UNIVERSITY OF CALIFORNIA
RIVERSIDE

# Sex Specific Mechanisms of Disease: Crosstalk Between Brain and Periphery in Inflammation

A Dissertation submitted in partial satisfaction
of the requirement for the degree of

Doctor of Philosophy

in

Neuroscience

by

Paula da Silva Frost

June 2023

Dissertation Committee:
Dr. Monica J. Carson, Chairperson
Dr. Vijayalakshmi Santhakumar
Dr. Marcus Kaul

The Dissertation of Paula da Silva Frost is Approved:

_____

_____

_____

Committee Chairperson

UNIVERSITY OF CALIFORNIA RIVERSIDE

ACKNOWLEDGEMENTS

There are many people who have helped tremendously in the completion of this work, and without them this would not have been possible. I would like to dedicate this thesis to my family. Thank you for believing in this dream of higher education. For my mother and my father, for all the opportunities their hard work was able to give me, for all the things they had to sacrifice so me and my sister could be here in the United States doing a PhD. I am incredibly thankful. Aline, my sister, thank you for stimulating me to try again, even when I had failed and thought I couldn't do it.

I want to thank my advisor, Dr. Monica Carson. For teaching me that science is made by people, for people. For pushing me throughout the years, for giving me the freedom to pursue my ideas, and for all the mentorship.

To all my labmates, for all the work put into obtaining data, for reminding me how exciting science is, and for constantly challenging me to become a better mentor. To Dorothy Estrada, for all the day-to-day friendship and the hard work that made the intestinal project become true. To Sirajan Kamara, who made our late nights of work a fun experience. You work incredibly hard and inspired me to do the same. Your contributions to the Alternaria chapter made this project what it is.

I want to thank my committee members. Dr. Marcus Kaul, for pushing me to think outside the box. And for Dr. Viji Santhakumar, I couldn't have asked for a more brilliant mentor. Thank you for listening to me and advising me throughout the years, and thank you for helping me make sense of the science.

I would like to thank all my collaborators, who made this work possible. I want to thank Dr. Lytle for introducing me to the world of intestinal physiology. Thank you for helping me understand how beautiful science can be, even when things go wrong. To Keziyah, for embracing the idea of a crazy experiment one month before my thesis deadline, which culminated with four figures in this dissertation.

I would like to thank all my UCR friends. Specially, Joseph Valdez and Edward Vizcarra, it was a lot of fun to create a podcast together, and your friendship helped me throughout the toughest years, including a pandemic.

To all my friends, whom which supported me to stay sane throughout this crazy journey. To Aaron, for making my days a breeze, I appreciate your friendship and your support. And could not have finished this degree without. For Emanuelle Vasconcellos, whose positive energy and hard work were a perfect match for us to develop multiple projects between the scientific communities of Brazil and the United States, including two international conferences. You have helped me understand how I can use my degree to create a positive impact in people's lives, and I will never forget.

To my beautiful partner Fernanda Arellano, the love of my life. Thank you for keeping me focused on the finish line, and to help me cross it. You inspire me every day. It is an understatement to say I couldn't have done it without you.

ABSTRACT OF THE DISSERTATION

Sex Specific Mechanisms of Disease: Crosstalk Between Brain and Periphery in Inflammation

by

Paula da Silva Frost

Doctor of Philosophy, Graduate Program in Neuroscience
University of California, Riverside, June 2023
Dr. Monica J. Carson, Chairperson

Sex is a variable that affects the immune response. Males and females have different innate and adaptive immune responses to pathogens, a fact that affects disease progression and treatment. However, only recently has sex has become more universally taken into account, and a lot of the mechanisms that dictate this variability are still being investigated. Correlative studies show that male and female immunologic responses to different pathogens continues to be different regardless of hormone levels, and suggest innate mechanism that differentiate sex response. Here, we used two different models of peripheral inflammation to study the sex-specific mechanisms of pathogenesis and its brain effects. The first model uses intraperitoneally injected LPS (IP-LPS), to drive systemic inflammation via TLR-4 receptor recognition. Using this model, we show in females but not males, that jejunum increases permeability, which is associated with recruitment of $CCR2^{+}$ macrophages and robust up regulation of inflammatory gene expression. To test whether macrophage activation was required for these effects, we used TREM2KO mice to "lock" macrophages in homeostatic state. We found that TREM2 deficiency prevented

the sex-specific effects of jejunum permeability, $CCR2^+$ macrophage recruitment, and metabolic gene expression. Using CCR2KO mice, we demonstrated that the recruited $CCR2^+$ cell population is directly responsible for functional alterations in the jejunum of IP-LPS treated females. The second model uses *Alternaria alternata* fungal extract to trigger allergic lung inflammation. Lungs contain nociceptors that relay the inflammatory response to the nuclei of the solitary tract (NTS), which controls breathing rhythms, bronchoconstriction, and can modulate inflammatory responses in the lung. We show males and females differentially regulate excitatory synaptic numbers in the NTS region; females decrease vglut2 and synaptophysin co-localized puncta, while males do not. The NTS also shows a sex-specific activation of protein signaling cascades PI3K/AKT and MAPK. Collectively the two models show how sex differentially impact peripheral immune response in inflammatory models, and how the brain plays a dual role by receiving and influencing that response.

# Contents

# List of Figures

# Chapter 1

## Introduction

### *Immune Response and Inflammation*

Inflammation is the collective response of cells to harmful stimuli, be it cellular injury, tissue malfunction or pathogenic invasion. It serves the purpose to alert surrounding cells, recruiting immune cells to the site of injury and returning the tissue to homeostasis. This orchestrated response is initiated by innate immune cells: macrophages and dendritic cells recognize danger molecular patterns (DAMPs) or pathogenic molecular patterns (PAMPs) via pattern recognition receptors. This initiates a signaling cascade that drive the production of pro-inflammatory mediators and culminate with the many symptoms of inflammation: swelling, redness, pain, and heat. They are associated with changes in blood vessel permeability, that allow the migration of immune cells to the injured site necessary for the immune system to remove the harmful stimuli and heal the tissue.

Among the PAMP receptors necessary for the innate immune system to recognize pathogenic molecules are a class of toll-like receptors (TLRs), that will be the focus of this introduction chapter. TLRs are highly conserved mammalian receptors, that can recognize many different pathogenic molecules. Each different PAMP is recognized by a different set of TLR, that range from 1-9. TLR 1,2,6 are responsible for lipoprotein and fungal extract recognition, while TLR3,7,9 can recognize RNA or DNA (Xu and Larbi, 2018). Upon activation toll-like receptors can elicit 2 different cascades of protein

phosphorylation: one uses the myeloid factor eighty-eight (MYD88) to activate the transcription factor nuclear factor kappa B (NFκB) and activating protein-1 (AP-1) (Park and Lee, 2013). The other uses the TIR-domain-containing adapter-inducing interferon-β (TRIF) to activate IRF3. The TLR activation from both signaling classically produce pro-inflammatory cytokines tumor necrosis alpha (TNFα), interleukin 6 (IL6), and interferon (IFNγ) (Schreiber *et al.*, 2006). These wide range of responses help the innate immune system produce a somewhat conserved first response, before the adaptive immune system builds a more specialized immunology response.

Around five days after the innate immunity is initiated, the tissue starts to shift toward an adaptive immune response, that is strongly and successfully mounted after seven days (Jain and Pasare, 2017). Animal models can make use of this timed response to isolate the innate immunity by using early time points of investigation, from a transitional period between the different types of immunity around day 5, and a later timepoint around seven days where adaptive immunity is prevalent. This time of response occurs because during tissue injury, dendritic cells travel to lymphoid organs carrying pathogenic molecules bound to MHCII receptors. Then, they present these pathogenic molecules to T cells, which in turn start their clonal expansion and generation of a specialized immune response with great specificity.

T cells can differentiate into a variety of subtypes during clonal expansion, depending on which pathogenic molecule was presented to them. $CD8^+$ T cells recognize infected cells and selectively induce apoptosis of them, while $CD4^+$ T cells act as stimulators of innate immunity by further controlling macrophages phagocytic capabilities (Sonnenberg *et al.*,

2011). T cells are also responsible to stimulate antibody production via its interaction with B cells, the second adaptive cell type to be covered in this introductory chapter. B cells are activated by T cell interaction via MHC class II receptors, and start producing immunoglobulins which further tag pathogenic molecules for phagocytosis of innate cells via opsonization (Pröbstel *et al.*, 2020).

This orchestrated response discussed here is beneficial to the tissue, as so is the inflammatory response. The body needs these series of adaptations to quickly recognize, neutralize and protect the body from harm. It is only when this response is dysregulated that inflammation becomes detrimental: chronic exposure to inflammatory mediators, or exacerbated acute inflammatory responses lead to tissue damage. This happens because the same inflammatory mediators used by the immune system to signal distress, change vascular permeability and fight pathogens can cause cellular stress and cell death (Rufo *et al.*, 2022). Reactive oxygen species often released by innate immunity prostaglandin-endoperoxide synthase 2 (COX-2) and inducible nitric oxide synthase (iNOS), cause oxidative damage in pathogenic molecules and cells alike, contributing to cell death during chronic inflammatory responses (Needleman and Manning, 1999).

So what are some of the mechanisms that ensure this inflammatory response will be physiologically beneficial instead of harmful? Or even if harmful, will the benefits out weight the costs? Many aspects influence this intricate balance of inflammatory response in disease, making treatments very hard to manage in clinic. One factor that heavily influences the immune response for example is sex, which is often overlooked in research.

Since the inflammatory regulation is sex-specific, models dissecting each sex contribution to inflammatory dysregulation is of major importance to aid specialized disease treatment.

## *Sex as a variable that influences the Immune response*

An important step when talking about the influence of sex in the immune response is defining what is sex and gender, since both can heavily influence the immune response of an individual. According to Wilkinson et al. sex is defined by 3 different characteristics: the chromosome composition (XX or XY), the gonadal hormones (testosterone and estrogen), and the reproductive system (ovaries, testes).

Wilkinson et al. defines gender as a social construct and refer to an individual's expression in clothes, pronouns, traits, but also to one sense of internal identity. Because of the way gender is constructed in society, it is hard to use animal models to study and isolate gender effects. However, extensive data documents in humans the effect gender have in the immune response: gender identity shapes the interaction of an individual with the health care system, as well as dictates lifestyle choices (smoking, stress, exercise, nutrition) that influence long-term health (Wilkinson *et al.*, 2022). This dissertation will focus on the effect of sex. Therefore, when males, females, men or women are used throughout this document, one should assume it is referring to sex and not gender.

Women are more affected by the majority of autoimmune diseases, with ratios that reach almost 10:1; below a table generated from epidemiological data in the United states shows the evolution of autoimmune affected individuals separated by sex (TABLE1). Females have higher prevalence in most diseases since 1997, which account for approximately 80%

of the United States' cases of autoimmunity (Jacobson *et al.*, 1997). At the same time, females have a lower prevalence of viral infections when compared to males. Men are more effected by Influenza virus, dengue viruses, oral HPV, West Nile viruses, among others (Gay *et al.*, 2021). And when females do get infected, viral loads tend to be lower, and symptoms less severe (Wang, Chen and Yeh, 2015). These evidences argue to the fact that females have a stronger innate and adaptive immune systems, and human studies do find strong evidence that sex is a major variable to influence immune responses (Ter Horst *et al.*, 2016). So what does explain the sex difference in immunity?

| Autoimmune Disease | Percent affected (women) |
|---|---|
| Addison's disease | 92.5% |
| Chronic Active Hepatitis | 88.3% |
| Hyperthyroidism | 94.6% |
| Insulin Dependent Diabetes | 47.9% |
| Multiple Sclerosis | 64.2% |
| Myasthenia Gravis | 72.7% |
| Pernicious anemia | 66.7% |
| Rheumatoid Arthritis | 74.8% |
| Sjorgren's | 93.7% |
| Systemic lupus | 88.2% |
| Thyroiditis | 94.6% |
| Vitiligo | 52.3% |

**Table 1.1 Sex influences prevalence of autoimmunity**
Different types of autoimmunity diseases and their prevalence in women in the United States population since 1997. Adapted from Jacobson et al., 1997.

Males and females express different chromosomes complement to their X, females have a second copy of an X chromosome, while males express chromosome Y. The X chromosome express over 1,000 genes; in the meantime, the Y chromosome only expresses between 45-75 genes (Wilkinson *et al.*, 2022). A lot of inflammatory genes are localized

to the X chromosome, including the expression of TLR7, TLR8, IRAK1, CD40L, and CXCR3 (Schurz *et al.*, 2019); but also the expression of X-linked non-coding microRNAs that regulate gene expression (Bianchi *et al.*, 2012). TLR4 on the other hand is not expressed in the X chromosome.

Because inflammatory genes are associated with the X chromosome, researchers have proposed the hypothesis of its influence in female inflammatory response; but it is hard to separate females XX hormone influence from XX chromosomal expression. Recently, this issue was circumvented by the generation of SRY expressing mice. SRY is expressed on the Y chromosome and drives testes development, by deleting sry gene from males one can generate XY mice that develop a uterus gonadotropin. With the same logic, one can express sry gene in XX females, this mutation allows female to develop testes even with an XX chromosome, separating the estrogen response from the equation (Arnold, 2020). In an animal model of experimental autoimmunity encephalomyelitis (EAE), animals with the same gonadal type expressed different XX or XY chromosomal pairs (e.g. XX and XY mice expressing testes). In this model, XX mice are more susceptible to EAE, regardless if the XX mice had testes or uterus (Smith-Bouvier *et al.*, 2008). This was not an isolated study, in stroke susceptibility XX mice have higher susceptibility with a higher immune cell infiltration and cytokine production in the infarct brain region regardless if they had uterus or testes (McCullough *et al.*, 2016). These animal models provide strong evidence that the sex influence in the immune response is mediated by an inherent mechanism from birth and not from hormonal levels.

In a study from the Human Functional Genomics Project, over 500 healthy subjects were challenged with bacterial, fungal, viral and non-pathogenic stimuli and a strong association between age and sex was found to affect the immune response. Moreover, the study found a remarkable fact: differences in circulating hormone levels did not explain sex differences. Most of the cytokines released to these different stimuli presented no correlation in men and women to the levels of progesterone and testosterone hormones (Ter Horst *et al.*, 2016). Another strong evidence that female increased innate responsive is due to birth gene expression, and not a hormonal regulation when comparing from male response.

As described above, the X chromosomes express a variety of inflammatory genes, but is that sufficient to drive sex differences to a variety of diseases? Chromosomal expression of genes is not the only described mechanism of sex specific immunity. TLR7, 8 and 9 activation in dendritic cells depend in the transcriptional regulation by an estrogen responsive element alpha (EREα) to elicit a pro-inflammatory cytokine response. ERE is the receptor for estrogen, that upon binding enters the nucleus and functions as a transcription factor to a number of genes (Cunningham *et al.*, 2012). Although estrogen is the main mediator of ERE activation, there are also non-canonical molecules that can activate ERE in an estrogen independent manner. This is the case for TLR7/8/9 activation, EREα transcription of inflammation genes occurs independently of estrogen levels (Cunningham *et al.*, 2014). One should not assume then, that hormonal fluctuations during the female menstrual cycle will be responsible for driving immune changes every time an estrogen receptor is present in the regulation of response.

This mechanism of inflammatory regulation poses a challenge to studying the effect of hormones in the immune response: administering estrogen artificially into animal models to high non-physiological levels would have estrogen participate in immune responses via estrogen responsive elements, something that as suggested above is not always a natural effect of the hormonal regulation of inflammation and can confound findings.

Now, the purpose of this dissertation is not to say that hormones have no role in the immune response. Estrogen, progesterone, and testosterone heavily influence the innate and adaptive immune responses and there is an extensive literature on the subject. Estrogen for example, can change innate immunity by producing a pro-inflammatory response in combination with TLR activation, that is abolished when estradiol is not present. Myeloid cells increase TLR-4 response to LPS in a mechanism dependent on estrogen by producing a higher level of cytokine release (Rettew, Huet and Marriott, 2009), ovariectomized females reduce serum levels of TNFα, IL6 and IL-10 in response to IP-LPS (Rettew, Huet and Marriott, 2009). At the same time, very high levels of estrogen that are supraphysiological have been shown to reduce the inflammatory response by IP-LPS (Deshpande *et al.*, 1997; Zhang *et al.*, 2001), suppressing these same cytokines TNFα, IL6 and IL-10. This is a mechanism in females that is used for the regulation of the immune response during pregnancy, where levels of estradiol vary from low to high, shifting the female response toward anti-inflammatory (Robinson and Klein, 2012), a mechanism thought to protect the developing embryo.

Hormonal levels also play a role in male inflammatory response: in vitro testosterone stimulation reduces TLR-4 expression in murine macrophages (Rettew, Huet-Hudson and

Marriott, 2008), this evidence is reproduced in vivo by orchiectomized male mice (Posma *et al.*, 2004), which have increased levels of TLR-4. Testosterone also influences the TLR-4 cytokine response, by decreasing its expression. Human epithelial cells exposed to LPS and dihydrotestosterone significantly downregulate IL-6, MCP-1, TLR4, and Cox-2 (Norata *et al.*, 2006). However, the fact is, hormone levels influence both male and female response and cause variability in both sexes, not just in one of them. For example, males have very strict social hierarchy in mice, α-males can have 10x more testosterone levels than other males lower in the social hierarchy within the same cage. A fact that can directly influence the variability in male response to inflammation, but it is rarely considered. And again, even at the light of hormones influencing immune responses, chromosomal expression is still the strongest factor that explains sex differences and researchers should consider its specific mechanisms of regulation. Therefore, works focusing on the intrinsic regulation of sex-specific inflammatory responses, regardless of hormonal influence in the interindividual variability, can be of great value to support novel treatments of inflammatory related diseases.

### *Systemic Inflammation Affects the brain*

The immune response that happens throughout the body uses blood vessels to communicate to distant locations. For example, intestinal or lung inflammation may recruit immune cells from outside via production of chemokines and cytokines that travel the blood. And pro-inflammatory mediators that initiate in peritoneal cavity, can travel throughout the body and have the capacity to influence distant organs, including the brain.

For some time, the brain was thought of as an immune privileged organ. Inflammation that happens throughout the body are filtered by the blood-brain barrier, protecting the brain from being affected. Indeed, the blood-brain barrier is responsible for filtering out molecules from the blood before then enter the brain: it is composed of endothelial cells with tight junction expression, which prevents the free passage of molecules from blood to brain; astrocytes have their end-feet in close proximity to endothelial cells, further filtering out substances that come from the blood; and pericytes are in close association with these cells, regulating the blood flow (Brown *et al.*, 2019). This view of immune privilege has changed over time.

Now we know that the blood-brain barrier does not cover every part of the brain, and that the area postrema within the brainstem does not possess a barrier, and blood molecules and inflammatory mediators can just impact function directly. Recently, we have also discovered lymphatic vases that arrive in the brain and directly carry immune cells to the brain, facilitating the impact of inflammation within (Louveau, Da Mesquita and Kipnis, 2016). Changes in systemic inflammation impact the blood-brain barrier, increasing permeability and facilitating cellular and inflammatory mediators migration (Galea, 2021). IP-LPS in the periphery for example increases levels of pro-inflammatory cytokines in the brain: TNFα, IL-1β, and increases the permeability of the blood-brain barrier to big molecules(Banks *et al.*, 2015; Zhao *et al.*, 2019). This increase in neuroinflammation impact brain function: cognitive performance decreases and animals have deficits in memory related tasks (Zhao *et al.*, 2019). Systemic inflammation also decreases motor

activity, food and water consumption and leads to social withdrawal, symptoms collectively known as sickness behavior (Dantzer *et al.*, 2008).

The access of cytokines via blood vessels by mechanisms described above are not the only ways the peripherical inflammation impact brain function, specially in the case of the sickness behavior control. Internal organs are innervated by sensory fibers such as nociceptors, that sense alterations in the inflammatory milieu and send the information to the brainstem in a region known as the nuclei of the solitary tract. This information than travels to a number of brain regions, including the hypothalamus and amygdala to influence the behavioral alterations necessary for sickness behavior (Dantzer *et al.*, 2008).

These physiological alterations to peripheral inflammation are a well-adapted response to direct our behavior for resting while we are feeling sick, but systemic inflammation can lead to maladaptive behaviors that culminate in brain injury. When inflammation is in high intensity, such as the case of sepsis, or when chronic, the brain is negatively impacted by decreasing synapse numbers, activating local immune cells the microglia and potentially leading to cellular death (González-Scarano and Baltuch, 1999). In fact, there is a growing hypothesis that neurodegenerative diseases development is influenced by chronic exposure to systemic inflammation (Houser and Tansey, 2017).

### *Microglial cells play a role in the brain effects of inflammation*

Microglial cells are resident immune cells that constantly surveil their microenvironment. This surveillance is part of their homeostatic role in the central nervous system (CNS), microglia participate in the active engulfment of synapses in a process known as synaptic

pruning, a normal developmental process that eliminates the excess synapses that are in formation in early age (Stevens *et al.*, 2007). The classification of microglia as immune cells should not blind us from their physiological role in the CNS. Indeed, their own similarity to the macrophage population is limited, since they have distinct embryonic origin. Tissue macrophages derive from a myeloid stem cell population that reside in the fetal liver in embryonic development and later from bone marrow (Gomez Perdiguero, Schulz and Geissmann, 2013). On the other hand, the myeloid progenitors that give rise to microglial cells are derived from the yolk sack, and they migrate to the central nervous system during early embryonic development (Ginhoux *et al.*, 2013). This microglial population from embryonic origin is a long-living brain resident throughout an individual's life and they have the ability to proliferate, regulating their numbers (Aguzzi, Barres and Bennett, 2013).

Upon the recognition of a pathogenic molecule in the CNS, microglial cells become reactive, a process in which they change their gene expression and morphology, retracting their processes and acquiring an amoeboid shape that has been extensively characterized (Kettenmann, Kirchhoff and Verkhratsky, 2013). This change in morphology permits the microglia to migrate to the site of inflammation, proliferate, and secrete a series of pro-inflammatory cytokines in order to reestablish homeostasis within the brain. These cytokines can also enter the blood, recruiting peripheral immune cells to assist them in the process. Since the cytokines produced have the ability to directly regulate neuronal transmission and neurogenesis (Sierra *et al.*, 2013), only when exacerbated they can lead to neuronal damage and can contribute to neurodegeneration (Ginhoux *et al.*, 2013).

Therefore, the microglia population needs a tight regulation when responding to alterations in their environment to prevent a cascade of damage they may trigger. If systemic inflammation leads to neuroinflammation, microglial cells will now act to amplify this neuroinflammatory response and actively contribute to damage when tight controls are not in place.

In neurodegenerative diseases microglial cells contribute to synapse loss by increasing phagocytosis of synaptic numbers. This mechanism depends on the orchestration of cellular mediators: astrocytes produce a complement system molecule 1q (C1q) that binds to synapses that need to be engulfed (Dejanovic *et al.*, 2022). On the other hand, microglial cells secrete another complement molecule C3, that binds to C1q. Microglia then recognize via C3R the tagged synapses and engulf them, a mechanism present in neurodegenerative diseases that drive synapse loss (Dejanovic *et al.*, 2022).

This is not the only way reactive microglia can negatively impact the brain. The changes in gene expression during certain neuroinflammatory environments generates by microglia reactive oxygen species COX2 and iNOS that decrease synaptic markers and induce memory deficits (Zhao *et al.*, 2019). Preventing microglial activation is a mechanism that prevents negative impact in brain health by systemic inflammation, as previously described (Frost *et al.*, 2019).

### *Crosstalk between sex, inflammation and the brain in this document*

Given the role of sex in affecting the inflammatory response, and how the inflammatory response impact the brain we use two different models of systemic inflammation to

understand sex-specific mechanisms of response. Chapters 3, 4 and 5 explore the sex-specific mechanisms of intestinal inflammatory strategies in response to a systemic inflammatory model. Chapter 6 focuses on the lung-brain axis, and how sex impacts the information from lung to brain, and its potential implication in brain to lung modulation. Chapter 2 goes over the methods and techniques used throughout this dissertation for both projects.

# Chapter 2

## Methods

### *Mice*

C57Bl/6J, TREM2KO, CCR2KO, and Nav1.8cre$^{+/-}$DTA$^{+/-}$ were maintained in standard mouse husbandry with standard Purina food chow under a 12-hour light/dark cycle in UCR campus vivarium. All experiments were performed in compliance with University of California Institutional Animal Care and Use Committee regulations. Genotyping of mice was conducted by Transnetyx.

#### C57Bl/6J Wild Type mice (WT)

C57Bl/6J mice were originally obtained from Jackson labs (ID#000664) and subsequently bre in house at UCR. This mouse model can be served as the background of many transgenic lines, it has low genetic individual variability (Corder *et al.*, 2023). Both sexes of these mice were used in experiment at ages of 2-3 months old unless stated otherwise.

#### Transient Receptor Expressed on Myeloid Cells (TREM) 2 knockout Mice

TREM2KO animals (T2KO) were donated by Dr. Marco Colonna and bred in house at UCR. They are generated by targeting exons 3 and 4 of the TREM2 gene, which encode the transmembrane and cytoplasmic domains of the receptor, as previously reported by (Turnbull *et al.*, 2006). Only homozygous TREM2KO mice were used in this studies at the

same ages as wild-type mice, unless stated otherwise. TREM2KO mice are 3 months old and both males and females are used throughout the experiments unless stated otherwise.

C-C-motif chemokine receptor 2 (CCR2) RFP knock-in/knock-out mice

CCR2 RFP KI/KO mice were purchased from Jackson laboratory (ID# 017586). These animals have a monomeric red fluorescent protein (RFP) sequence replaces the expression of the CCR2 gene. When heterozygous, the mice exhibit a marker for CCR2 expressing cells, these animals were named CCR2 RFP thought this manuscript. When homozygous the animals do not express the CCR2 gene, therefore these animals were named CCR2KO throughout this manuscript.

Nav1.8cre x DTA mice

Nav1.8-cre knock-in/knock-out mice (ID# 036564) and Rosa/DTA STOP mice (ID#009669) were purchased from Jackson laboratory and breed to generate Nav1.8cre x DTA. In brief, Nav1.8 cre knock-in/knock-out have a cre expression under the translation initiation site of the scn10a gene. The gene transcribes for the voltage-gated sodium channel alpha (Nav1.8), which is expressed in a subtype of sensory neurons known as nociceptors (Nassar *et al.*, 2004). Rosa/DTA STOP mice have a STOP cassette between two loxp sites and a Gt(ROSA)26Sor promoter driving diphterin toxin a (DTA) expression (Voehringer, Liang and Locksley, 2008), under normal conditions the STOP cassette prevents the expression of the toxin. When the animals are breed together, the cre

expression drives DTA expression in Nav1.8 expressing cells, ablating the nociceptor subtype as previously used (Talbot *et al.*, 2015).

## *Treatment*

### LPS administration

At 3-5 months of age, male and female, C57Bl/6J, TREM2KO and CCR2KO mice were administered lipopolysaccharide (LPS, Sigma-Aldrich, 1mg/mL) intraperitoneally (IP) 5mg/kg.

### Chamber Exposure to Alternaria Fungi

Mice are kept in their home cage with food and water *ad libidum,* with a 12h light/dark cycle for the duration of experiment. The cages are put inside an acrylic chamber, where the air flow is controlled as described by Peng et al. 2017. Specifically, compressed air is filtered by a series of passages through different materials: silica (moisture absorption), activated carbon (organic absorption), hopcalite (CO absorption) and purafil (NOx absorption). Pressure is applied to guarantee a constant flow of air and aerosolized particles. *Alternaria alternata* non-infectious extracts are diluted in PBS1X and converted to an aerosol spray at a constant flow of 6L/min by a nebulizer. The concentration of *Alternaria alternata* is kept constant at 750μg/cm$^2$ for the 7day duration of experiment by a condensation particle counter as previously described (Peng *et al.*, 2018). A control chamber is concomitant exposing mice to filtered air for the duration of the 7day experiment, and a reversal group receives *Alternaria alternata* non-infectious extracts for

7days and are then transferred to a filtered air chamber for another 7days to verify reversal of lung and brain effects.

## *Ex vivo intestinal experiments*

Ussing chamber Experiments

24h post IPLPS animals were anesthetized with isoflurane and sacrificed with cervical dislocation. Intestine was collected 9cm after stomach and a 6cm jejunum segment was isolated in Parson's solution as previously described (Chen *et al.*, 2020), with or without D-glucose-1,2,3,4,5,6,6-d7 (Sigma-Aldrich), adjusted to 305 mosmol/kgH2O by the addition of NaCl or water. Indomethacin was added to solution (1µM/ Cambridge Isotope Laboratories, Tewksbury, MA). Segment was further dissected into 3 pieces of 2cm each, intestine was then mounted in 0.3cm2 chamber slider aperture and inserted in chamber. Luminal side received 3mL Parson's solution with mannitol (10Mm) and indomethacin (1µM), while serosal side received Parson's solution with D-glucose (10mM) and indomethacin (1µM). Temperature was controlled to 37°C, tissues received a mixed gas (CO2 5%, O2 95%) throughout the duration of experiments. Tissues remained in chambers for approximately 30min before current was measured at rest and after a 2mV pulse (Physiological Instruments VCC-MC2). Glucose solution (300mM) was added to lumen and peak of current increase was recorded in voltage clamp mode (0mV). 3µL of forskolin was added to serosal side, and peak of current increase in voltage clamp was recorded. Forskolin activates cAMP dependent chloride secretion and indicates tissue viability. Tissues that did not respond to forskolin ($\Delta I<12\mu A$) were excluded from analysis.

4kDa FITC-dextran quantification

40uL 4kDa FITC-dextran (Abcam, 80mg/ml) was applied to luminal side in Ussing chambers. After a 1hr incubation period, 200uL of solution from serosal side was collected for analysis. Samples were kept in -80°C until quantification on Veritas Microplate luminometer (Turner Biosystems, Sunnyvale, CA), using GloMax software (Promega, Madison, WI). Sample concentration was determined using a 4kDa FITC-dextran dilution curve.

Cd11b cell isolation and co-culture

Spleen is removed from isoflurane anesthetized animals and homogenized in HBSS1x (Thermo Fischer), contents are passed through a 70um cell strainer into a 50mL conical tube and centrifuged for 10min 1000rpm. Supernatant is discarded and pellet is resuspended. This cell suspension is now centrifuged for 10min at 300g and cells are resuspended in 90uL of MACS Buffer per 107 cells. 10uL of cd11b beads (MACS) are used per 107 cells and incubated at 2-8°C for 15min. Cells are centrifuged at 300g 10min and resulting pellet is resuspended in 500uL of buffer. Solution is passed through MACS beads separation column (MiniMACS) according to manufacturer's instructions. Cd11b+ separated cells are diluted in DMEM media 25mM HEPES, L-Glutamine and 4.5g/l D-Glucose (sigma-aldrich) and added to the bottom of a 12well plate (500,000 cells per well). T84cells cultured in same DMEM media 12-mm permeable Transwell inserts (Corning, Corning, NY) until confluent and then are added to the cd11b cell population. Co-culture

is maintained for 48hrs, transepithelial resistance (TEER) is measured at 4h, 24h and 48h post cell plating.

## *BALF collection and Analysis*

BALF collection

Animals are anesthetized with isofluorane followed by euthanasia via cervical dislocation. Animals had their trachea perforated using a 23G needle and the bronchio-alveolar lavage fluid (BALF) was recovered through intratracheal washing of ice-cold PBS (3x 0.8mL each) as previously described (Chen Gang *et al.*, 2016). Collected BALF is centrifuged at 1500rpm to generate a cell pellet and resuspended in fresh PBS.

Flow cytometry of lung tissue

Resuspended BALF is centrifuged at 1500rpm for 7min and resuspended in 100µL of zombie Yellow dye (biolegend) for assessment of cellular death. After staining, cells were washed in FACS Buffer, centrifuged and resuspended in 1:50 dilution of anti-Fc block (BD Pharmigen) for 10min. Cells are then incubated for 30min with the following cellular markers: anti-CD45 FITC (BioLegend, 30-F11), anti-CD19 Percp-Cy5.5 (eBioscience, eBio1D3), anti-CD3 APC-Cy7 (BioLegend, 17A2), anti-Ly6G BV510 (BioLegend, 1A8), anti-CD11b BV421 (BioLegend, M1/70), anti-CD11c PE-Cy7 (BioLegend, N418) and anti-SiglecF APC (BioLegend, S17007L). Samples are washed with FACS buffer, incubated with PFA1% overnight and run through flowcytometer NovoCyte Quanteon

(Agilent Technologies). Gating strategies were used according to previously described (Biddle *et al.*, 2023) and analyzed using FlowJo software (Version 10.81).

## *Histological analysis*

Jejunum Collection

Mice are anesthetized by isofluorane, and cervical dislocated. Jejunum intestinal segment is isolated by measuring 9cm after stomach, and a 10cm measured section is isolated and flushed using ice cold PBS to empty contents of intestinal lumen. Tissue is them flushed with PFA4% and post-fixed in this solution for 24hrs, then further incubated in a solution of PBS +30%sucrose for 48hrs. Tissue was mounted on optimal cutting temperature compound (OCT) and sectioned (16µm). Samples were incubated for 20min at 60-80°C in Citrate Buffer, followed by permeabilization in PBS, 0.5% Tween 20 for 10min (Sigma-Aldrich). Tissues were blocked by a solution containing PBS, 5%Normal Goat Serum (NGS, Vector Laboratories) and 0.1% Tween for 1hr prior to claudin-3 antibody (Abcam) incubation overnight. Secondary antibody anti-rabbit 488 (Invitrogen) was used 16hrs later during a 1hr incubation. Tissue sections were mounted in Prolong Gold with DAPI and imaged in spinning-disk confocal imager (Yokogawa, Japan) attached to a Zeiss Axio Observer inverted microscope.

Claundin-3 puncta quantification

Pictures were taken at 63X magnification on spinning-disk confocal imager (Yokogawa, Japan). Animals have 2 sections of their intestine collected. For each section, 3 images are

taken at 63X in different regions of their jejunum. For each image at least 5 cells are quantified per villi. Internalized puncta is quantified in Image J software manually, any puncta smaller than 0.065μm$^2$ was excluded from counts.

Brain Collection

Mice are anesthetized with isofluorane and intracardiacally perfused using ice cold PBS (20mL) followed by 4%PFA (20mL). The whole brain is then removed and dissected for the brain regions of interest, and post-fixed 24hrs in 4%PFA. Brains are then transferred to a 30%sucrose in PBS solution for 48hrs and mounted on OCT. Samples are sectioned at 5μm for GeoMx and puncta quantification, while they are sectioned at 20μm for IBA1 quantification.

Brain immunofluorescence

Samples were incubated for 20min in high-pressure cooker with Citrate Buffer. Tissues were blocked by a solution containing PBS, 5%Normal Goat Serum (NGS, Vector Laboratories) and 0.1% Tween for 1hr prior to primery antibody incubation overnight. The following antibodies were used: anti-rabbit IBA1 (WAKO), anti-mouse synaptophysin (abcam), anti-rabbit PSD95 (abcam), anti-guinea pig vglut2 (EMDmillipore). Secondary antibody anti-rabbit 594 (Invitrogen), anti-guinea pig 647 (Invitrogen), anti-mouse 488 (Invitrogen) were used 16hrs later during a 1hr incubation. Tissue sections were mounted in Prolong Gold with DAPI and imaged in spinning-disk confocal imager (Yokogawa, Japan) attached to a Zeiss Axio Observer inverted microscope. Images for puncta analysis

were taken at 63X. Microglial analysis were taken with z-stack at 20x (1.19um z-step, 14 slices) and 63X (0.37um z-step, 45 slices).

Synaptic Puncta Quantification

63X images from synaptic markers were taken from the nuclei of the solitary tract (NTS) in air and *Alternaria alternata* exposed mice. Each animal had 3 sections collected, and each section were taken 3 pictures of the NTS region. parameters for each synaptic marker (vglut2, synaptophysin and PSD95) were set per batch of analysis; samples had the same brightness and contrast and exposure time at the microscope. Images were analyzed for puncta separately using ImageJ software for particle analysis, only puncta within 0.5-10$\mu m^2$ size were considered. Values were normalized by a positive control sample and graphed in GraphPad Prism.

Puncta co-localization was analyzed according to previously published data (Nguyen *et al.*, 2020). In brief, vglut2 and synaptophysin were transformed to an 8-bit image and an ImageJ plugin colocalization was used. Samples were superimposed and a third image with the superimposed puncta was generated, a threshold of 160 is applied and puncta is quantified by particle analysis. Once again, only puncta within 0.5-10$\mu m^2$ are considered in quantification. Values are normalized by a positive control sample and graphed in GraphPad Prism.

## *mRNA isolation*

Jejunum was dissected from animals and immediately placed in RNA later at 4°C before RNA extraction. 500uL of Trizol (Invitrogen, Carlsbad, CA, USA) per 1mg of tissue was used for homogenization; samples were incubated in room temperature (RT) for 5min, then 250uL of chlorophorm was used for phase separation. Samples are then centrifuged (12,000g 15min 4°C) and up to 400uL of supernatant is collected. 500uL of isopropanol is used for RNA precipitation at RT for 5min, then 700uL of solution is pippeted into RNeasy mini kit columns (Qiagen, cat: 74106). Manufacturer's protocol is followed, ensuring high quality RNA, which is further characterized in Nanodrop 2000 for purity and on Agilent 2100 Bioanalyzer for quality Absorbance ratios 260/280 below 1.85 or RIN below 7.9 are criteria used for sample exclusion.

## *Nanostring highthroughput assays*

nCounter gene expression analysis

RNA extracted from samples were incubated with Reporter probe and Capture probe for 16hr at 65°C, 50ng of RNA samples were pippeted into inflammation panel cartridge or metabolic panel cartridge for imaging on nCounter SPRINT Profiler. Raw gene counts were obtained and normalized by housekeeping genes by a built-in analysis on Rosalind website. Principal component analysis and pathway scoring are obtained by software. Volcano plots comparing males and females response were generated by analyzing differential expression of individual genes, multiple comparison p-value adjustment was obtained by Benjamin-Hochberg analysis.

GeoMx spatial protein analysis

Brains dissected from perfused animals as described previously (Immunofluorescence section) are sectioned at 5um thickness for protein quantification via GeoMx procedure. Slides are then incubated with anti-tyrosine hydroxylase antibody conjugated with Alexa fluorophore 594 (ThermoFischer) and with the kits provided by NanoString company for the following: neuronal cell profiling core, autophagy module, MAPK module, PI3K/AKT module and glial subtype module. A complete list of probes used in this study are depicted in figure 2.1. In brief, samples are imaged in GeoMx machine and the nucleus of the solitary tract is selected as region of interest (ROI). Machine collects probes in 96-wells, and they are hybridized at 67C for 17hours before being pipetted into cartridges for readout on nCounter machine. Data is obtained as raw counts of proteins per sample. Any protein counts with levels close to background are excluded from the analysis. To decide excluded proteins in brief, counts were normalized by the negative control probes (Rabbit IgG, Rat IgG2b, Rat IgG2a) geometric mean, then data is transformed by its logarithmic on base 2 value (Figure 2.1). Any protein counts with its $75^{th}$ percentile below the background level of 0 is interpreted as below detection as counts are close to background levels, therefore they are excluded from analysis. This does not include proteins which part of the counts are at or below background level and part of it is above, as this might have biological significance. Proteins excluded are: MHCII, CD163, ki-67, CD39, SPP1, GPNMB, MET. Any samples with more than 50% of protein counts below the geometric average of negative probes are excluded from analysis.

There are 3 additional methods to normalize data across samples based on housekeeping protein expression, negative probes and nuclei counts. The best method for normalization is investigated using a correlation plot of all 3 possible normalizing factors. The factor that best correlates across the datasets is more equipped to be used as representative of the data for normalization. First, we must decide if all housekeeping proteins should be used as housekeeping normalization or if one should be excluded. Next, we must analyze if within the negative probes one should be excluded or if they should all be used. Last, we must generate geometric averages with the probes chosen for housekeeping and the probes chosen for negative/background probes and check which parameter best correlates with the data: nuclei counts, housekeeping proteins or negative probes.

To decide which housekeeping proteins to use in our normalization, raw counts for S6, histone H3 and GAPDH are plotted (Fig2.2 A). The r squared value is calculated per plot, and values below 0.6 are used as an indicator of poor correlation. In our analysis the correlation between GAPDH and histone H3 values has an $r^2$ value of 0.57; therefore one of them must be excluded from our final geometric average for housekeeping, but further analysis is necessary to decide which one of the two. The next two graphs show r squared values of 0.7 plotting GAPDH and S6, and 0.86 plotting histone H3 and S6. Therefore, GAPDH has the poorest correlative value between them and is excluded from analysis. A geometric mean using S6 and histone H3 raw counts is generated per sample.

To decide whether all 3 negative control probes should be used for normalization we generate correlation plots for Rabbit IgG, Rat IgG2a and Rat IgG2b (Fig. 2.2 B). All graphs

have high correlation and high $r^2$ values. Therefore, a geometric mean is generated using all 3 negative probes per sample.

Next, we must decide between the different methods of normalization which one fits our data better. Again, correlation plots are generated to look for consistency between different parameters (Fig. 2.2 C). The housekeeping (HK) protein geometric average is an indicator of signal in our data; the negative probes geometric average is an indicator of background in the data. In a perfect dataset in which all samples are comparable, the higher the signal the higher the background obtained, therefore high correlation. Indeed, we observe a high correlation between our signal (HK geo mean) and our background (IgG geo mean), suggesting they are both good parameters to be used as normalization factors. To choose between them a second correlation plot is generated using nuclei counts. Each ROI has a distinct area and a consequently a distinct number of nuclei. Assuming a perfect dataset in which all signal is obtained, the number of nuclei in a given ROI correlates with the amount of signal and background. We can see that in our dataset, the housekeeping protein parameter correlates the most with the nuclei counts and therefore is the best method to be used as a normalization factor.

After the choices for normalization are made the samples are inputed into the GeoMx software for quantification and it automatically normalizes samples by the parameter chosen: housekeeping proteins S6 and histone H3 geometric mean. Normalized values are used to generate volcano plots using the LOG2 of fold change by the -LOG10(adj. p-value). Data is compared using linear mixed models and p-value is adjusted by Benjamini-Hochberg method.

### *Statistical Analysis*

Bars graphs show mean ± SEM. Samples were compared by unpaired two-tailed or one-tailed Student t-test for single comparisons; one-way ANOVA was used for multiple comparisons, and post-test Tukey was used. Groups were analyzed with two-way ANOVA when appropriate. A p value lower then 0.05 was used for statistical significance. Data was graphed in GraphPad Prism Software. Differentially expressed genes was analyzed in NanoString Advanced Analysis nCounter software and graphed in GraphPad Prism software, multiple comparisons corrected p value was generated by Benjamini-Hochberg test. Heatmaps were generated by nCounter Analysis software by comparing normalized gene expression average via Euclidian distance clustering.

## *Figures and Legends*

**Figure 2.1 List of proteins quantified by GeoMx**
Data is expressed by normalized values. In brief, protein counts per sample are divided by the geometric mean of the negative control probes (Rabbit IgG, Rat IgG2b, Rat IgG2a). Then, the logarithmic value on base 2 of this ratio is obtained and plotted. Puncta expresses each ROI obtained in the analysis, data expressed as average with box extending to 25 to 75 percentile, whiskers go to minimum and maximum value obtained. Dashed line represents background, proteins with distribution majoritarily (75 percentile bar) bellow dashed line are excluded from analysis.

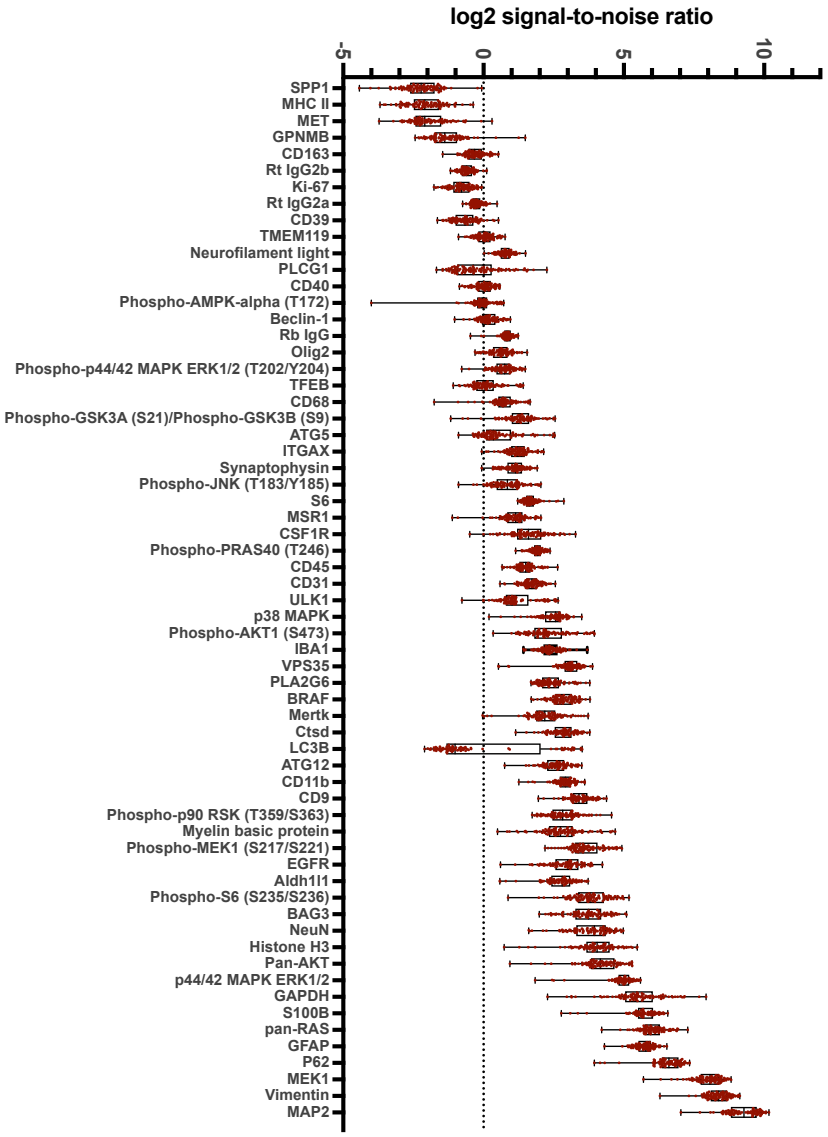
log2 signal-to-noise ratio
-5
0
5
10
SPP1
MHC II
MET
GPNMB
CD163
Rt IgG2b
Ki-67
Rt IgG2a
CD39
TMEM119
Neurofilament light
PLCG1
CD40
Phospho-AMPK-alpha (T172)
Beclin-1
Rb IgG
Olig2
Phospho-p44/42 MAPK ERK1/2 (T202/Y204)
TFEB
CD68
Phospho-GSK3A (S21)/Phospho-GSK3B (S9)
ATG5
ITGAX
Synaptophysin
Phospho-JNK (T183/Y185)
S6
MSR1
CSF1R
Phospho-PRAS40 (T246)
CD45
CD31
ULK1
p38 MAPK
Phospho-AKT1 (S473)
IBA1
VPS35
PLA2G6
BRAF
Mertk
Ctsd
LC3B
ATG12
CD11b
CD9
Phospho-p90 RSK (T359/S363)
Myelin basic protein
Phospho-MEK1 (S217/S221)
EGFR
Aldh1l1
Phospho-S6 (S235/S236)
BAG3
NeuN
Histone H3
Pan-AKT
p44/42 MAPK ERK1/2
GAPDH
S100B
pan-RAS
GFAP
P62
MEK1
Vimentin
MAP2

**Figure 2.2 Housekeeping proteins are used as normalization factor based on correlation**
**A**. Raw counts of the data are used to generate correlation plots for housekeeping.
**B**. Raw counts of the data are used to generate correlation plots for background.
**C**. Geometric average of chosen housekeeping and negative probes are used to generate correlation. plots between themselves and nuclei.

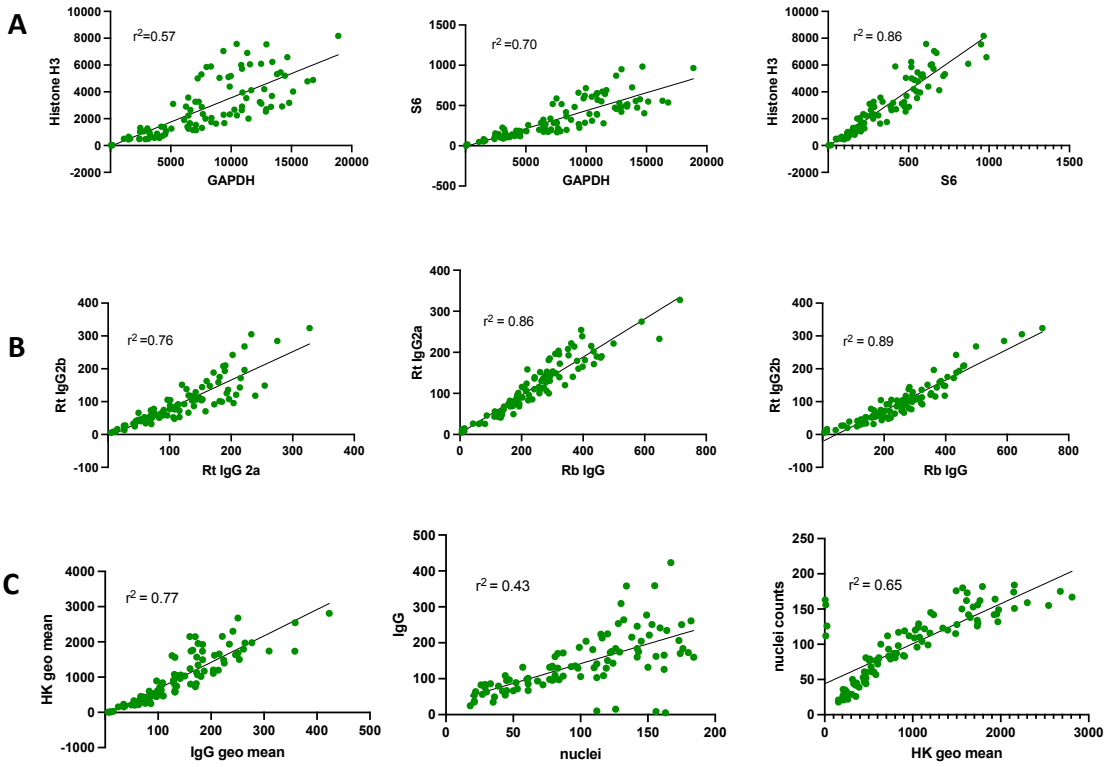
A
Histone H3
GAPDH
r2=0.57
S6
GAPDH
r2 =0.70
Histone H3
S6
r2 = 0.86
B
Rt IgG2b
Rt IgG 2a
r2 =0.76
Rt IgG2a
Rb IgG
r2 = 0.86
Rt IgG2b
Rb IgG
r2 = 0.89
C
HK geo mean
IgG geo mean
r2 = 0.77
IgG
nuclei
r2 = 0.43
nuclei counts
HK geo mean
r2 = 0.65

# Chapter 3

## Sex Influences the Intestinal Inflammatory Response

### *Introduction*

In this chapter we try to characterize the sex-specific intestinal alterations in response to a well characterized model of systemic inflammatory response that uses intraperitoneal lipopolysaccharide (IP-LPS) administration. The introduction is divided in sub-sections, the first two introduce the LPS molecule and its receptor recognition in immune cells. Meanwhile the third sub-section provides information on current models of IP-LPS that investigated sex-alterations. The forth sub-section explores the idea that metabolic changes are intertwined with alterations with immune responses, which is important to understand the metabolic changes we present later in the results section of this chapter. The fifth section introduces the intestinal tissue, and its relationship to metabolism, inflammation and sex, illustrating why we chose to focus in this tissue in our models.

#### Lipopolysaccharide structure

Lipopolysaccharide (LPS) administration is a well characterized model to study systemic inflammatory responses in animal models. LPS is an endotoxin present in gram-negative bacteria and consists of 3 regions: a lipid A region, anchored to the cellular membrane; a core oligosaccharide structure; and a polysaccharide chain denominated the O-antigen (Erridge, Bennett-Guerrero and Poxton, 2002). This well conserved structure, varies from species to species of bacteria, with changes in the composition of the polysaccharide chain

of the O-antigen and the core, being most prevalent (Lerouge and Vanderleyden, 2002), but alterations in lipid-A region have also been found (Migale *et al.*, 2015). This heterogeneity in LPS exists even in bacteria of the same species, if we use pathogenic *Escherichia coli* as an example, the LPS composition varies from different strains and each variation receives a unique name such as O55:B5 LPS, O111:B4 LPS and O127:B8 LPS, among others (Nedrebø and Reed, 2002).

As discussed before, the immune system is able to recognize evolutionary conserved pathogenic molecular patterns, and despite the alterations in serotype composition of LPS, all forms of LPS bind and activate TLR-4. That is not to say that are no alterations in its response, as different serotypes of pathogenic *E. coli* LPS have shown different lethal dosages (Nedrebø and Reed, 2002), different inflammatory mediator responses (Migale *et al.*, 2015), and a difference in symptoms (Pieterse *et al.*, 2016; Anhê *et al.*, 2021). The lethal dosage of O127:B8 is 10mg/kg while the lethal dosage for O111:B4 is half that dose: 4.9mg/kg (Nedrebø and Reed, 2002). Cytokine wise, the different serotypes O55:B6, O127:B8 and O111:B4 had differences in levels of mmp3, IL6 and COX2, and the serotype O111:B4 activated c-jun signaling cascade more strongly than the others (Migale *et al.*, 2015). Not surprisingly, given the altered responses of the animals to these strains, their symptomatic presentation also differs: O127:B8 increases albumin extravasation in a variety of tissues, with a most drastic effect in small intestine, while serotype O111:B4 does not.

As mentioned, the differences in strain response are not associated with a difference in receptor recognition: TLR-4 knockout mice do not respond to LPS, regardless of strain

used (*LPS from E. coli, Serotype O55:B5 (TLRGRADE®) (Ready-to-Use)*, 2022)Then what explains the drastic difference in animal response to strains of LPS pertaining to a same bacterial species? It is possible that the differences in LPS structure in the different strains cause a different interaction between LPS and the TLR4 receptor. This would activate different signaling cascades of TLR-4 and elicit a different cytokine response, a hypothesis supported by other researchers in the field (Migale *et al.*, 2015). In fact, removal of a polysaccharide side chains and acyl groups from the lipid A structure of LPS drastically decreases the TLR4 mediated pro-inflammatory response (Mata-Haro *et al.*, 2007).

LPS and TLR4 receptor activation

The TLR4 receptor uses adaptor protein CD14 and LBP to help with LPS recognition. Because of the lipophobic nature of LPS, the molecule aggregates and form micelles, which are harder to recognize by the immune cells. Therefore, LBP binds to LPS and monomerizes the molecule, presenting it to CD14, which then transfers it to TLR4 receptors (Jiang *et al.*, 2005; Płóciennikowska *et al.*, 2015). Upon recognition of LPS, TLR4 receptor dimerizes, and a signaling cascade is initiated in its cytosolic domain. The myeloid differentiating factor 88 (Myd88) is recruited to the receptor, associating with Mal and generating the TIRAP assembly. By then IRAK kinases assemble together with TIRAP in a complex to further continue the signaling cascade, activating TRAF-6 and culminating with NF-κB and AP-1 activation (Park and Lee, 2013). These transcription factors are responsible for pro-inflammatory cytokine production. NF-κB produces TNF-α, IL-6 and

iNOS (Schreiber *et al.*, 2006); AP-1 activates IL-8, RANTES and COX-2. TLR-4 can also generate a Myd88 independent signaling cascade, in which TRIF is recruited and activated. This pathway then produces and secretes interferon type-I proteins, via IRF-3, and is usually associated when the TLR-4 receptor and its ligand are endocytosed (Figure 3.1).

Activation of TLR4 serves two different purposes: initiate the pro-inflammatory cascade to alert the vicinity cells of a bacterial pathogen and drive appropriate recruitment of immune cells; and to up-regulate the phagocytic capability of myeloid cells to actively engulf and digest the bacterial pathogen.

When LPS is administered intraperitoneally (IP), the first cells to recognize the molecules are peritoneal macrophages. Activation of TLR receptor in those cells secrete pro-inflammatory cytokines that travel the blood and influence other organs. At the same time, depending on LPS concentration, the increase in permeability facilitates LPS to travel via blood vessels and then LPS itself affect other tissues, including the intestine. Even though TLR4 is primarily expressed by immune cells, other non-immune cells also express this receptor. In jejunum tissue for example, this expression is very high in intestinal epithelial cells (Dheer *et al.*, 2016) and on sensory nerve fibers (Barajon *et al.*, 2009). On lung tissue, TLR4 is highly expressed in nociceptor fibers (Hiroki *et al.*, 2021). And non-classical activation of TLR-4 receptors can both contribute to immune responses or signal the brain the occurrence of an immune response (Maruyama, 2022).

Sex affects the IP-LPS response

Peritoneal macrophages have a difference in number between males and females: females have an increased total amount of cells in the peritoneal cavity, which reflects in a higher macrophage, T cell and B cell population than males (Scotland *et al.*, 2011). This is also reflected on a baseline increased expression of several chemokines: cxcl1, ccl2, cxcl12, ccl5, and TLR receptors: TLR2, TLR3, TLR4 (Scotland *et al.*, 2011). When isolated peritoneal macrophages are treated with zymosan, a yeast cell wall particle, females engulf more efficiently the molecule than males (Scotland *et al.*, 2011), evidence reproduced by different treatments (Spitzer, 1999). This suggests that female macrophages have a higher phagocytic capacity than macrophages in male mice, an idea supported by many authors (Wilkinson *et al.*, 2022). With this amount of evidence supporting a strong innate immune response, one would hypothesize that the inflammatory response in female peritoneal cavity would be stronger or more robust than males. However, that is not what happens: after *in vitro* LPS treatment to peritoneal macrophages, males and females have similar levels of TNFα, IL6, ccl2 and TGF-β production (Scotland *et al.*, 2011). Many different works started to characterize the inflammatory response to IP-LPS in males and females. Data from different models support the idea that females have a higher phagocytic capability than males (Weinstein, Ran and Segal, 1984; Spitzer, 1999) although it is still unclear which sex responds with a stronger pro-inflammatory release.

In a work published as a pre-print in 2023, 2hrs after IP-LPS (O111:B4, 0.25mg/kg) males and females secreted similar levels of IL-1β, IL6 and TNFα, but females had a higher secretion of ccl3, ccl4, cxcl2 in plasma; while males had a higher increase of cxcl10 and

ccl5 than females (Finnell, Speirs and Tronson, 2023). At 24h timepoint all increased circulating proteins returned to baseline levels. This suggests that in models using a single administration of a low dose IP-LPS, there is a very transient effect in cytokine and chemokine release, and a very rapid return to homeostasis despite of sex.

In another investigation, IP-LPS (O111:B4, 0.3mg/kg) caused a more robust effect in female mice. Females had higher plasma levels of almost all cytokines and chemokines investigated, including IL-1β, IL6, TNFα, IL-10 among others (Nonoguchi *et al.*, 2022) at 6hr timepoint. This difference in susceptibility cannot be explained by mouse strain or bacterial strain and external factors that drive sex-response remains to be discovered.

Despite this controversy, a lot of papers cite that males have a stronger TLR4 response to IP-LPS. This data is based on analysis of sickness behavior in mice, where males are more affected by the same IP-LPS dose (Cai *et al.*, 2016); on papers that do show males with higher response to IP-LPS, which are present in the literature (Deny *et al.*, 2022); and data on human cohorts.

Data obtained from LPS exposure in men and women does show that circulating levels of cytokines are higher in men after LPS challenge. 1ug/mL of LPS elicits an increased male response of TNFα only (Aulock *et al.*, 2006), fact supported and reproduced by bigger cohorts (Ter Horst *et al.*, 2016). While no differences are found in IL-10, IFNγ nor IL6 response between sexes (Aulock *et al.*, 2006; Ter Horst *et al.*, 2016).

Regardless of the susceptibility controversy, there is a very strong consensus in the field that sex influences the immune response, disease susceptibility and IP-LPS regulation.

Metabolism changes are associated with changes in immune response

Immune cells after recognizing molecular patterns and activating signaling cascades to produce a pro-inflammatory response are now posed with the challenge of increasing protein synthesis and proliferating. Those activities are extremely metabolic demanding. Therefore, during the normal course of an immune response, cells change their preferential metabolic source to glycolysis to be able to quickly undergo the necessary changes and mount a proper immune response. This has a variety of consequences for immune cells.

Macrophages first upregulate GLUT1 expression to increase glucose absorption (Freemerman *et al.*, 2014). Second, they start aerobic glycolysis producing lactate from pyruvate, instead of allowing pyruvate to go to the TCA cycle (Figure 3.2). The change to aerobic glycolysis is orchestrated by hypoxia inducible factor-α (HIF1-α) after mTOR activation, HIF1-α upregulates genes that will change the metabolic dependency to glycolysis by preventing pyruvate from entering the TCA cycle, such as lactate dehydrogenase A (LDHA), phosphoinositide-dependent kinase-1 (PDK1) (Figure 3.2). LDHA increases the use of pyruvate for lactate production, while PDK1 inhibits the use of pyruvate the in TCA cycle, thus reducing oxidative mitochondrial dependency during an immune response, while upregulating glycolysis (Kelly and O'Neill, 2015).

LPS upregulation of mTOR consequently increases ccl2 activation to recruit blood monocytes to tissue (Ribeiro *et al.*, 2018), as well as decreases ccr7 expression, preventing dendritic cells to migrate outside of resident tissue and recruit adaptive immune cells (Jang *et al.*, 2006).

Metabolism than, not only affects the immune response of innate cells, but also how they interact with adaptive immune cells, programming the whole immune response. In tumor environments, macrophages and dendritic cells also up-regulate an enzyme called indole-amine 2,3-dioxygenase (IDO). This enzyme is responsible for dictating tryptophan catabolism, and production of kynurenine metabolite. Since tryptophan is an essential amino acid for T cells, decreases in tryptophan inhibit T cell response in these microenvironments (Munn *et al.*, 1999). In a model of study of innate immunity, these tryptophan/kynurenine shifts can occur early (24hrs), and could be a predictor of later adaptive response, but not an indicator of adaptive immune regulation since recruited adaptive immune cells would only influence tissue around 5-7 days after PAMP encounter. During LPS response, the shutdown of the TCA cycle with an up-regulation of glycolysis also has an implication to the reactive oxygen species generation. Since pyruvate is primarily prevented from coming into the TCA to allow electron transport chain to happen, LPS can elicit a reverse transportation of electrons through this pathway (Mills *et al.*, 2016). This reverse flow counter oxidative phosphorylation and promotes the production of ROS, this stabilizes HIF-1α and culminates with *il1b* production (Mills *et al.*, 2016). However, the role of oxidative phosphorylation in the inflammatory response to LPS is dual. LPS signaling also increases production of itaconate metabolite, which disrupts TCA cycle and the electron transport chain, at the same time it acts as a major down-regulator of the inflammatory response suppressing a number of pro-inflammatory genes (Lampropoulou *et al.*, 2016). This highlights the fact that immunity is tightly regulated,

and metabolism supports this regulation even in a microenvironment that favors a highly characterized pro-inflammatory response in the presence of LPS.

During periods of decrease glucose availability, the cells might start to use fatty acids as a metabolic source to fuel the TCA cycle and continue energy production. This phenomenon is called fatty acid oxidation. During immune responses, this mechanism has been proposed to aid in tissue repair, by changing macrophage gene expression to produce anti-inflammatory genes, and affecting the genome landscape with epigenetic modifications in histones (Vats *et al.*, 2006). However, simply preventing fatty acid oxidation has contradictory results in inhibits this macrophage role (Van den Bossche and van der Windt, 2018). It is possible the fatty acid oxidation is a consequence of tissue repair, not a requirement, but more data is necessary to draw a conclusion on this subject. Nonetheless, the anabolic role of fatty acid metabolism: fatty acid synthesis, has been shown to be necessary for proper pro-inflammatory responses in a variety of works, as reviewed (Stunault *et al.*, 2018). The gene responsible for driving fatty acid synthesis *ascl*, decreases TNFα, IL-1β and CCL2 expression when deleted (Kanter *et al.*, 2012).

Glutamine is the most available amino acid in the human body and is used in several metabolic processes during inflammatory responses. Immune cells use glutamine at high rates during cellular division, as a precursor for nucleotide synthesis (Cruzat *et al.*, 2018). Degradation of glutamine produces pyrimidines and purines for both DNA and RNA synthesis (Cruzat *et al.*, 2018). This metabolite seems to be particularly important for macrophages specializing in tissue repair, instead of a potent pro-inflammatory response (Satoh *et al.*, 2010).

Recapitulating, innate immune cells change their metabolism in response to PAMP recognition. During LPS activation of TLR4, glycolysis is up-regulated by HIF-1α, and mitochondrial oxidation is downregulated. Nucleotide and protein synthesis are necessary during this process. Amino acid metabolism regulate both nucleotide and protein synthesis, as well as adaptive immune response. Fatty acid oxidation is associated with tissue repair and an anti-inflammatory response, while fatty acid synthesis is necessary for a pro-inflammatory response.

This response in innate immune cells is not isolated from the tissue they reside; the cells always communicate with each other to further control tissue homeostasis. In the intestinal tissue for example, the intestinal epithelial cells actively communicate with the immune cells and themselves can also generate an immune response by TLR recognition, further contributing to the changes in tissue metabolism.

The Intestine responds to systemic inflammation

The intestinal tissue is composed of a single layer of columnar intestinal epithelial cells that separates the intestinal lumen, filled with organic matter and microorganisms, from the lamina propria, a structure with fenestrated capillaries and a myriad of resident immune cells. The intestine is tightly regulated, as breaches in intestinal permeability affect the intricate balance of the tissue: bacterial molecules from the lumen can now access the lamina propria and elicit a pro-inflammatory response in resident immune cells, and an exacerbated inflammatory response can travel through the blood and become systemic, as well as act in a positive loop to further cause epithelial cell damage and increase

permeability. Therefore, changes in systemic inflammation that increase permeability dysregulate this intricate balance and might create a positive feedback of pro-inflammatory amplification that damages the intestinal epithelium.

To avoid this from happening, the intestinal epithelial cells and innate immune cells have a series of specializations to dampen the immune response and prevent its amplification.

Intestinal epithelial cells are composed of different cell lineages: goblet cells, absorptive enterocytes, enteroendrine-cells and Paneth cells. Goblet cells auxiliate with protection from microorganisms by producing mucus on top of the epithelial cell layer, this produces another barrier that needs to be overcome before contacting the lamina propria. Paneth cells are specialized in the production of anti-microbial peptides. Entero-endocrine cells produce hormones that control intestinal function. Enterocytes have specialized transporters to absorb nutrients, while filtering out unwanted substances. This happens via two distinct mechanisms: first, the epithelial cells express tight junctions that prevent the free passage of molecules between lumen and lamina propria, second, they create an ionic concentration reducing the energy use of this demanding task. For example, glucose absorption happens via the sodium glucose co-transporter 1 (SGLT1), that uses the transportation of sodium, in favor of its gradient, to drive glucose transportation across the epithelium (Röder *et al.*, 2014).

All of these cell types are organized in vili, a strategy to further amplify the absorption of nutrients increasing the surface area of the intestinal organ. The cells all come from the same stem cell population that reside in intestinal crypts and are always dividing. Not surprisingly, the metabolic demands between the two regions are quite different. The stem

cell niche in constant division adopts glycolysis as their main metabolic source to maintain the high rate of division; while the intestinal epithelial cell layer uses mainly mitochondrial oxidation in their cellular functions (Rath and Haller, 2022).

Regardless, the intestinal epithelial cells express toll-like receptors to recognize bacterial molecules (Peterson and Artis, 2014). This is an important role, since the lumen of the intestine has microorganisms that are essential for intestinal function and must be ignored by the immune system, at the same time it provides a route for pathogenic bacteria and virus to induce infection, which must be recognized, and an immune response must be mounted. It seems important than, that immune cells and intestinal epithelial cells have some tolerance to the bacterial molecules they must respond, unlike other organs.

Resident intestinal macrophages have been shown to prevent this amplification of inflammatory response. Upon recognition of a bacterial molecule the cells increase its phagocytic capacity without releasing pro-inflammatory mediators such as nitric oxide, and preventing the negative impacts of an inflammatory response (Smythies *et al.*, 2005). Moreover, in the presence of microbiota released metabolites, macrophages respond with IL-10 production (Kim *et al.*, 2018). Macrophages help preserve the integrity of intestinal epithelial cells, a population cd121b+ stays in close proximity to the epithelial population phagocyte intestine epithelial cells, helping with cell turnover (Kang *et al.*, 2019). When csf1is deleted, a gene that ensures macrophage survival, mice display impaired intestinal epithelial cell differentiation and renewal (Huynh *et al.*, 2013). Macrophages are extremely plastic cells that are influenced by their environment (Yip *et al.*, 2021). Not surprisingly, the heterogeneity of environmental cues in the different specializations of the intestinal

tissue (small and large intestine, vili, crypt-associated, lamina propria) generates a heterogeneity of macrophage cells within each niche (Viola and Boeckxstaens, 2021).

When a inflammatory response in generated, macrophages from outside the intestinal tissue are recruited via a series of chemokine signals: ccl8, ccl2, cxcl9. These monocytes have specialized receptors like CCR2 that recognize these migrating signals and reallocate to the intestinal tissue. This migrating population initially do not possess the same break mechanisms to prevent an exacerbated immune response and only acquire this phenotype over time: they decrease CCR2 expression, increasing CXCR1 and MHCII over the course of 5-6 days. As a consequence, they increase genes associated with phagocytosis, complement pathway and IL10 signaling (De Schepper *et al.*, 2018). The initial migration of immune cells can therefore amplify the pro-inflammatory response.

Since this intricate balance of immune cells and epithelium can be dysregulated with the arrival of cells outside the tissue, mouse models have tried to understand these mechanisms by studying systemic inflammation and its impact in intestinal health, including the use of IP-LPS as a model. To this point we have shown how sex impacts the IP-LPS cytokine response, but there is very little information in the literature about the effect of sex in intestinal permeability to IP-LPS. Small intestine increases epithelial cell apoptosis close to 1.5hrs after a high-dose of IP-LPS, and an increase in intestinal permeability 5hrs later (Williams *et al.*, 2013), but the study was performed in males only.

Diseases with dysregulated inflammatory responses affect intestinal permeability in humans, and are influenced by sex. In Crohn's disease (CD) females have a higher incidence throughout their lifetime. On the other hand, for ulcerative colitis (UC), there

was no sex effect until the age of 45, then males were shown to have a higher incidence of UC (Shah *et al.*, 2018). Other diseases that again have an immune component such as celiac disease also have a higher incidence in women (Jansson-Knodell *et al.*, 2018). Given the epidemiological data it is non-surprising to find differences in intestinal immune response between males and females to change throughout life. Jejunal biopsies of healthy adults shows a sex-difference in their transcriptomic profile. In woman's samples, genes associated with a pro-inflammatory response were upregulated, including ones associated with IL2 and IL1 response. The signaling cascade of activation of NFkB a major orchestrator of inflammation showed upregulation in a series of key genes, among them Myd88, TRAF6, JNK and MAPKp38 (Sankaran-Walters *et al.*, 2013). Regardless of the disease, it seems like sex plays a factor in its susceptibility, a phenomenon not well studied. Moreover, these diseases have very intricate inflammatory responses that are still not completely understood in the light of sex. Using mice models of early IP-LPS administration allows us to understand the innate immune responses early in the inflammatory process, and its sex-specific tissue regulation.

Here, we demonstrate that a model of IP-LPS in mice provides clues into the differences in innate immune response between male and female, and its effect in intestinal function. Females increase jejunum permeability in response to IP-LPS, concomitantly rearranging tight junction claudin-3 and increasing gene expression of chemokines, molecules associated with TLR signaling cascade and pro-inflammation response. Males at the same timepoint do not change permeability in response to IP-LPS. Reduce gene expression of inflammatory mediators including nfkb and increase glucose absorption in jejunum tissue.

Metabolic changes are associated with both male and female jununum. Collectively, the data suggests sex is a major influence in innate immune response to IP-LPS, and differentially impacts jejunum health with a greater susceptibility in females at 24hrs.

## *Results*

Intestinal permeability is increased in females but not male jejunum

To understand the effects of systemic inflammation in the intestinal response during innate immunity, male and female C57Bl/6J mice were injected with IP-LPS and jejunal intestinal tissue was collected 24hrs later. Jejunum was then added to using chamber for an *ex vivo* assessment of intestinal permeability as previously described (Chen *et al.*, 2020). Female mice had a significant decrease in transepithelial resistance (TEER) after IP-LPS, while male jejunum did not (Figure 3.3 A). Only female jejunum showed an increased permeability to 4kDa FITC-dextran in response to IP-LPS (Figure 3.3 B). *Ex vivo* measurements of short circuit current under baseline conditions was stimulated in the female jejunum following in vivo LPS exposure, but not in males (Figure 3.3 C).

Changes in permeability are associated to alterations in tight junction expression (Lee, 2015). We investigated claudin-3 tight junction alterations in our model. Claudin-3 is a tight junction that becomes internalized after an inflammatory response and is associated with changes in TEER in intestinal tissue (Prasad *et al.*, 2005). Female mice internalize claudin-3 tight junction after IP-LPS, while male mice do not (Figure 3.3 D-F).

One of the major functions of the jejunum intestinal segment is the absorption of nutrients. We measured the glucose absorption in *ex vivo* jejunum tissue in our experimental models to see the effect of IP-LPS in intestinal function. The measurement is done indirectly by assessing changes in current after glucose administration as previously described (Overduin *et al.*, 2023). Male jejunum increase glucose associated current after IP-LPS, while female jejunum does not (Figure 3.3 G).

Female jejunum has a robust change in the expression of inflammatory genes while male jejunum does not

Because IP-LPS is shown to increase the inflammatory response, and changes in intestinal permeability are associated with a higher inflammatory response we decided to investigate changes in gene expression of inflammatory genes in jejunum of males and females. For this purpose, the Nanostring Inflammatory gene expression panel was used. This technology allows for the quantification of genes associated with a specific biological function, in this case inflammation, without amplifying gene products. A list of all probes analyzed are available online (*nCounter Mouse Inflammation V2 Panel Gene List*, 2021). 248 genes were assessed in male and female jejunum 24hr after IP-LPS and volcano plots were generated to measure changes in gene expression correcting for multiple comparisons.

Females have a more robust regulation of the inflammatory response, with a higher number of genes up- and downregulated (Figure 3.4 A-E). None of the genes changed between males and females are shared, as sex-brings the most differences to the immune response (Figure 3.4 F). In female jejunum, molecules associated with limiting or inhibiting pro-inflammatory innate immune responses are downregulated (Rps6ka5, Mapk3, Max), while molecules associated with promoting inflammation are downregulated in males (jun, ccl20). Furthermore, the female jejunum robustly upregulates transcription of genes promoting proinflammatory innate immune responses (tlr8, Cxcl9, Cxcl10, hif1a mapk8, Mx2, nod1, stat3), amplifying TLR mediated responses (il6ra, il1rap) as well as

chemokines associated with recruiting blood derived inflammatory monocytes and neutrophils being amongst the molecules showing the most robust upregulation (Ccl2, Ccl8, cxcl9). None of those up-regulated genes are present in the male dataset.

Collectively this data suggests a more robust responsiveness of female jejunum to IP-LPS.

Female jejunum pathway score analysis shows gene expression identity associated with pro-inflammatory response

To further understand the role of gene expression changes, the data was analyzed by pathway scores. In this analysis the genes are grouped into specific biological pathways according to function as described by NanoString (*nCounter Mouse Inflammation V2 Panel Gene List*, 2021), genes with a higher change in gene expression, regardless of direction of regulation, receive a higher score. In this analysis we can differentiate the biological pathways changing the most in our dataset (Figure 3.5 A), allowing an unbiased look into the biological roles of the network of changing genes. The pathway with the most alteration is the cytokine activity pathway, with a global significance score close to 2.5. Immune Response, Innate Immune Response and Inflammatory Response also appear in the list suggesting a tight control of immunity (Figure 3.5 A).

The next pathways with the most amount of change in females are external side of plasma membrane, extracellular space and extracellular region (Figure 3.5 A), suggesting a lot of the up-regulation genes are being secreted to act elsewhere, again suggesting a role in immune cell recruitment.

To further understand how those pathways are altered we generated heatmaps with the identity of genes associated with each pathway. This then allows us to infer directionality of pathway with high scores and infer function (Figure 3.5 B-N), as well as look at variability. The biological replicates pertaining to different groups show a very similar regulation of gene expression (Figure 3.5 B-N).

In females the high scored pathways for immune response mentioned show most genes with an up-regulation, and all these genes participate in the generation of a pro-inflammatory response (Figure 3.5 B, D, I, M). The pathway for cytokine activity shows upregulation of cxcl9 and cxcl10, two chemokines associated with the recruitment of immune cells and with the pathophysiology of dysregulated inflammatory diseases of the small intestine (Ostvik *et al.*, 2013; Zhao *et al.*, 2017).

Despite the alterations showed, the pathway for negative regulation of apoptosis appears in the most changed pathways. Suggesting a role for both hif1a and mapk8 upregulation to prevent apoptosis in our model (Figure 3.5 J).

Collectively, the data shows a robust change in pathways associated with female inflammatory response, and the identity of the genes confirms a profile toward a pro-inflammatory response.

Male pathway score analysis shows similar pathways to females, but downregulated

The same pathway score analysis was performed in males to investigate biological function. Only two pathways show significant regulation in male mice: cytokine activity

and immune response both showing a downregulation of genes as previously discussed (Figure 3.6 A-C).

Gene expression analysis suggests that females have a higher pro-inflammatory response than males; consistent with the jejunum profile observed.

Metabolic analysis of gene expression shows sex-specific regulations of response

Changes in inflammatory response are accompanied by shifts in the metabolic profile of immune cells. Therefore, we investigated gene expression of the metabolic profile of male and female jejunum. To pursue these questions, NanoString metabolic panel was used to assess gene expression in jejunum tissue after IP-LPS in males and females. A list of full genes associated with NanoString metabolic panel is available online (*Mouse Metabolism Panel Gene List*, 2022).

Consistent with previous data, we noticed a different profile of expression between males and females (Figure 3.7 A, B). Female jejunum seems to be more responsive than male jejunum, with an overall robust up-regulation of genes, not present in males. Females shows a log2 fold change that reaches 5, while males fluctuate around 2 (Figure 3.7 C, D). When we look at the identity of these genes once again those associated with a pro-inflammatory immune response and chemokine expression are among the ones with the highest fold change (Figure 3.7 C-G), including cxcl9, a neutrophil chemokine, cd14 a protein that assists with TLR signaling. Non-surprisingly, a lot of genes involved with TLR signaling are also upregulated in females but not in males, including tlr1, traf6, myd88, mapk8 genes (Figure 3.7 H), as observed with the inflammatory panel. Males once again

downregulate most genes, including a major orchestrator of the inflammatory response nfkb (Liu *et al.*, 2017).

Since the changes in inflammatory response are usually accompanied by an increase in in glycolysis as a metabolic source (Stunault *et al.*, 2018). In innate immune cells such as macrophages, this happens via hif1a activation, a transcription factor activated by mTOR signaling that upregulate the glycolytic response (Cheng *et al.*, 2014). We next asked if genes involved with this pathway would be changed in a sex-specific manner. Females do indeed increase expression of hif1a, while males do not (Figure 3.7 H). However, genes associated with the glycolysis pathway show an up- and downregulation in both males and females (Figure 3.7 A-H). Since this is a jejunum gene expression it is possible that different cell types are having different metabolic shifts, and the glycolytic pathway is becoming a preferred metabolic source in some cells but not others, a limitation of our technique.

In conclusion, male and females have a different metabolic shift, again showing a robust upregulation of gene expression in females, but not male jejunum.

Identity of pathways changing in females suggest fatty acid oxidation as the major metabolic source and a tight control in mTOR pathway

Having stablished a very different profile in gene expression between males and females (Figure 3.7 G), and a mixed response in the glycolytic pathway modulation we decided to further explore changes in metabolism between males and females. Once again, the

pathway score analysis from NanoString would offer an unbiased way of understanding which metabolic pathways are having more changes in both sexes.

First, the female pathways were organized in ascending order according to their pathway score (Figure 3.8 A), then the genes associated with each pathway were graphed in a heatmap for analysis of directionality (Figure 3.8 B-AD).

Females show the most change in pathways associated with fatty acid and amino acid metabolism (Figure 3.8 A). Fatty Acid oxidation is the most changed pathway in females, and it is associated with a macrophage production of anti-inflammatory cytokines (Vats *et al.*, 2006). Since fatty acid is the most changed pathway, we also analyzed the individual genes associated with the pathway to understand the directionality of fatty acid oxidation (Figure 3.8 B), again there is a mixed response in its directionality, genes associated with an increase in fatty acid oxidation such as acadl and acat1 are respectively up- and downregulated in females suggesting a cell specific response that modulates this pathway. At the same time, the majority of genes that drive fatty acid oxidation acat1, acox1, hadh, ehhadh are downregulated, suggesting that even with cellular heterogeneity the pathway is shifting toward downregulation after IP-LPS (Figure 3.8 B).

For metabolic changes in amino acid usage, several pathways show a major regulation after IP-LPS in females: tryptophan/kynurenine pathway, glutamine metabolism, amino acid synthesis and amino acid transporters. Amino acid synthesis is necessary for production of proteins during inflammation and resolution, but both synthesis and catabolism of proteins are among the most changed pathways, again suggesting a mixed tissue response and a cell specific directionality of amino acid pathways. Confirming this hypothesis once more, all

pathways mentioned above have an up-regulation and downregulation of gene expression after IP-LPS administration, suggesting a concomitant activation and repression of these pathways that could be a confounding factor of whole tissue analysis (Figure 3.8 A-H).

mTOR and AKT/PI3K pathway are orchestrators of this change in metabolism and are activated by TLR signaling (Ribeiro *et al.*, 2018). mTOR appears among the most changed pathway is females with a tight regulation of response with a big change in gene expression (Figure 3.8 G). Again, genes show both an up- and downregulation, suggesting a mixed tissue response. However, just like fatty acid oxidation, most genes associated with an activation of mTOR pathway are up-regulated, this includes akt1, akt2, prkaa2, prkab1 braf and fnip2, which could suggest an overall positive regulation of the pathway in female jejunum after IP-LPS, but more experiments would be necessary to confirm this hypothesis.

Collectively, the data shows a dramatic shift in major metabolic sources in females including mTOR pathway, as well as amino acid and fatty acid dependent regulation.

Male jejunum metabolism shows a different profile than that of the female

The same pathway analysis was performed in male jejunum for comparison of its metabolic shifts after IP-LPS. Initial analysis shows that both mTOR and fatty acid metabolism that appear as the most regulated ones in females (Figure 3.8) do not show up in male jejunum regulation. Instead, mitochondrial respiration is one of the metabolic pathways showing most regulation and most genes associated with pathway activation are downregulated (Figrue 3.9 A-J). This suggests male jejunum prefers to shift its metabolism toward a

decrease dependency in mitochondrial respiration, a different regulation than female jejunum.

Again, strikingly, male jejunum exclusively shows 2 interesting pathways most highly regulated, that are involved with changes in inflammatory response: reactive oxygen species and c-myc. Reactive Oxygen Species are usually a preferred change in metabolism to drive the destruction of pathogenic bacteria during a pro-inflammatory immune response (Mills *et al.*, 2016). This pathway can also cause damage to tissues, including jejunum epithelial cells, contributing to the detrimental effects of an inflammatory response (Farré *et al.*, 2020). In male jejunum this pathway shows a great modulation, with most genes showing a downregulation (Figure 3.9 B).

c-myc on the other hand is a pathway that can be active by TLR response independent of hif1a (Lee *et al.*, 2010). This pathway that is exclusively regulated in males, shows an overall downregulation after IP-LPS at the 24h timepoint (Figure 3.9 D).

Collectively, the pathway analysis has shown a sex-specific metabolism shift after IP-LPS, which in males is characterized by changes in mitochondrial respiration, reactive oxygen species and c-myc.

## *Discussion*

This third chapter of my dissertation proposes the following hypothesis: that male and female mice have different innate immune responses in the intestinal tissue. This is not a new idea, throughout the years many different authors have proposed the fact that immunity is influenced by sex (Wilkinson *et al.*, 2022). Dendritic cells, macrophages, neutrophils have differences in number and expression of TLR receptors. Females present a higher amount of peritoneal macrophages, with a more efficient phagocytic response to pathogenic and non-pathogenic stimuli, and a higher expression of TLR receptors at baseline levels than males (Scotland *et al.*, 2011). Activation of TLR receptors 8, 7 and 9 elicit stronger responses in female innate immune cells (Torcia *et al.*, 2012; Griesbeck *et al.*, 2015).

For TLR4 however, the receptor that recognizes LPS, there is a mixed response in the literature of sex-specific effects. Male macrophages produce higher levels of CXCL10 than females, while females produce higher levels of prostaglandin (PGE2) (Torcia *et al.*, 2012). Early in the response to LPS males have higher circulating TNFα levels (Card *et al.*, 2006; Sylvia and Demas, 2018), while females present higher levels of CCL1, IL10, IL-5 around 28hrs post IP-LPS (Erickson *et al.*, 2018). This effect is corroborated by data obtained from humans, as an ex vivo LPS challenge can produce higher circulating cytokines in males than females including TNFα, IL6, IL-1β and IFNγ (Ter Horst *et al.*, 2016), the classical cytokines responsible for a series of systemic effects that culminate in sickness behavior (Dantzer *et al.*, 2008).

However, this sex-specific effect in circulatory cytokines still needs to be further explored in different tissues. In the intestine, innate immune cells have been shown to inhibit the response to LPS (Nakata *et al.*, 2006). Moreover, the LPS not necessarily reaches the intestinal tissue. The intraperitoneal LPS administration is first recognized by peritoneal macrophages and it is more likely that peritoneal macrophages started the response and intestinal macrophages responded to the TNFα or other pro-inflammatory cytokines produced, than responding to LPS itself. The question then remains: how can the systemic immune response to a high dose of IP-LPS influence sex-specific jejunum function? And how does that affect resident tissue innate immune response and its metabolic shift?

Here, we show that in contrast to the systemic response reported in other studies, the jejunum tissue has a stronger effect in female. Females show an increase in tissue permeability 24hrs after IP-LPS, while males do not. The comparison of sex-specific permeability changes is not entirely understood and very little studied. A recent pre-print has tried to understand the changes in jejunum permeability to different stimuli (Doney *et al.*, 2023). Using IP-LPS (O127:B8, 0.83mg/kg) they showed a decrease in tight junction expression in male jejunum only, suggesting male jejunum to be more susceptible to IP-LPS, as an apparent contrast to what was shown here with LPS (O55:B5, 5mg/kg).

The data from this preprint combined to the experiments here suggest a couple of interesting ideas about jejunum function in response to inflammation. First, it suggests that the use of different strains and its TLR-4 changes in ligand interaction, affect sex-susceptibility of response. In fact, LPS isolated from different strains increase different sets of pro-inflammatory cytokines (Migale *et al.*, 2015). Therefore, this opens the possibility

that sex-effects are mediated by the activation of different signaling cascades in different immune cells and depend on receptor-ligand interaction.

The same pre-print that showed male susceptibility to IP-LPS (Doney *et al.*, 2023), also shows a shift in sex-susceptibility when the inflammatory stimuli is changed to a stress paradigm: female jejunum shows a decrease in tight junction expression that is not seen in male mice. This data only strengths the idea that the concentration of stimuli, or specificity of receptor recognition, shifts the sex-specific susceptibility.

In our study, disorganization in claudin-3 tight junction is shown in female, but not male jejunum. Claudin-3 has been shown to become internalized in response to an inflammatory response (Doney *et al.*, 2023). And gene expression analysis obtained from nanostring panels in our data show a more robust up-regulation of genes involved with a pro-inflammatory immune response in female jejunum only.

All TLR receptors from TLR1-TLR9 are investigated in this Nanostring inflammatory panel. TLR expression is usually induced after activation in a positive feedback mechanism to amplify recognition of ligand (Krivan *et al.*, 2019). Strikingly, TLR4 receptor does not increase expression after IP-LPS exposure in our animals, suggesting the receptor was not the one eliciting the inflammatory response of the tissue at the 24hr timepoint. This corroborates with the idea that jejunum innate immune cells are responding to factors released from peritoneal macrophages, and not recognizing LPS themselves. Further experiments are necessary to confirm this hypothesis.

Among all TLR genes, only TLR1 and TLR8 are up-regulated (Figure 3.4 and 3.5). TLR8 up-regulation has been associated with female ulcerative colitis and Crohn's disease

mucosal inflammation (Saruta *et al.*, 2009), this provides a mechanism in which female innate immunity influences IBD. Moreover, TLR8 activation is associated with an enhancement of classical cytokines TNFα, IL6 and IL-1β (Moen *et al.*, 2019), and its expression is localized to the X chromosome (Jaillon, Berthenet and Garlanda, 2019). TLR1 forms heterodimers with TLR2 receptors to recognize bacterial molecules, specifically it has been shown to induce a response to lipoprotein, but not essential for LPS mediated response (Takeda and Akira, 2005). In intestinal function TLR1 activation decreases the inflammatory response (Kamdar *et al.*, 2016).

Genes associated with a downstream signaling activation of TLRs and cytokine receptors are also upregulated in females only: Myd88, traf6, mapk8, suggestive of a myd-88 dependent activation instead of TRIF dependent. MAPK8 transcribes JNK, a major signaling mechanism that increases chemokine expression and in intestinal tissue is associated with changes in barrier function (Zhou and Boutros, 2020). The increase expression of chemokines ccl2, ccl8 attract monocytes from circulation, and increase in cxcl9 attracts T cells (Zimmerman *et al.*, 2008). This could lead to two different outcomes that are not mutually exclusive: the initial inflammatory response is amplified by the migration of immune cells; or the immune cells start resolving the inflammatory response and engaging with tissue repair.

In contrast to this female response, males downregulate nfkb expression. Together with the fact that males do not upregulate pro-inflammatory genes, signaling cascades nor chemokines, it makes a compelling case that males are downregulating the jejunum pro-inflammatory response. Consistent with a lack of intestinal permeability changes after IP-

LPS. That is not to say that the jejunum at this time-point is unresponsive to IP-LPS. Males have an increase in glucose transportation after LPS exposure.

Intestinal epithelial cells, as mentioned before, have polarity with an apical side facing the lumen and a basolateral side, facing the lamina propria. The apical side expresses a Na+-glucose co-transporter (SGLT1), that uses a sodium symport mechanism to also transport glucose inside the lumen against its concentration gradient. Therefore, measuring increases in current in using chambers are used as an indirect method to assess glucose transportation, as previously described (Clarke, 2009). This has its own disadvantage, since other molecules can influence ionic distribution and could indirectly affect glucose transportation, including claudins, such as claudin-15 (Rosenthal *et al.*, 2020), and $Na^+/K^+$-ATPase (Thorsen, Drengstig and Ruoff, 2014). Measuring SGLT1 levels would be a first step in determining whether this glucose transporter transduces in an increased glucose transportation in males only. In fact, an increase in SGLT-1 mediated glucose uptake protects intestinal epithelial cells against LPS mediated cell death (Yu, Turner and Buret, 2006), by increasing crypt cellular proliferation (Zhou *et al.*, 2018). This could be a possible mechanism used by males to prevent changes in intestinal permeability.

Both the change in inflammatory profile of immune cells in female jejunum, and the increased glucose absorption in male jejunum suggested that metabolic changes in the tissue would take place. Moreover, this difference in intestinal response by sex suggests the metabolic changes are also sex-specific.

Female jejunum had among the most regulated pathways are fatty acid oxidation, tryptophan/kynurenine metabolism, glutamine metabolism. All of which are not associated

with a TLR4 pro-inflammatory activation (van Teijlingen Bakker *et al.*, 2022), and the genes associated with theses pathways are majoritarily downregulated in our model. In intestinal tissue the microbiota population produces short-chain fatty acid lipids that undergo lipid oxidation a main source of epithelium metabolism fueling the TCA cycle (Donohoe *et al.*, 2011; Smith *et al.*, 2021).

Hypoxia, mTOR and amino acid synthesis also show very high scores within the pathway analysis. Hypoxia and mTOR pathways are controlled by a pro-inflammatory immune response, activating akt, hif1a signaling cascades; for these pathways most genes are showing an upregulation. Consistent with these, most pathways being regulated in female mice are also inflammation pathways: cytokine and chemokine signaling, reactive oxygen response, TLR signaling, endocytosis, NFκB and antigen presentation. However, despite this profile, glycolysis pathway does not seem to be changing very significantly, nor protein synthesis, which are contradictory to the idea of an innate immunity pro-inflammatory response. Moreover, the genes in each of those pathways have contrasting responses, as genes that both activate and inhibit a specific biological function are being regulated in similar direction. This opens up the possibility that different cells are acquiring different metabolic phenotypes, causing the data to have mixed results, a disadvantage of our whole tissue gene expression analysis.

In fact, intestinal epithelial cells themselves have many different cellular compositions, with different functions and contrasting metabolic responses, which could explain in part the data obtained. For example, crypt cells have a stem cell niche and rely on glycolysis to be constant dividing (Rath and Haller, 2022), which could hinder the glycolytic alterations

in immune cells from being detected. Moreover, differentiation and maturation of these stem cells into intestinal epithelial cells rely heavily on mitochondrial respiration (Zhou *et al.*, 2018), again contributing for our apparently contradictory data.

In males on the other hand, the most regulated pathways are reactive oxygen response, mitochondrial respiration and c-myc. First, none of the pathways acquire as high score as the females, showing that the regulation in response to LPS are not as substantial. Second, those pathways show a downregulation of response, again highlighting how mixed the intestinal metabolic profile is, as reactive oxygen species are usually up-regulated during inflammation, while mitochondrial respiration are usually downregulated.

Collectively, the data suggests the jejunum intestinal response in females is more pro-inflammatory than males, even to LPS-TLR4 ligand, a classically described signaling that elicits a higher circulating pro-inflammatory response in males.

*Figures and Legends*

**Figure 3.1. LPS elicits two different signaling cascades, one Myd88 dependent, the other Myd88 independent, and activates PI3K and mTOR pathways**
TLR-4 activates myd88 and culminates with TRAF-6 activation that will in turn activate two different pro-inflammatory transcription factors: NF-κB and AP-1. On the other hand it is capable of activating TRIF and TRAF-3, which in turn will activate IRF-3 and initiate interferon genes transcriptions. Image generated and adapted from Biorender.

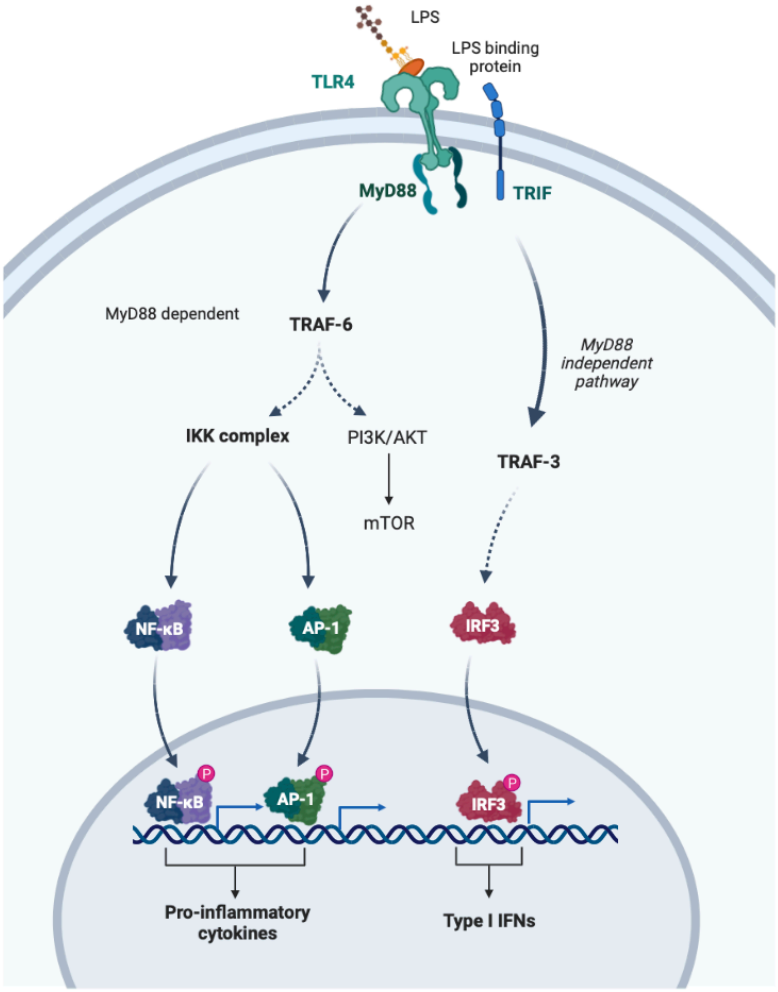

**Figure 3.2. HIF1α elicits a series of metabolic changes within the cell to fuel protein and nucleotide synthesis necessary during an immune response**
TLR-4 and cytokine activation can increase PI3K and AKT pathways that in turn activate mTOR. mTOR then is responsible for increasing ccl2 production and release; and activate HIF1α. HIF1α acts as a transcription factor that activates protein synthesis and nucleotide synthesis and changes the metabolic profile toward glycolysis, inhibiting mitochondrial respiration. HIF1α increases the insertion of GLUT1 glucose transporter to cell membrane, increases PDK1 and LDHA expression, which will respectively prevent pyruvate from entering the TCA cycle and increase the usage of pyruvate in lactate production. In green: positive alterations driven by HIF, red arrows represent inhibition or decreased function. Image generated and adapted from biorender.

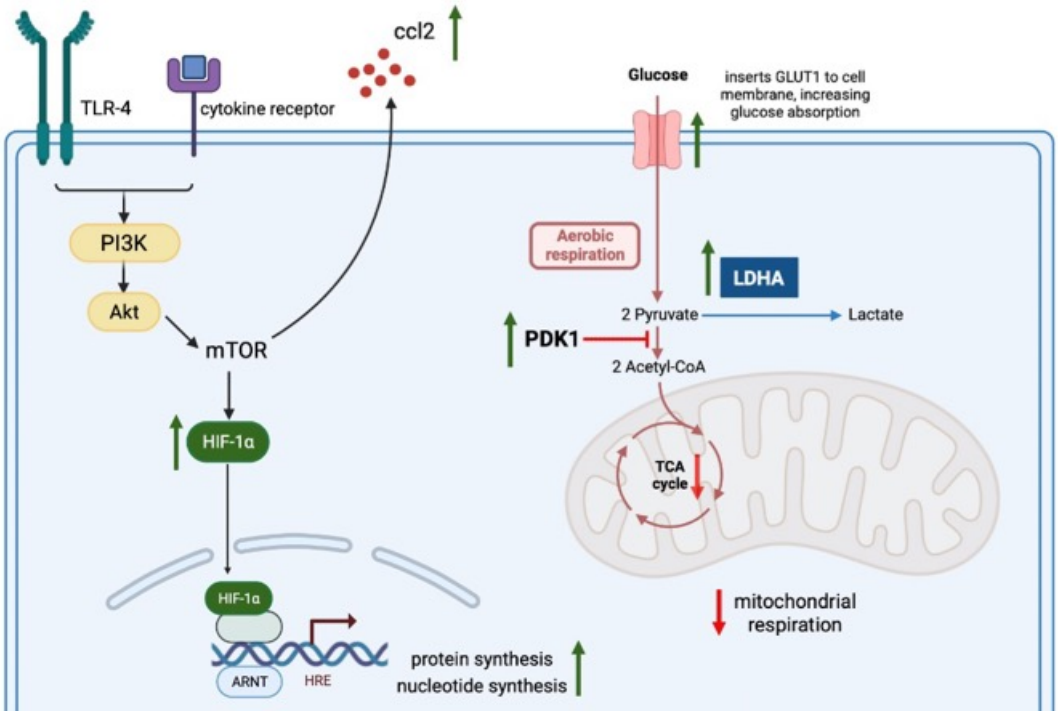

**Figure 3.3 IP-LPS increases female jejunum permeability and male glucose absorption**
**A –**Ussing chamber transepithelial resistance (TEER) of jejunum in WT naive and 24h after IP-LPS in male and female mice. n=WT F (6), WT+LPS F (5), WT M (6), WT+LPS M (6) mice, total jejunum segments.
**B –** 4kDa dextran FITC-conjugated permeability in jejunum of male and female WT naive and 24h after IP-LPS mice. n=WT F (5), WT+LPS F(5), WT M(6), WT+LPS M (6) mice.
**C –** Current at rest in jejunum of male and female mice WT naïve and 24h after IP-LPS n=WT F (7), WT+LPS F(5), WT M(5), WT+LPS M (6) mice, total jejunum segments.
**D –** zoom of 63X representative images for jejunum vili of WT naive and 24h after IP-LPS. Green represents claudin-3 (cld3), white arrows represent internalized cld3 puncta. Scale bar 5μm.
**E, F –** Total internalized claudin-3 puncta per cell per animal in females (E) and males F).
G – Peak of current after glucose in lumen of male and female jejunum WT naive and 24h after IP-LPS. n=WT F (6), WT+LPS F (5), WT M (5), WT+LPS M (6) mice, total jejunum segments).
Data showed as mean ± SEM, analyzed with unpaired one-tailed t-test (E and F), or one-way ANOVA, Tukey multiple comparison analysis post-test (**A-C, G**). *$p<0.05$, **$p<0.01$, ****$p<0.0001$.

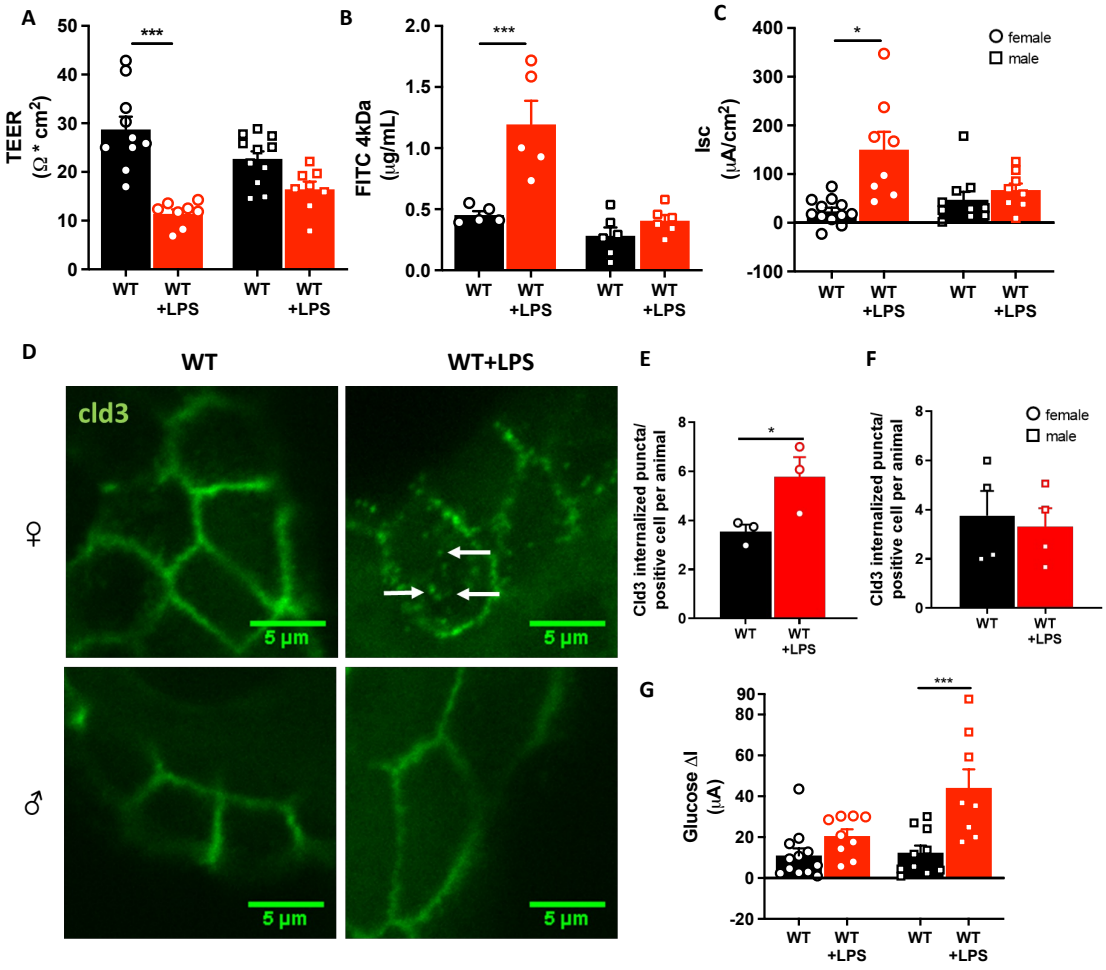
A
TEER
(Ω * cm²)
***
WT
WT +LPS
WT
WT +LPS
B
FITC 4kDa
(μg/mL)
***
C
Isc
(μA/cm²)
*
female
male
D
WT
WT+LPS
cld3
5 μm
♀
♂
E
Cld3 internalized puncta/ positive cell per animal
*
F
Cld3 internalized puncta/ positive cell per animal
female
male
G
Glucose ΔI
(μA)
***

**Figure 3.4 – LPS changes gene expression in both males and females, with females showing a greater upregulation of inflammatory genes**

**A,D** – NanoString inflammatory panel Volcano plot analysis of differentially regulated gene expression in response to inflammation in females (A) and males (E). Red represents significantly upregulated genes and blue represents significantly downregulated genes with p-value adjusted to multiple comparisons by Benjamin-Yekutieli method. n=3 animals per group

**B, C, F, G** – Fold change and adj.p-value of genes from volcano plot analysis in females (B, C) and males (F, G).

**D, H** – Venn Diagram of genes changing in both males and females in response to IP-LPS. Females significantly downregulated and upregulated genes are displayed in grey; males significantly downregulated and upregulated genes are displayed in green.

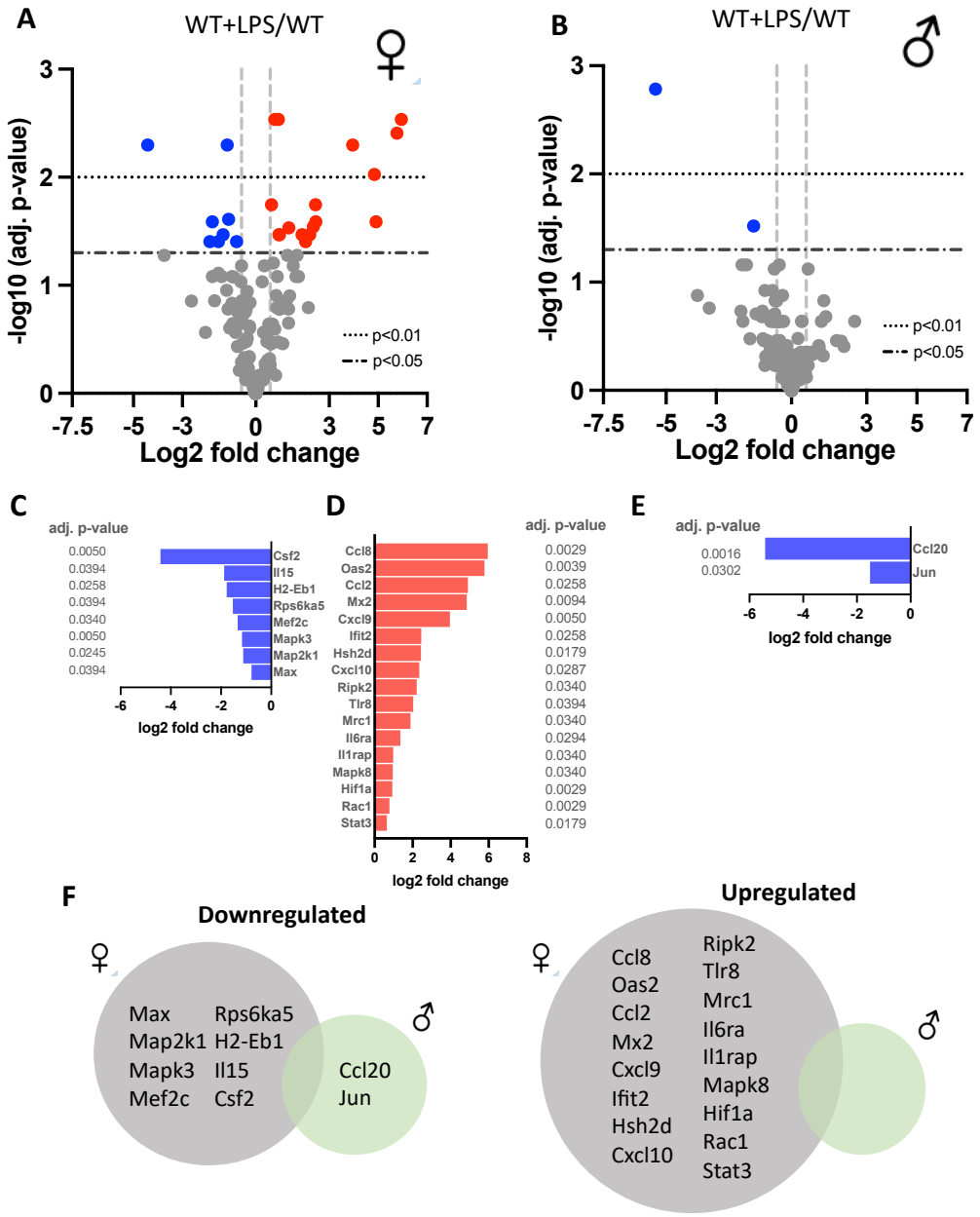
A
WT+LPS/WT
♀
-log10 (adj. p-value)
Log2 fold change
p<0.01
p<0.05
B
WT+LPS/WT
♂
-log10 (adj. p-value)
Log2 fold change
p<0.01
p<0.05
C
adj. p-value
0.0050
0.0394
0.0258
0.0394
0.0340
0.0050
0.0245
0.0394
Csf2
Il15
H2-Eb1
Rps6ka5
Mef2c
Mapk3
Map2k1
Max
log2 fold change
D
adj. p-value
0.0029
0.0039
0.0258
0.0094
0.0050
0.0258
0.0179
0.0287
0.0340
0.0394
0.0340
0.0294
0.0340
0.0340
0.0029
0.0029
0.0179
Ccl8
Oas2
Ccl2
Mx2
Cxcl9
Ifit2
Hsh2d
Cxcl10
Ripk2
Tlr8
Mrc1
Il6ra
Il1rap
Mapk8
Hif1a
Rac1
Stat3
log2 fold change
E
adj. p-value
0.0016
0.0302
Ccl20
Jun
log2 fold change
F
Downregulated
♀
Max
Map2k1
Mapk3
Mef2c
Rps6ka5
H2-Eb1
Il15
Csf2
♂
Ccl20
Jun
Upregulated
♀
Ccl8
Oas2
Ccl2
Mx2
Cxcl9
Ifit2
Hsh2d
Cxcl10
Ripk2
Tlr8
Mrc1
Il6ra
Il1rap
Mapk8
Hif1a
Rac1
Stat3
♂

**Figure 3.5 NanoString Inflammatory biological pathways impacted by IP-LPS in female jejunum**

**A** – List of Pathway Global Significance Scores in NanoString Inflammatory cartridge panel. Only pathways with a higher score than 2 are included in analysis. Global significance scores are calculated based on the sum of the combined t-tests of differentially expressed genes in each pathway. N=3 per group

**B-N** – Pathways showing all genes z-scores per sample before and after IP-LPS

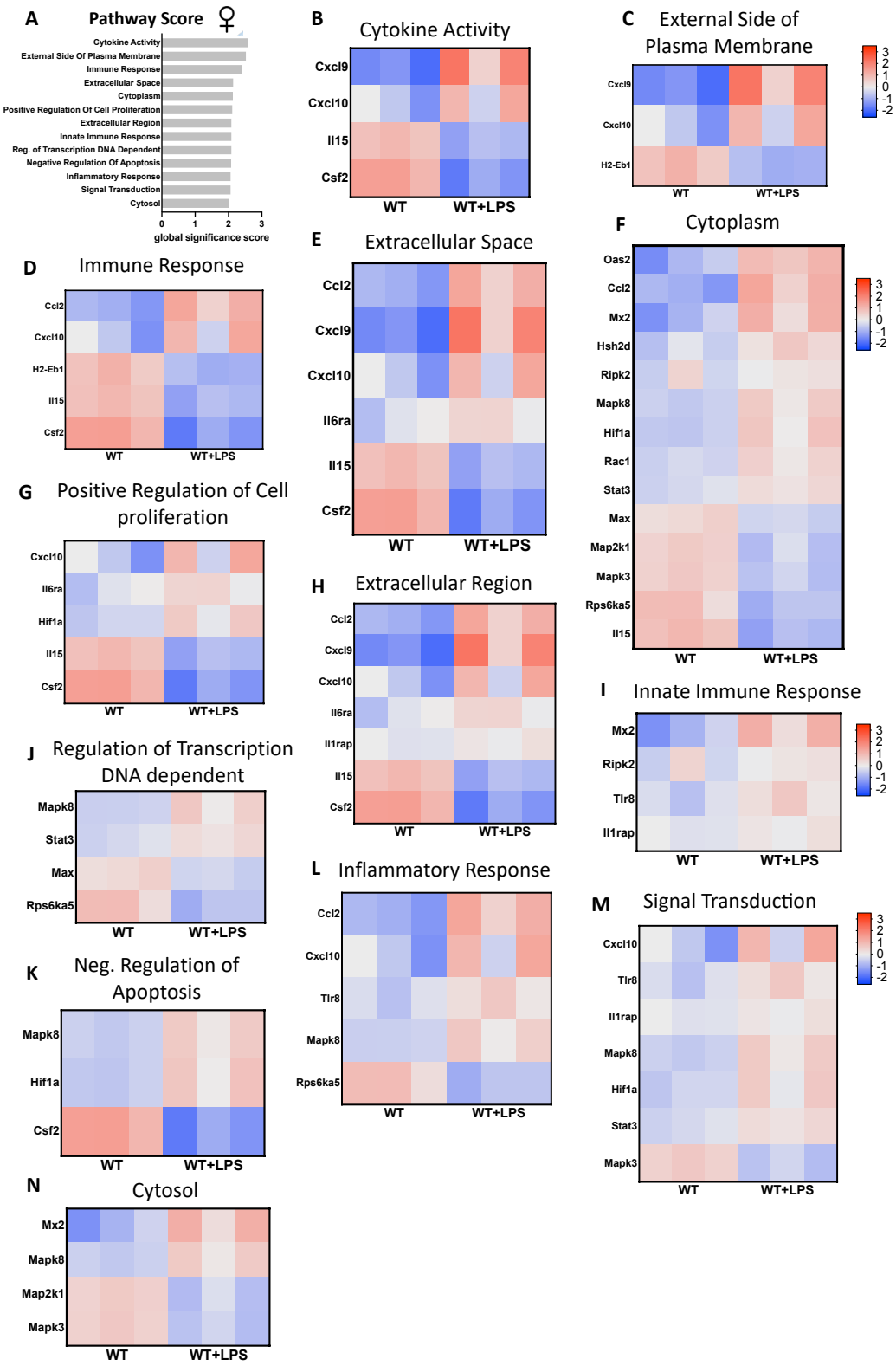
A
Pathway Score
Cytokine Activity
External Side Of Plasma Membrane
Immune Response
Extracellular Space
Cytoplasm
Positive Regulation Of Cell Proliferation
Extracellular Region
Innate Immune Response
Reg. of Transcription DNA Dependent
Negative Regulation Of Apoptosis
Inflammatory Response
Signal Transduction
Cytosol
0 1 2 3
global significance score
B
Cytokine Activity
Cxcl9
Cxcl10
Il15
Csf2
WT WT+LPS
C
External Side of Plasma Membrane
Cxcl9
Cxcl10
H2-Eb1
WT WT+LPS
3 2 1 0 -1 -2
D
Immune Response
Ccl2
Cxcl10
H2-Eb1
Il15
Csf2
WT WT+LPS
E
Extracellular Space
Ccl2
Cxcl9
Cxcl10
Il6ra
Il15
Csf2
WT WT+LPS
F
Cytoplasm
Oas2
Ccl2
Mx2
Hsh2d
Ripk2
Mapk8
Hif1a
Rac1
Stat3
Max
Map2k1
Mapk3
Rps6ka5
Il15
WT WT+LPS
3 2 1 0 -1 -2
G
Positive Regulation of Cell proliferation
Cxcl10
Il6ra
Hif1a
Il15
Csf2
WT WT+LPS
H
Extracellular Region
Ccl2
Cxcl9
Cxcl10
Il6ra
Il1rap
Il15
Csf2
WT WT+LPS
I
Innate Immune Response
Mx2
Ripk2
Tlr8
Il1rap
WT WT+LPS
3 2 1 0 -1 -2
J
Regulation of Transcription DNA dependent
Mapk8
Stat3
Max
Rps6ka5
WT WT+LPS
L
Inflammatory Response
Ccl2
Cxcl10
Tlr8
Mapk8
Rps6ka5
WT WT+LPS
M
Signal Transduction
Cxcl10
Tlr8
Il1rap
Mapk8
Hif1a
Stat3
Mapk3
WT WT+LPS
3 2 1 0 -1 -2
K
Neg. Regulation of Apoptosis
Mapk8
Hif1a
Csf2
WT WT+LPS
N
Cytosol
Mx2
Mapk8
Map2k1
Mapk3
WT WT+LPS

**Figure 3.6 NanoString metabolic pathways in response to jejunum IP-LPS in males**
**A** – List of Pathway Global Significance Scores in NanoString Inflammatory cartridge panel. Only pathways with a higher score than 2 are included in analysis. Global significance scores are calculated based on the sum of the combined t-tests of differentially expressed genes in each pathway. N=3 per group
**B-C** – Pathways showing all genes z-scores per sample before and after IP-LPS

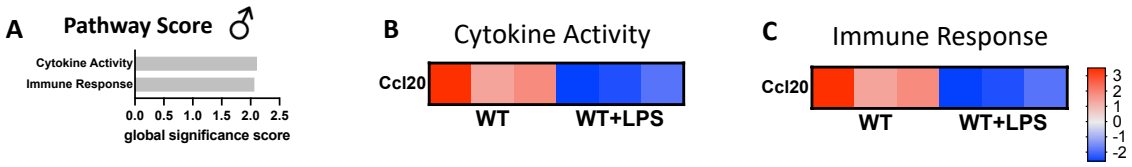
A
Pathway Score
♂
Cytokine Activity
Immune Response
0.0 0.5 1.0 1.5 2.0 2.5
global significance score
B
Cytokine Activity
Ccl20
WT
WT+LPS
C
Immune Response
Ccl20
WT
WT+LPS
3
2
1
0
-1
-2

**Figure 3.7 – LPS changes gene expression in both males and females, with females showing a greater upregulation of metabolic genes**

**A, B** – NanoString metabolic panel Volcano plot analysis of differentially regulated gene expression in response to inflammation in females (A) and males (B). Red represents significantly upregulated genes and blue represents significantly downregulated genes with p-value adjusted to multiple comparisons by Benjamin-Yekutieli method. n=3 animals per group

**C-F** – Fold change and adj.p-value of genes from volcano plot analysis in females (C, D) and males (E, F).

**G** – Venn Diagram of genes changing in both males and females in response to IP-LPS. Females significantly downregulated and upregulated genes are displayed in grey; males significantly downregulated and upregulated genes are displayed in green.

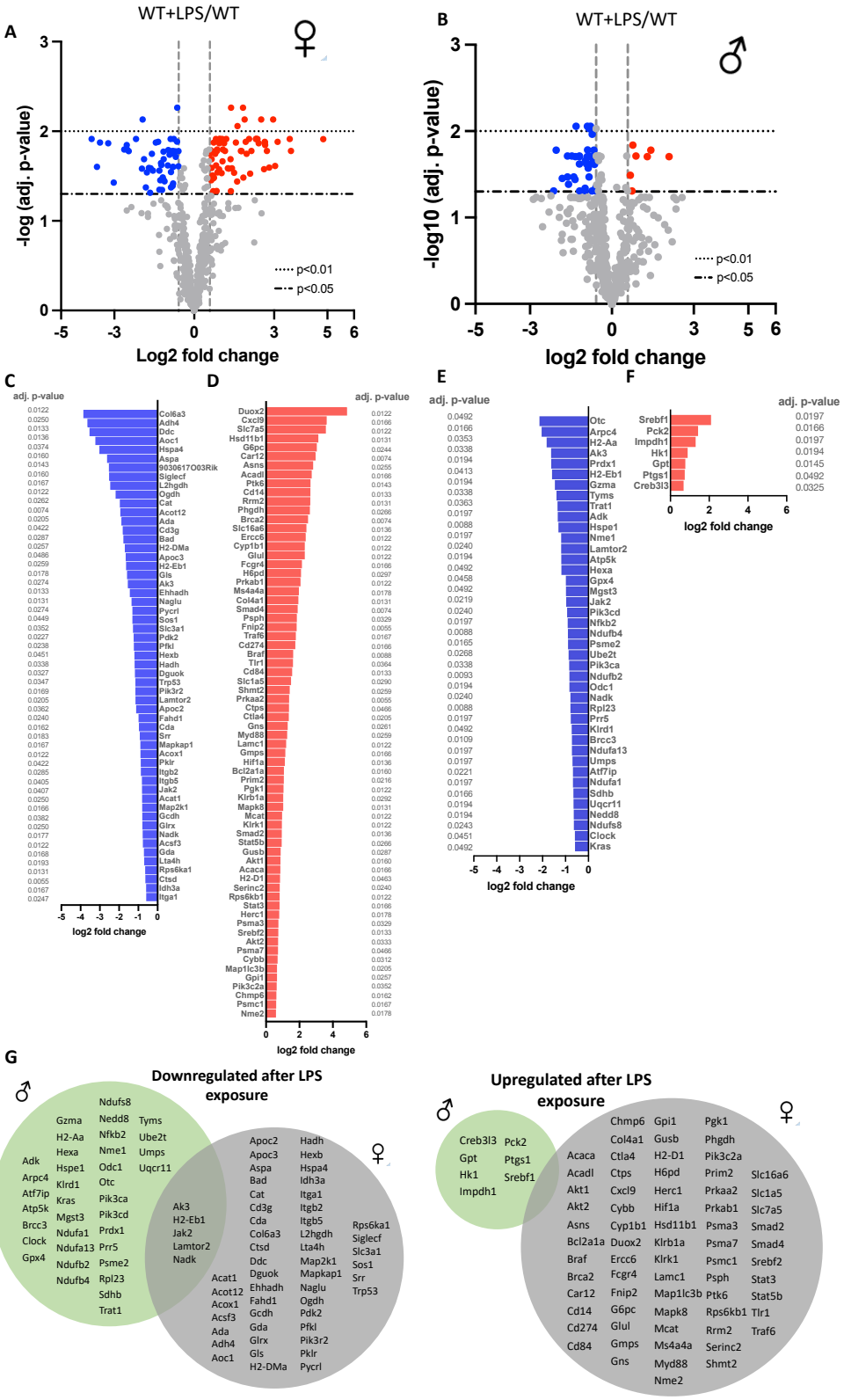
A
WT+LPS/WT
♀
-log (adj. p-value)
Log2 fold change
p<0.01
p<0.05
B
WT+LPS/WT
♂
-log10 (adj. p-value)
log2 fold change
p<0.01
p<0.05
C
adj. p-value
log2 fold change
D
adj. p-value
log2 fold change
E
adj. p-value
log2 fold change
F
adj. p-value
log2 fold change
G
Downregulated after LPS exposure
♂
♀
Upregulated after LPS exposure
♂
♀

**Figure 3.8 – NanoString Metabolic biological pathways impacted by IP-LPS in female jejunum**

**A** – List of Pathway Global Significance Scores in NanoString Metabolic cartridge panel. Only pathways with a higher score than 2 are included in analysis. Global significance scores are calculated based on the sum of the combined t-tests of differentially expressed genes in each pathway. N=3 per group

**B-AD** – Pathways showing all genes z-scores per sample before and after IP-LPS

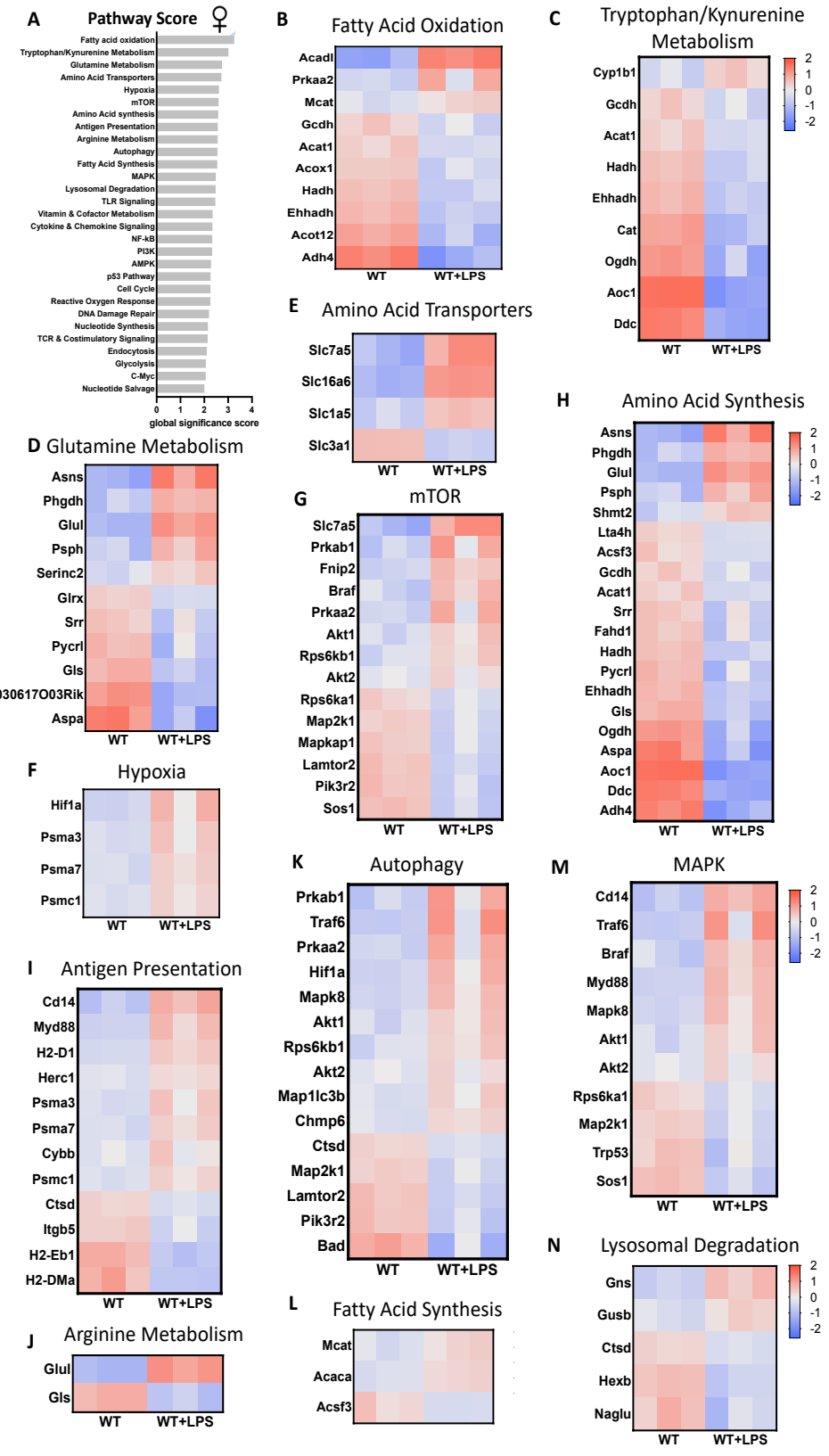
A
Pathway Score ♀
Fatty acid oxidation
Tryptophan/Kynurenine Metabolism
Glutamine Metabolism
Amino Acid Transporters
Hypoxia
mTOR
Amino Acid synthesis
Antigen Presentation
Arginine Metabolism
Autophagy
Fatty Acid Synthesis
MAPK
Lysosomal Degradation
TLR Signaling
Vitamin & Cofactor Metabolism
Cytokine & Chemokine Signaling
NF-kB
PI3K
AMPK
p53 Pathway
Cell Cycle
Reactive Oxygen Response
DNA Damage Repair
Nucleotide Synthesis
TCR & Costimulatory Signaling
Endocytosis
Glycolysis
C-Myc
Nucleotide Salvage
0 1 2 3 4
global significance score
B
Fatty Acid Oxidation
Acadl
Prkaa2
Mcat
Gcdh
Acat1
Acox1
Hadh
Ehhadh
Acot12
Adh4
WT WT+LPS
C
Tryptophan/Kynurenine Metabolism
Cyp1b1
Gcdh
Acat1
Hadh
Ehhadh
Cat
Ogdh
Aoc1
Ddc
WT WT+LPS
2 1 0 -1 -2
D Glutamine Metabolism
Asns
Phgdh
Glul
Psph
Serinc2
Glrx
Srr
Pycrl
Gls
9030617O03Rik
Aspa
WT WT+LPS
E
Amino Acid Transporters
Slc7a5
Slc16a6
Slc1a5
Slc3a1
WT WT+LPS
F
Hypoxia
Hif1a
Psma3
Psma7
Psmc1
WT WT+LPS
G
mTOR
Slc7a5
Prkab1
Fnip2
Braf
Prkaa2
Akt1
Rps6kb1
Akt2
Rps6ka1
Map2k1
Mapkap1
Lamtor2
Pik3r2
Sos1
WT WT+LPS
H
Amino Acid Synthesis
Asns
Phgdh
Glul
Psph
Shmt2
Lta4h
Acsf3
Gcdh
Acat1
Srr
Fahd1
Hadh
Pycrl
Ehhadh
Gls
Ogdh
Aspa
Aoc1
Ddc
Adh4
WT WT+LPS
2 1 0 -1 -2
I
Antigen Presentation
Cd14
Myd88
H2-D1
Herc1
Psma3
Psma7
Cybb
Psmc1
Ctsd
Itgb5
H2-Eb1
H2-DMa
WT WT+LPS
J
Arginine Metabolism
Glul
Gls
WT WT+LPS
K
Autophagy
Prkab1
Traf6
Prkaa2
Hif1a
Mapk8
Akt1
Rps6kb1
Akt2
Map1lc3b
Chmp6
Ctsd
Map2k1
Lamtor2
Pik3r2
Bad
WT WT+LPS
L
Fatty Acid Synthesis
Mcat
Acaca
Acsf3
M
MAPK
Cd14
Traf6
Braf
Myd88
Mapk8
Akt1
Akt2
Rps6ka1
Map2k1
Trp53
Sos1
WT WT+LPS
2 1 0 -1 -2
N
Lysosomal Degradation
Gns
Gusb
Ctsd
Hexb
Naglu
WT WT+LPS
2 1 0 -1 -2

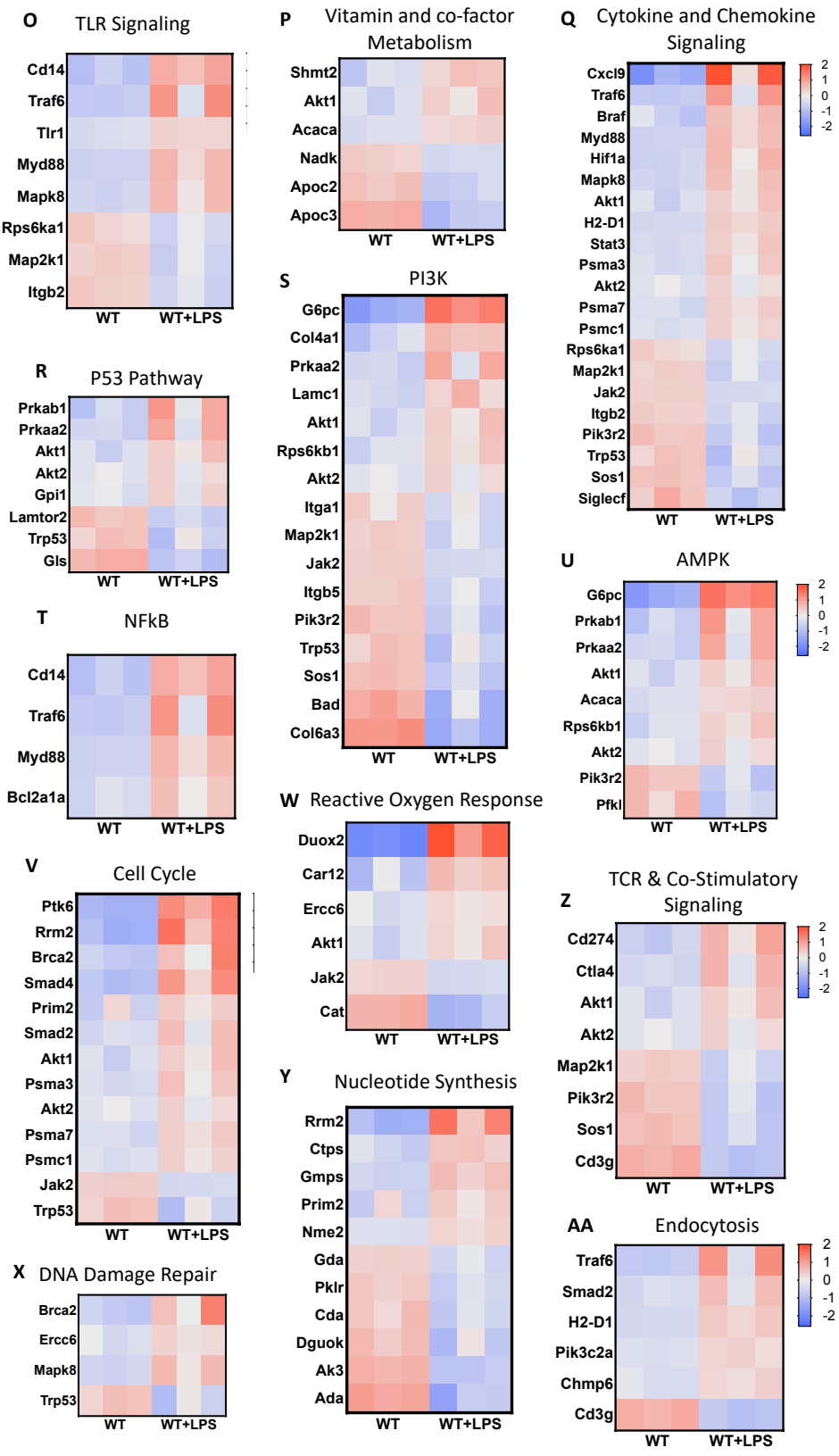
O
TLR Signaling
Cd14
Traf6
Tlr1
Myd88
Mapk8
Rps6ka1
Map2k1
Itgb2
WT
WT+LPS
P
Vitamin and co-factor Metabolism
Shmt2
Akt1
Acaca
Nadk
Apoc2
Apoc3
WT
WT+LPS
Q
Cytokine and Chemokine Signaling
Cxcl9
Traf6
Braf
Myd88
Hif1a
Mapk8
Akt1
H2-D1
Stat3
Psma3
Akt2
Psma7
Psmc1
Rps6ka1
Map2k1
Jak2
Itgb2
Pik3r2
Trp53
Sos1
Siglecf
WT
WT+LPS
2
1
0
-1
-2
R
P53 Pathway
Prkab1
Prkaa2
Akt1
Akt2
Gpi1
Lamtor2
Trp53
Gls
WT
WT+LPS
S
PI3K
G6pc
Col4a1
Prkaa2
Lamc1
Akt1
Rps6kb1
Akt2
Itga1
Map2k1
Jak2
Itgb5
Pik3r2
Trp53
Sos1
Bad
Col6a3
WT
WT+LPS
U
AMPK
G6pc
Prkab1
Prkaa2
Akt1
Acaca
Rps6kb1
Akt2
Pik3r2
Pfkl
WT
WT+LPS
2
1
0
-1
-2
T
NFkB
Cd14
Traf6
Myd88
Bcl2a1a
WT
WT+LPS
W
Reactive Oxygen Response
Duox2
Car12
Ercc6
Akt1
Jak2
Cat
WT
WT+LPS
V
Cell Cycle
Ptk6
Rrm2
Brca2
Smad4
Prim2
Smad2
Akt1
Psma3
Akt2
Psma7
Psmc1
Jak2
Trp53
WT
WT+LPS
Y
Nucleotide Synthesis
Rrm2
Ctps
Gmps
Prim2
Nme2
Gda
Pklr
Cda
Dguok
Ak3
Ada
WT
WT+LPS
Z
TCR & Co-Stimulatory Signaling
Cd274
Ctla4
Akt1
Akt2
Map2k1
Pik3r2
Sos1
Cd3g
WT
WT+LPS
2
1
0
-1
-2
X
DNA Damage Repair
Brca2
Ercc6
Mapk8
Trp53
WT
WT+LPS
AA
Endocytosis
Traf6
Smad2
H2-D1
Pik3c2a
Chmp6
Cd3g
WT
WT+LPS
2
1
0
-1
-2

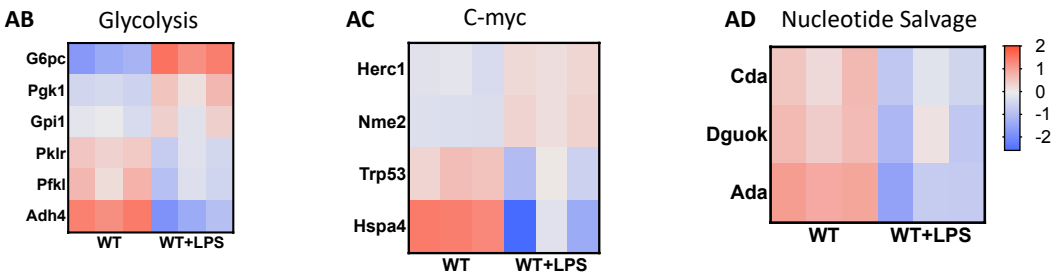
AB
Glycolysis
G6pc
Pgk1
Gpi1
Pklr
Pfkl
Adh4
WT
WT+LPS
AC
C-myc
Herc1
Nme2
Trp53
Hspa4
WT
WT+LPS
AD
Nucleotide Salvage
Cda
Dguok
Ada
WT
WT+LPS
2
1
0
-1
-2

**Figure 3.9 – NanoString Metabolic biological pathways impacted by IP-LPS in female jejunum**

**A** – List of Pathway Global Significance Scores in NanoString Metabolic cartridge panel. Only pathways with a higher score than 2 are included in analysis. Global significance scores are calculated based on the sum of the combined t-tests of differentially expressed genes in each pathway. N=3 per group

**B-J** – Pathways showing all genes z-scores per sample before and after IP-LPS

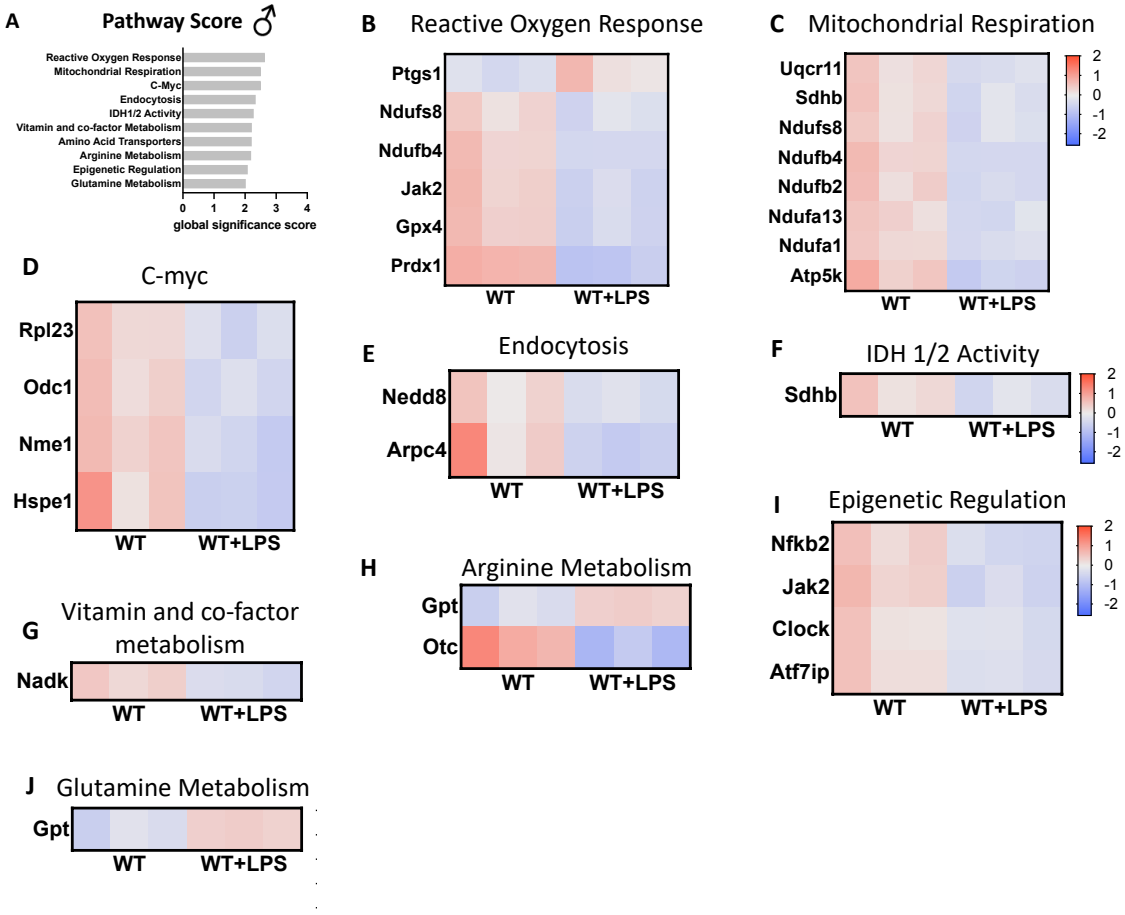
A
Pathway Score ♂
Reactive Oxygen Response
Mitochondrial Respiration
C-Myc
Endocytosis
IDH1/2 Activity
Vitamin and co-factor Metabolism
Amino Acid Transporters
Arginine Metabolism
Epigenetic Regulation
Glutamine Metabolism
0 1 2 3 4
global significance score
B Reactive Oxygen Response
Ptgs1
Ndufs8
Ndufb4
Jak2
Gpx4
Prdx1
WT WT+LPS
C Mitochondrial Respiration
Uqcr11
Sdhb
Ndufs8
Ndufb4
Ndufb2
Ndufa13
Ndufa1
Atp5k
WT WT+LPS
2 1 0 -1 -2
D C-myc
Rpl23
Odc1
Nme1
Hspe1
WT WT+LPS
E Endocytosis
Nedd8
Arpc4
WT WT+LPS
F IDH 1/2 Activity
Sdhb
WT WT+LPS
2 1 0 -1 -2
G Vitamin and co-factor metabolism
Nadk
WT WT+LPS
H Arginine Metabolism
Gpt
Otc
WT WT+LPS
I Epigenetic Regulation
Nfkb2
Jak2
Clock
Atf7ip
WT WT+LPS
2 1 0 -1 -2
J Glutamine Metabolism
Gpt
WT WT+LPS

# Chapter 4

## TREM2 modulates the sex-specific inflammatory response

### *Introduction*

By the year 2000, researchers knew that a series of receptors existed in myeloid cells and were responsible for modulating the inflammatory response of these cells with a potential role for disease pathogenesis. Up to this point, very few groups worked in this characterization. In 2001 TREM-1 and TREM-2 were identified for the first time by Marco Colonna group (Bouchon, Dietrich and Colonna, 2000). The manuscript focused on TREM-1 however, due to the observation that after LPS administration neutrophils and monocytes up-regulated TREM-1 expression, while downregulated TREM2 expression.

During those first years, DAP12 was identified as the obligate partner mediating downstream signaling cascade of activated TREM2 (Daws *et al.*, 2001). Initially, anionic lipids were identified as TREM2 ligands (Daws *et al.*, 2003). In 2002, two different groups suggested a rather important role of TREM2 at the exact same time that started the boom of research in this field. First, Leena Peltonen group published in September that homozygous mutations in the TREM2 receptor were associated with the development of Nasu-Hakola Disease: a disease characterized by frontotemporal dementia and abnormalities in bone density (Paloneva *et al.*, 2002). While Monica Carson group in December of the same year characterized the expression of TREM2 in a population of

myeloid cells in the brain: the microglial cells (Schmid *et al.*, 2002). For the very first time in the literature, they hinted at the fact that this receptor would be associated with Alzheimer's disease and other types of dementia. The prediction would only become true almost 10 years later, when in 2012 polymorphisms in TREM-2 gene expression with single-amino acid substitutions were linked to Alzheimer's Disease (Jones, 2013), and later that would implicate a 3-4 fold increased risk of developing the disease when mutations were present. After the correlation of TREM2 with the development of two different types of dementia, there was a boom in research for understanding the role of TREM2 in myeloid cells, especially since its expression varies from brain-to-brain region (Schmid *et al.*, 2002).

TREM2 activation by LPS decreases TREM2 expression, while increases TREM-1. For a very long time these molecules were thought to have opposing effects, with TREM2 acting as an anti-inflammatory molecule and TREM-1 as a pro-inflammatory molecule (Turnbull *et al.*, 2006). In fact, the most classical described role of TREM-2 is an inhibitor of TLR4 mediated inflammation (Turnbull *et al.*, 2006). New evidence has now shown how flexible the role of TREM2 is in the inflammatory response and consequently in neurodegenerative disease pathogenesis.

TREM2 expression in myeloid cells and its control of inflammatory response

TREM2 is a receptor expressed in myeloid cells including macrophages, microglia, and dendritic cells (Genua *et al*, 2014). One of its first described functions in macrophages was its recognition of lipidic molecules such as bacterial lipopolysaccharide (LPS) and

consequent inhibition of the downstream signaling cascade of TLR4 activation, generating an anti-inflammatory response (Genua *et al*, 2014). This response occurs via downregulation of two major pro-inflammatory transcription factors: JNK and NFkB (Hamerman *et al.*, 2006). And consequently downregulate the expression of pro-inflammatory cytokines such as TNFα and IL6 (Turnbull *et al.*, 2006).

It does seem a little counterintuitive how T2KO models can show exacerbated inflammatory reactions or increased disease severity if the main role of TREM2 is to downregulate inflammation. What was found is that TREM2 has the capacity of activating a series of other roles such as phagocytosis and metabolic shifts. Each role is dependent on a separate signaling cascade in which the regulating mechanisms are still unknown.

For its phagocytic role, activation of TREM2 by ligands such as LPS, starts a signaling cascade with DNAX-activating protein of 12 kDa (DAP12), and recruits the spleen tyrosine kinase (SYK). Activation of SYK leads to a phagocytic response of myeloid cells as demonstrated by increased internalization of LPS expressing bacteria *E. coli* (Yao *et al.*, 2019), among other phagocytic targets (Crowley *et al.*, 1997). The Syk signaling cascade of phagocytosis is a known target that upregulates the inflammatory response of myeloid cells via PI3K/AKT and is a conserved signaling cascade used by other receptors that up-regulate inflammation (Crowley *et al.*, 1997). Therefore, TREM2 anti-inflammatory role must happen independent of SYK, PI3K and AKT (Yao *et al.*, 2019). And blocking SYK, PI3K or AKT is enough to prevent the phagocytic role of TREM2 activation, without affecting its anti-inflammatory response (Yao *et al.*, 2019). For its effect in anti-

inflammation, particularly to antagonize TLR4 activation is still under investigation. It is still under investigation the signaling cascades that determine this anti-inflammatory role. Binding of low affinity molecules to TREM2 receptor is capable of activating inositol phosphatase (SHIP1). This molecule then acts to inhibit SYK by dephosphorylation, consequently preventing PI3K and AKT signaling to block activation of TREM2 receptor (Peng *et al.*, 2010). TREM2 receptor can also recruit DAP10 as a heterodimer to DAP12, or DAP10 only homodimers to its intracellular site of activation. DAP10-TREM2 signaling happens independent of SYK, mTOR pathways and leads to myeloid cell proliferation (Wang *et al.*, 2022). Contrasting to the effect in macrophages, dendritic cell activation of TREM2 is a classically described response of pro-inflammation (Correale *et al.*, 2013; Hall and Agrawal, 2017).

TREM2 effect on metabolism

Given the role of PI3K and AKT signaling in regulating mTOR and metabolism, it is not surprising that TREM2 signaling also regulates metabolic fitness of immune cells. TREM2 is necessary for the proper activation of myeloid cells and the metabolic changes necessary for them to fully exert a pro-inflammatory response. This was discovered after an observation that T2KO microglia in a murine model of Alzheimer's Disease, start undergoing autophagy cell death as disease progresses. Autophagy occurs during metabolic stress, when the cell is not able to find sufficient metabolic sources for its survival and starts to digest cytosolic components to recycle some of its own organelles as energy (Kroemer, Mariño and Levine, 2010). Autophagy is downregulated by mTOR.

Since T2KO microglia have mTOR dysregulation in AD, it was suggested that TREM2 signaling could be responsible for changing the metabolic profile of immune cells and prevent the autophagy mediated cell death in AD.

The recognition of DAMP is very metabolic demanding, as previously discussed in this dissertation: the immune cells start a shift in metabolic source toward glycolysis, inhibiting mitochondrial mediated cell respiration in a process necessary to properly mount a pro-inflammatory response. TREM2 then is a major regulator of this process: the pro-inflammatory response mounted by SYK recruitment of the TREM2 receptor is necessary for mTOR and HIF1α activation and the cell shifts to glycolysis to be able to respond to the metabolic demand (Keren-Shaul *et al.*, 2017). In fact, in T2KO microglia both glycolysis and mitochondrial respiration are decreased (Ulland *et al.*, 2017).

TREM2 impact on intestine

In the intestine, an organ in close proximity with a bacterial population and a myriad of immune cells it is not surprising that TREM2 plays a role in disease mechanisms. Mutations in the TREM2 receptor are suggested to be associated with the development of intestinal bowel disease (Natale *et al.*, 2019), and animal models are used to dissect its control in tissue response. In models of intestinal colitis, TREM2 increases inflammation and pathological scores induced by dextran-sulfate (Correale *et al.*, 2013) as well as the expression of pro-inflammatory genes TNFα, IL-1β and MMP-3.

At the same time, TREM2 signaling is necessary for wound healing by dampening the pro-inflammatory response and recruiting $TREM2^{+}$ macrophages (Seno *et al.*, 2009). Given

TREM2 is a major controller of the innate immune response by both inhibition and activation, it is likely the different models recruit different signaling cascades downstream of TREM-2, although that remains to be investigated.

Sex is a known variable to influence the immune response (Takahashi and Iwasaki, 2021) and it is surprising to find very few reports of sex-specific mechanisms of immunity. Females have a better phagocytic capability in innate immune cells than males (Scotland *et al.*, 2011), a role controlled by TREM2. For intestinal inflammatory disorders, ulcerative colitis is more prevalent and severe in men, while epidemiological data shows Chron's disease to be more prevalent and severe in women rather than men (Goodman, Erkkila and Pizarro, 2020). And TREM2 is found to be up-regulated in humans with intestinal bowel disease (Correale *et al.*, 2013). Thus, here we want to bridge this gap in literature by understanding the role of TREM2 in controlling sex-specific jejunum innate immune inflammatory responses using IP-LPS as a model. We show a drastic divergence between sex in intestinal inflammation and a rather clear pro-inflammatory role of TREM2 signaling in female jejunum.

## *Results*

Sex-specific alterations in jejunum tissue are TREM2 dependent

To investigate the modulation of the innate-immune response in jejunum and its sex-specific dependency, we used T2KO animals to assess regulation of inflammatory response. 24hrs after IP-LPS administration, jejunum section was collected and tissue was analyzed in ussing chambers for measurements of ex vivo jejunum permeability, as previously described in this dissertation. No changes were found in TEER, IsC nor FITC in response to IP-LPS in male and female jejunum (Figure 4.1 A-C). This data suggests that TREM2 is required for female jejunum increases in permeability by IP-LPS.

Once again, claudin-3 becomes disorganized after an inflammatory response and in females 24hrs after IP-LPS (Figure 3.2). In T2KO animals, there is no change in claudin-3 cellular reorganization (Figure 4.1 D-F).

TREM2 is also required for male jejunal effects. Glucose absorption does not increase in male jejunum after IP-LPS (Figure 4.1 G).

Collectively, this data indicates that myeloid TREM2 is required for sex-specific jejunal responses to IP-LPS.

Sex-specific changes in inflammatory gene expression are TREM2 dependent

Three different facts were used to hypothesize the role of TREM2 in IP-LPS jejunal gene expression. First, the fact that jejunum permeability is driven by pro-inflammatory mediators; second, the fact that TREM2KO abolished the jejunal permeability changes in females; third, the fact that other authors have stipulated a role for TREM2 in controlling

the inflammatory response of myeloid cells, as explored in the introduction portion of this chapter. Therefore, we hypothesized that TREM2 would change both males and females inflammatory gene expression in response to IP-LPS.

Females completely abolished the changes in inflammatory gene expression in T2KO jejunum (Figure 4.2 A). While males increase their gene expression profile (Figure 4.2 B-D). Male jejunum now shows a robust downregulation of gene expression in response to IP-LPS. Overall, there is a regulation toward pro-inflammatory responses by decreasing expression of il10rb; and increased *cxcl9* chemokine. Among the genes up-regulated *ifit2, mx2, ligp1* lead to an interferon response, and *hsh2d* is involved with T cell activation, suggesting once more a pro-inflammatory regulation. At the same time, male jejunum decreases pro-inflammatory response by downregulating *nfkb, jun, map3k1, map2k6*. This shows that in the absence of TREM2, there is a dysregulation of the inflammatory control of IP-LPS response, with a mixed pro- and anti-inflammatory response in male jejunum.

It is very clear that the sex-specific effect remains, but it is now inverted. T2KO males regulate more inflammatory genes after IP-LPS than female jejunum (Figure 4.2 E).

Collectively, the data suggests TREM2 to drive the upregulation of the inflammatory response in females, causing intestinal permeability; while showing a complex regulation of the inflammatory response in males in the absence of permeability changes.

Pathway score analysis suggest TREM2 controls biological pathways associated with transcriptional regulation in males

To further understand the role of TREM2 loss of function in the intestinal immune response, the genes were organized in biological pathways according to NanoString Inflammation panel. A global significance score was attributed to each gene, representing the sum of t-tests of each differentially expressed gene. The bigger the change in a biological pathway, the bigger the global significance score being used to represent that pathway (Figure 4.3 A). Females did not show any changes in pathway score analysis, consistent with a lack of gene expression changes from volcano plot analysis.

Most pathways changed in males demonstrate a transcriptional control of the response: Regulation of Transcription by RNA pol. II promoter, Transcription DNA dependent, Negative and Positive Regulation of Transcription DNA dependent, and Nucleus are among the pathways most regulated in T2KO mice. This suggests that IP-LPS generates a shift in the transcriptional regulation to the inflammatory response of male jejunum independently of TREM2 (Figure 4.3 A).

To further understand the direction of these biological pathways and its role in regulating biological function, each pathway was organized by individual gene expression using Z-score (Figure 4.3 B-J). Most transcriptional factors are downregulating gene expression after IP-LPS, including as described previously, nfkb a major regulator of inflammatory response (Figure 4.3 C, E, F, G); and jun and fos regulators of cellular activation. IP-LPS shifts the expression of major controllers of transcription in the absence of TREM2 in males.

Transcriptional factors that upregulate inflammatory response are also downregulated in male jejunum: mapk3, mapk3k1, irf1, rps6ka5, ddit3. As well as pro-inflammatory mediators such as il15, mmp9, ccl24 associated with the extracellular space since they are secreted molecules (Figure 4.3 K, J). Overall pathway analysis shows several transcription factor are being used after IP-LPS to control the mixed inflammatory response independent of TREM2 in male jejunum.

Metabolic response is also shifted in TREM2 dependent manner

TREM2 investigations in microglial cells have shown that loss of function of this receptor affect changes in metabolic shifts dependent on hif1a and mTOR (Ulland *et al.*, 2017), regulators present in female IP-LPS response (Chapter 3). We hypothesized that in T2KO, female jejunum would fail to metabolically regulate these pathways.

For males, the IP-LPS response increases glucose absorption after IP-LPS (Chapter 3), which was TREM2 dependent (Figure 4.1G). We then hypothesized that the absence of TREM2 metabolism would shift differently than females, affecting glucose metabolism.

To explore that possibility, NanoString Metabolic panel was used to investigate the metabolic response in naïve and 24h after IP-LPS jejunum of male and female mice (Figure 4.4).

As hypothesized, the female jejunum failed to shift the metabolic response after IP-LPS, as no genes are found significantly altered in our analysis (Figure 4.4 A), again suggesting that the female jejunum is not responding to IP-LPS in the absence of TREM2 signaling.

In males, there was a greater shift in metabolic gene expression (Figure 4.4 B-E), that is different than the WT profile. This suggests IP-LPS to drive changes in metabolism in the absence of TREM2 expression. Once again, the data suggests that in the absence of TREM2 there is a shift in the sex-specific response: male jejunum is more responsive to IP-LPS than female jejunum.

Metabolic pathways in T2KO mice highlight male and female specific effects

Females only had one pathway significantly regulated (Figure 4.5 A), while males had a very robust biological response (Figure 4.5 B). Among the pathways up-regulated by males, the profile is very similar to the one obtained by female WT jejunum: changes in fatty acid oxidation, glutamine metabolism and hypoxia. This suggests a TREM2-independent modulation these metabolic pathways after IP-LPS. Most genes associated with these pathways showed a downregulation of its expression (Figure 4.5 C-Y).

At the same time, there are shifts in the metabolic profile that are divergent of the female response: fatty acid synthesis, glycolysis and lysosomal degradation show high scores in male pathway analysis. All these pathways are correlated with inflammatory responses and phagocytic functions (Jung, Zeng and Horng, 2019). The glycolysis pathway, which we hypothesized would show alterations, presented a downregulation of adh genes, which are implicated in alcohol production from glycolysis use (Yuki and Thurman, 1980). This result does not explain the changes in male glucose absorption, and could point toward microbiota alterations, although more experiments are necessary to understand this data.

Overall, the T2KO male response is very divergent in the metabolic profile than the male WT response, suggesting the TREM2 receptor shifted the metabolic profile in WT IP-LPS response. The data differs between male and female, suggesting a role of TREM2 in regulating sex-specific responses to IP-LPS. Moreover, collectively, the female jejunum does not seem to respond to IP-LPS in the absence of TREM2.

## *Discussion*

TREM2 regulates phagocytosis and metabolic shifts necessary for a pro-inflammatory response at the same time they can downregulate TLR-4 mediated proinflammatory responses. Given this dual role of TREM2 in mediating a myriad of functions in immunity it is not surprising that mutations of this receptor are associated with dysregulated inflammatory disorders. Single amino acid substitutions to the receptor increase by 3 fold the risk of developing Alzheimer's disease (Guerreiro *et al*, 2013; Bianchin *et al*, 2013), and when mutations are homozygous it causes frontotemporal dementia and Nasu-Hakola disease.

TREM2 is not only expressed in the brain myeloid population, as macrophages and dendritic cells also express the receptors and are present in almost every organ of the body. Here, we use IP-LPS as a model to generate systemic inflammation, and at the 24hr timepoint to study the effect of innate immunity in intestinal inflammation. As we have previously characterized in this dissertation, the intestinal response has a sex-specific phenotype, with female jejunum producing higher levels of inflammatory mediators and an increased intestinal permeability. To further understand how that inflammatory response is controlled we acquired mice with a null mutation in the TREM2 receptor.

TREM2 was able to fully reverse female effect: T2KO prevented the changes in inflammatory and metabolic gene expression and prevented changes in intestinal permeability. This suggests (1) TREM2 is required for the female response to IP-LPS, and (2) TREM2 up-regulates the pro-inflammatory response, increasing intestinal permeability in females only. This was not the first-time intestinal inflammation was driven by TREM2.

In a model of DSS colitis, T2KO mice decreased the intestinal inflammatory response. The effect seems to be dependent on dendritic cell signaling (Correale *et al.*, 2013). In our model, we have not investigated the cellular contribution of TREM2 response in macrophages versus dendritic cells, and it is possible dendritic cells are the ones eliciting this strong phenotype in females.

It has been stablished that female macrophages have a higher phagocytic capacity than male macrophages (Scotland *et al.*, 2011). Since TREM2 is responsible for phagocytosis in myeloid cells, it is possible that TREM2 is more active in females after IP-LPS, a function that is regulated independent of the anti-inflammatory role of TREM2. In fact, the mTOR pathway that is regulated by TREM2 and necessary for a pro-inflammatory response is more upregulated in female jejunum. As discussed in chapter 3 females have a higher expression of genes affecting the mTOR pathway including *hif1a, akt1, akt2*. Given how dependent the female response is in mTOR signaling it is not surprising that T2KO completely abolishes the changes in inflammatory and metabolic gene expression in females.

The TREM2 regulation of mTOR is a pathway described to keep microglial cells in a high metabolic state during pro-inflammatory responses. When that fails, autophagic pathways are recruited to help maintain the metabolic status and can lead to cell death by autophagy (Ulland *et al.*, 2017). T2KO models shows an upregulated autophagic vesicles (Ulland *et al.*, 2017). In our model, we did not detect changes in autophagy in T2KO female intestine. In fact, in the absence of TREM2, the female jejunum seemed to not notice the IP-LPS response at all and did not elicit responses in the parameters we measured.

Male jejunum did not change permeability in response to IP-LPS, but instead showed an up-regulation of glucose absorption. T2KO male jejunum also reverted the effects of IP-LPS, thus TREM2 was responsible for the glucose generated current in male jejunum. This suggests that myeloid cells expressing TREM2 are interacting with intestinal epithelial cells and modulating nutrient absorption during inflammatory conditions. More importantly, it suggests this happens via TREM2. This is the first time in the literature that TREM2 expression is shown to modulate glucose absorption in the intestine. More investigations into the mechanisms that drive these alterations are necessary to draw further conclusions.

T2KO also shifted the inflammatory and metabolic profile of gene expression in males to a new direction. Unlike the female response it represented a more robust up- and downregulation of gene expression. The profile seems to have characteristics of both pro- and anti-inflammatory responses: *nfkb2, jun* and several mapk are downregulated. At the same time, il10 is downregulated and *duox2, cxcl9*, *myd88*, *cd14* are all up-regulated and associated with a pro-inflammatory response (Chen *et al.*, 2018). The downregulation of nfkb is present in male WT jejunum, and is not changed after TREM2 is knocked out. Since IP-LPS is being administered, it is non-surprising that immune cells generate an immune response in the absence of TREM2, myeloid cells express TLR-4 receptors, and circulating cytokine levels reach the jejunum tissue from peritoneal macrophages response regardless. But the fact the intestine is more responsive in T2KO, suggests TREM2 dampens the pro- and anti-inflammatory response in the male jejunum after IP-LPS administration.

Since male jejunum do not seem to be recruiting mTOR related genes (Figure 3.4), it suggests TREM2 acts independently of mTOR to regulate male alterations. TREM2 mtor independent signaling is classically described as an anti-inflammatory response that acts on TLR-4 mediated signaling (Yao *et al.*, 2019). Whether or not males and females activate different signaling cascades upon TREM2 activation in jejunum remains to be investigated. This dual role of TREM2 activation has been shown in different models of disease. In cancer for example, tumor associated macrophages suppress T cell response via TREM2 receptor (Binnewies *et al.*, 2021). Blocking TREM2 using antibodies promotes anti-tumor immunity. At the same time, a lack of function of the TREM2 receptor worsens Alzheimer's Disease prognostics by preventing phagocytosis of amyloid-beta proteins, molecular mediators of the cognitive deficits in Alzheimer's Disease (Ulland *et al.*, 2017). In fact, the use of antibodies that activate TREM2 in Alzheimer's Disease are capable of enhancing the phagocytic response of microglia and prevent detrimental metabolic changes in microglial cells (van Lengerich *et al.*, 2023). These models of disease highlight the versatility of the TREM2 receptor in promoting and inhibiting inflammatory responses, depending on the role of innate immunity when driving pathogenesis.

Collectively, this chapter has shown how TREM2 is responsible for different roles in the inflammatory response to IP-LPS that are sex-specific. In males TREM2 is responsible for up-regulating glucose absorption, which does not happen in females. In females, TREM2 is responsible for upregulating the inflammatory response and to increase intestinal permeability. Overall, more experiments are necessary to further understand how TREM2 regulates this sex difference.

## *Figures and Legends*

**Figure 4.1 TREM2 is necessary for IP-LPS increased female jejunum permeability and male glucose absorption**

**A –**Ussing chamber transepithelial resistance (TEER) of jejunum in T2KO naive and 24h after IP-LPS in male and female mice. n=4-6 mice, points represent total jejunum segments.

**B –** 4kDa dextran FITC-conjugated permeability in jejunum of male and female T2KO naive and 24h after IP-LPS mice. n=4-6 mice

**C –** Current at rest in jejunum of male and female mice T2KO naïve and 24h after IP-LPS =4-6 mice, total jejunum segments.

**D –** zoom of 63X representative images jejunum, vili of T2KO naive and 24h after IP-LPS, green represents claudin-3 (cld3), white arrows represent internalized cld3 puncta, scale bar 5μm.

**E, F –** Total internalized claudin-3 puncta per cell per animal in females (E) and males (F).

**G** – Peak of current after glucose in lumen of male and female jejunum WT naive and 24h after IP-LPS. n=4-6 mice, total jejunum segments.

Data showed as mean ± SEM, analyzed with unpaired one-tailed t-test (E and F), or one-way ANOVA, Tukey multiple comparison analysis post-test (A-C, G). *$p<0.05$, **$p<0.01$, ****$p<0.0001$.

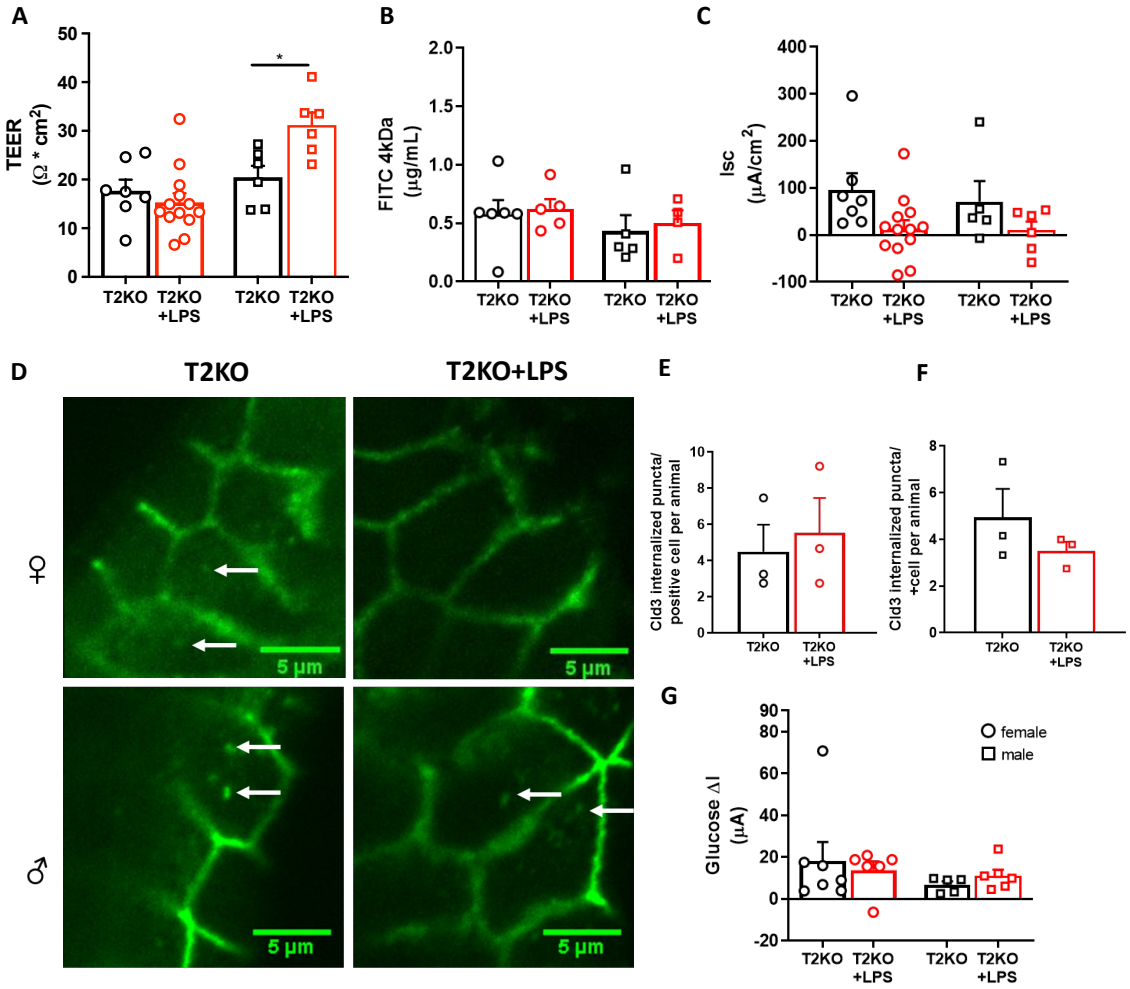
A
TEER
(Ω * cm²)
T2KO
T2KO +LPS
T2KO
T2KO +LPS
*
B
FITC 4kDa
(µg/mL)
C
Isc
(µA/cm²)
D
T2KO
T2KO+LPS
♀
♂
5 µm
E
Cld3 internalized puncta/ positive cell per animal
F
Cld3 internalized puncta/ +cell per animal
G
Glucose ΔI
(µA)
female
male

**Figure 4.2 – T2KO animals have sex-specific regulations of inflammatory gene expression after IP-LPS**

**A,B** – NanoString inflammatory panel Volcano plot analysis of differentially regulated gene expression in response to inflammation in females (A) and males (B). Red represents significantly upregulated genes and blue represents significantly downregulated genes with p-value adjusted to multiple comparisons by Benjamin-Yekutieli method. n=3 animals per group

**C, D** – Fold change and adj.p-value of genes from volcano plot analysis in males. Blue represents downregulated genes after IP-LPS (C), red represents upregulated genes after IP-LPS (D).

**E** – Venn Diagram of genes changing in both males and females in response to IP-LPS. Females significantly downregulated and upregulated genes are displayed in grey; males significantly downregulated and upregulated genes are displayed in green.

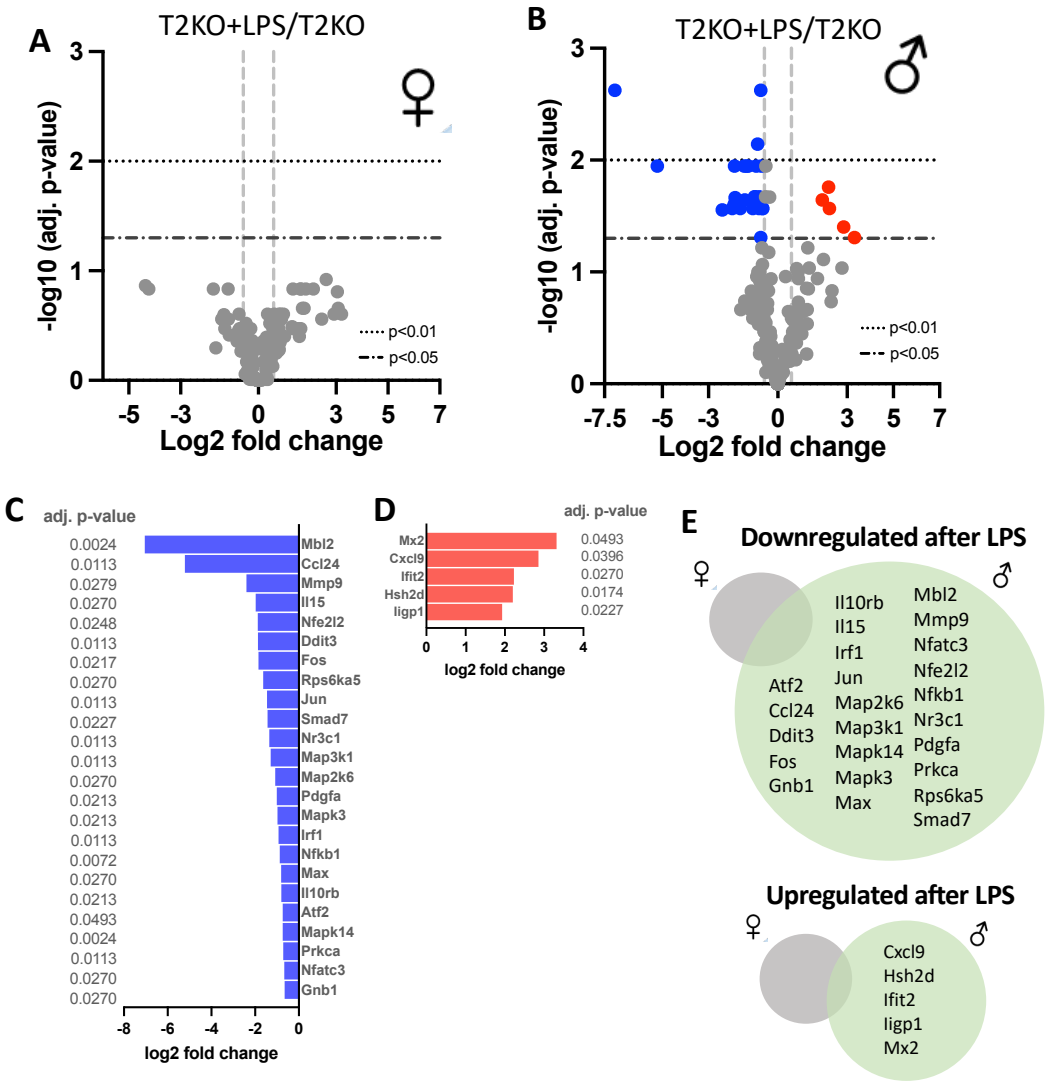
A
T2KO+LPS/T2KO
♀
-log10 (adj. p-value)
Log2 fold change
p<0.01
p<0.05
B
T2KO+LPS/T2KO
♂
-log10 (adj. p-value)
Log2 fold change
p<0.01
p<0.05
C
adj. p-value
0.0024 Mbl2
0.0113 Ccl24
0.0279 Mmp9
0.0270 Il15
0.0248 Nfe2l2
0.0113 Ddit3
0.0217 Fos
0.0270 Rps6ka5
0.0113 Jun
0.0227 Smad7
0.0113 Nr3c1
0.0113 Map3k1
0.0270 Map2k6
0.0213 Pdgfa
0.0213 Mapk3
0.0113 Irf1
0.0072 Nfkb1
0.0270 Max
0.0213 Il10rb
0.0493 Atf2
0.0024 Mapk14
0.0113 Prkca
0.0270 Nfatc3
0.0270 Gnb1
log2 fold change
D
adj. p-value
Mx2 0.0493
Cxcl9 0.0396
Ifit2 0.0270
Hsh2d 0.0174
Iigp1 0.0227
log2 fold change
E
Downregulated after LPS
♀
♂
Atf2
Ccl24
Ddit3
Fos
Gnb1
Il10rb
Il15
Irf1
Jun
Map2k6
Map3k1
Mapk14
Mapk3
Max
Mbl2
Mmp9
Nfatc3
Nfe2l2
Nfkb1
Nr3c1
Pdgfa
Prkca
Rps6ka5
Smad7
Upregulated after LPS
♀
♂
Cxcl9
Hsh2d
Ifit2
Iigp1
Mx2

**Figure 4.3 NanoString inflammatory biological pathways impacted by IP-LPS in T2KO male jejunum**

**A** – List of Pathway Global Significance Scores in NanoString Inflammatory cartridge panel. Only pathways with a higher score than 2 are included in analysis. Global significance scores are calculated based on the sum of the combined t-tests of differentially expressed genes in each pathway. N=3 per group

**B-K** – Pathways showing all genes z-scores per sample before and after IP-LPS in T2KO male jejunum.

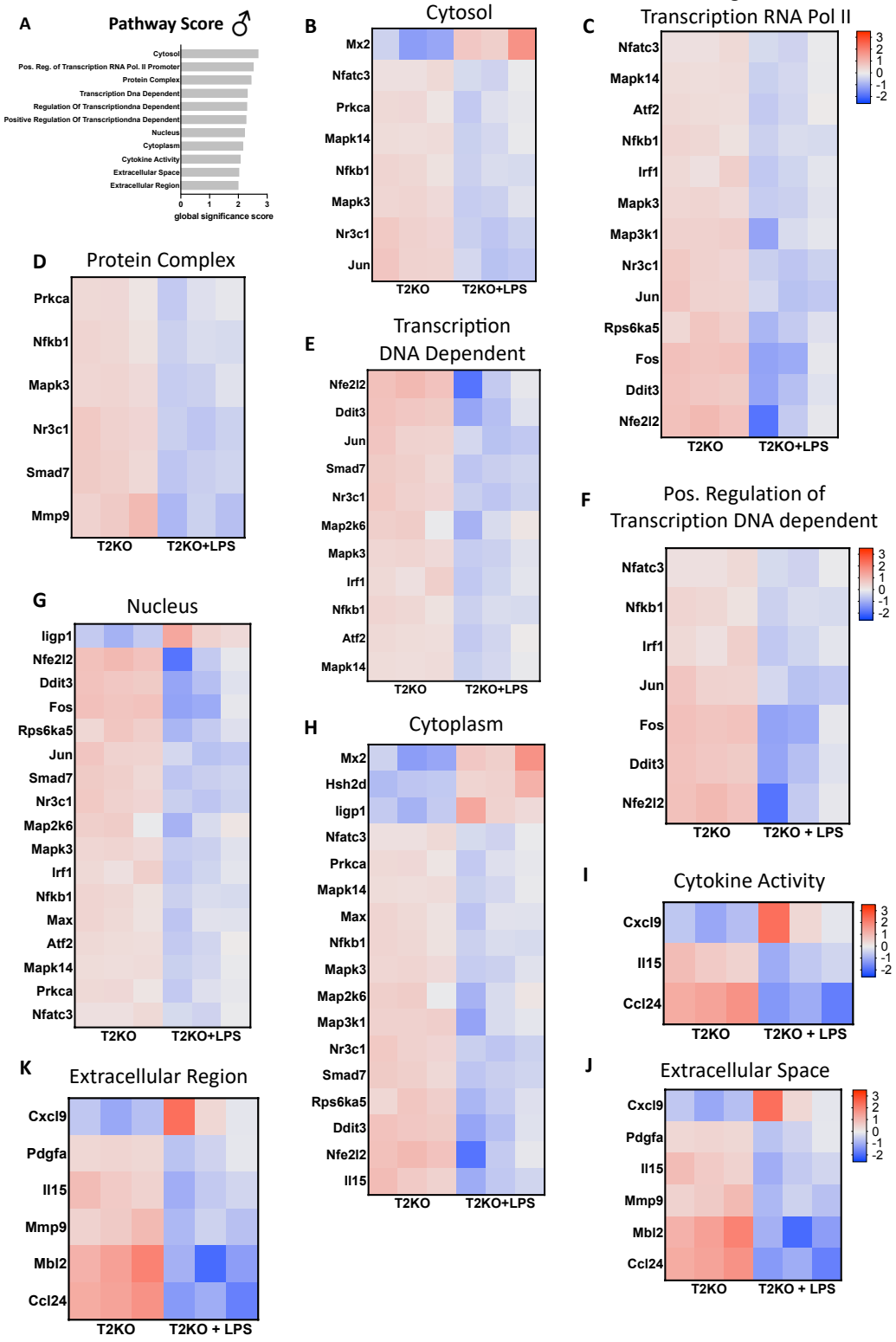
A
Pathway Score
Cytosol
Pos. Reg. of Transcription RNA Pol. II Promoter
Protein Complex
Transcription Dna Dependent
Regulation Of Transcriptiondna Dependent
Positive Regulation Of Transcriptiondna Dependent
Nucleus
Cytoplasm
Cytokine Activity
Extracellular Space
Extracellular Region
0 1 2 3
global significance score
B
Cytosol
Mx2
Nfatc3
Prkca
Mapk14
Nfkb1
Mapk3
Nr3c1
Jun
T2KO T2KO+LPS
C
Pos. Regulation of Transcription RNA Pol II
Nfatc3
Mapk14
Atf2
Nfkb1
Irf1
Mapk3
Map3k1
Nr3c1
Jun
Rps6ka5
Fos
Ddit3
Nfe2l2
T2KO T2KO+LPS
3 2 1 0 -1 -2
D
Protein Complex
Prkca
Nfkb1
Mapk3
Nr3c1
Smad7
Mmp9
T2KO T2KO+LPS
E
Transcription DNA Dependent
Nfe2l2
Ddit3
Jun
Smad7
Nr3c1
Map2k6
Mapk3
Irf1
Nfkb1
Atf2
Mapk14
T2KO T2KO+LPS
F
Pos. Regulation of Transcription DNA dependent
Nfatc3
Nfkb1
Irf1
Jun
Fos
Ddit3
Nfe2l2
T2KO T2KO + LPS
3 2 1 0 -1 -2
G
Nucleus
Iigp1
Nfe2l2
Ddit3
Fos
Rps6ka5
Jun
Smad7
Nr3c1
Map2k6
Mapk3
Irf1
Nfkb1
Max
Atf2
Mapk14
Prkca
Nfatc3
T2KO T2KO+LPS
H
Cytoplasm
Mx2
Hsh2d
Iigp1
Nfatc3
Prkca
Mapk14
Max
Nfkb1
Mapk3
Map2k6
Map3k1
Nr3c1
Smad7
Rps6ka5
Ddit3
Nfe2l2
Il15
T2KO T2KO+LPS
I
Cytokine Activity
Cxcl9
Il15
Ccl24
T2KO T2KO + LPS
3 2 1 0 -1 -2
J
Extracellular Space
Cxcl9
Pdgfa
Il15
Mmp9
Mbl2
Ccl24
T2KO T2KO + LPS
3 2 1 0 -1 -2
K
Extracellular Region
Cxcl9
Pdgfa
Il15
Mmp9
Mbl2
Ccl24
T2KO T2KO + LPS

**Figure 4.4 – TREM2 is necessary for female metabolic response and changes males metabolic response to IP-LPS**

**A,B** – NanoString metabolic panel Volcano plot analysis of differentially regulated gene expression in response to inflammation in T2KO females (A) and males (B). Red represents significantly upregulated genes and blue represents significantly downregulated genes with p-value adjusted to multiple comparisons by Benjamin-Yekutieli method. n=3 animals per group

**C, D** – Fold change and adj.p-value of genes from volcano plot analysis in T2KO males. Blue represents downregulated genes after IP-LPS (C), red represents upregulated genes after IP-LPS (D).

**E** – Venn Diagram of genes changing in both T2KO males and females in response to IP-LPS. Females significantly downregulated and upregulated genes are displayed in grey; males significantly downregulated and upregulated genes are displayed in green.

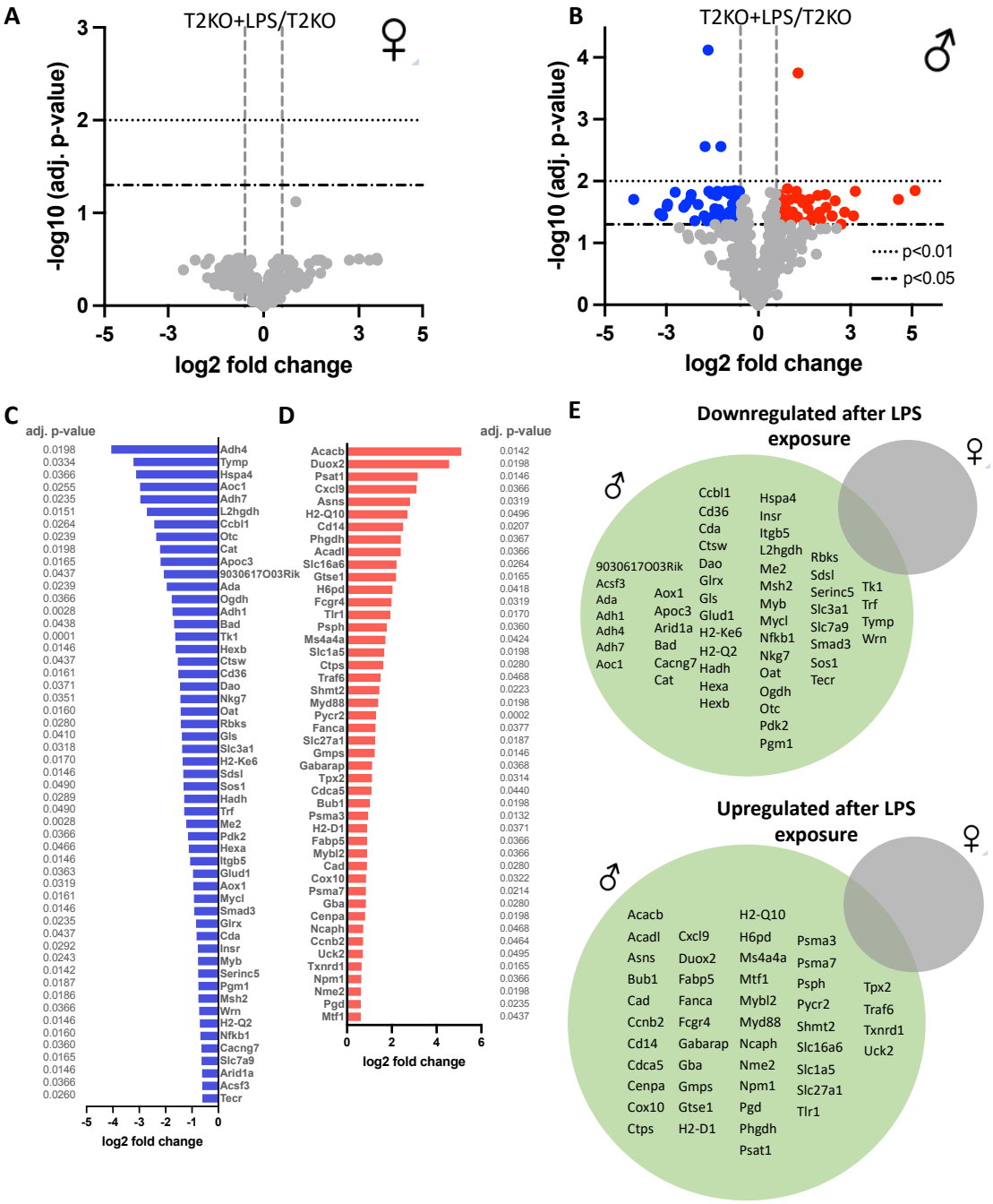
A
T2KO+LPS/T2KO
♀
-log10 (adj. p-value)
log2 fold change
B
T2KO+LPS/T2KO
♂
-log10 (adj. p-value)
log2 fold change
p<0.01
p<0.05
C
adj. p-value
0.0198 Adh4
0.0334 Tymp
0.0366 Hspa4
0.0255 Aoc1
0.0235 Adh7
0.0151 L2hgdh
0.0264 Ccbl1
0.0239 Otc
0.0198 Cat
0.0165 Apoc3
0.0437 9030617O03Rik
0.0239 Ada
0.0366 Ogdh
0.0028 Adh1
0.0438 Bad
0.0001 Tk1
0.0146 Hexb
0.0437 Ctsw
0.0161 Cd36
0.0371 Dao
0.0351 Nkg7
0.0160 Oat
0.0280 Rbks
0.0410 Gls
0.0318 Slc3a1
0.0170 H2-Ke6
0.0146 Sdsl
0.0490 Sos1
0.0289 Hadh
0.0490 Trf
0.0028 Me2
0.0366 Pdk2
0.0466 Hexa
0.0146 Itgb5
0.0363 Glud1
0.0319 Aox1
0.0161 Mycl
0.0146 Smad3
0.0235 Glrx
0.0437 Cda
0.0292 Insr
0.0243 Myb
0.0142 Serinc5
0.0187 Pgm1
0.0186 Msh2
0.0366 Wrn
0.0146 H2-Q2
0.0160 Nfkb1
0.0360 Cacng7
0.0165 Slc7a9
0.0146 Arid1a
0.0366 Acsf3
0.0260 Tecr
log2 fold change
D
adj. p-value
Acacb 0.0142
Duox2 0.0198
Psat1 0.0146
Cxcl9 0.0366
Asns 0.0319
H2-Q10 0.0496
Cd14 0.0207
Phgdh 0.0367
Acadl 0.0366
Slc16a6 0.0264
Gtse1 0.0165
H6pd 0.0418
Fcgr4 0.0319
Tlr1 0.0170
Psph 0.0360
Ms4a4a 0.0424
Slc1a5 0.0198
Ctps 0.0280
Traf6 0.0468
Shmt2 0.0223
Myd88 0.0198
Pycr2 0.0002
Fanca 0.0377
Slc27a1 0.0187
Gmps 0.0146
Gabarap 0.0368
Tpx2 0.0314
Cdca5 0.0440
Bub1 0.0198
Psma3 0.0132
H2-D1 0.0371
Fabp5 0.0366
Mybl2 0.0366
Cad 0.0280
Cox10 0.0322
Psma7 0.0214
Gba 0.0280
Cenpa 0.0198
Ncaph 0.0468
Ccnb2 0.0464
Uck2 0.0495
Txnrd1 0.0165
Npm1 0.0366
Nme2 0.0198
Pgd 0.0235
Mtf1 0.0437
log2 fold change
E
Downregulated after LPS exposure
♂
♀
9030617O03Rik
Acsf3
Ada
Adh1
Adh4
Adh7
Aoc1
Aox1
Apoc3
Arid1a
Bad
Cacng7
Cat
Ccbl1
Cd36
Cda
Ctsw
Dao
Glrx
Gls
Glud1
H2-Ke6
H2-Q2
Hadh
Hexa
Hexb
Hspa4
Insr
Itgb5
L2hgdh
Me2
Msh2
Myb
Mycl
Nfkb1
Nkg7
Oat
Ogdh
Otc
Pdk2
Pgm1
Rbks
Sdsl
Serinc5
Slc3a1
Slc7a9
Smad3
Sos1
Tecr
Tk1
Trf
Tymp
Wrn
Upregulated after LPS exposure
♂
♀
Acacb
Acadl
Asns
Bub1
Cad
Ccnb2
Cd14
Cdca5
Cenpa
Cox10
Ctps
Cxcl9
Duox2
Fabp5
Fanca
Fcgr4
Gabarap
Gba
Gmps
Gtse1
H2-D1
H2-Q10
H6pd
Ms4a4a
Mtf1
Mybl2
Myd88
Ncaph
Nme2
Npm1
Pgd
Phgdh
Psat1
Psma3
Psma7
Psph
Pycr2
Shmt2
Slc16a6
Slc1a5
Slc27a1
Tlr1
Tpx2
Traf6
Txnrd1
Uck2

**Figure 4.5 NanoString metabolic biological pathways impacted by IP-LPS in T2KO male and female jejunum**

**A, B** – List of Pathway Global Significance Scores in NanoString Metabolic cartridge panel in T2KO females (A) and males (B). Only pathways with a higher score than 2 are included in analysis. Global significance scores are calculated based on the sum of the combined t-tests of differentially expressed genes in each pathway. N=3 per group

**C-Y** – Pathways showing all genes z-scores per sample before and after IP-LPS in T2KO male jejunum.

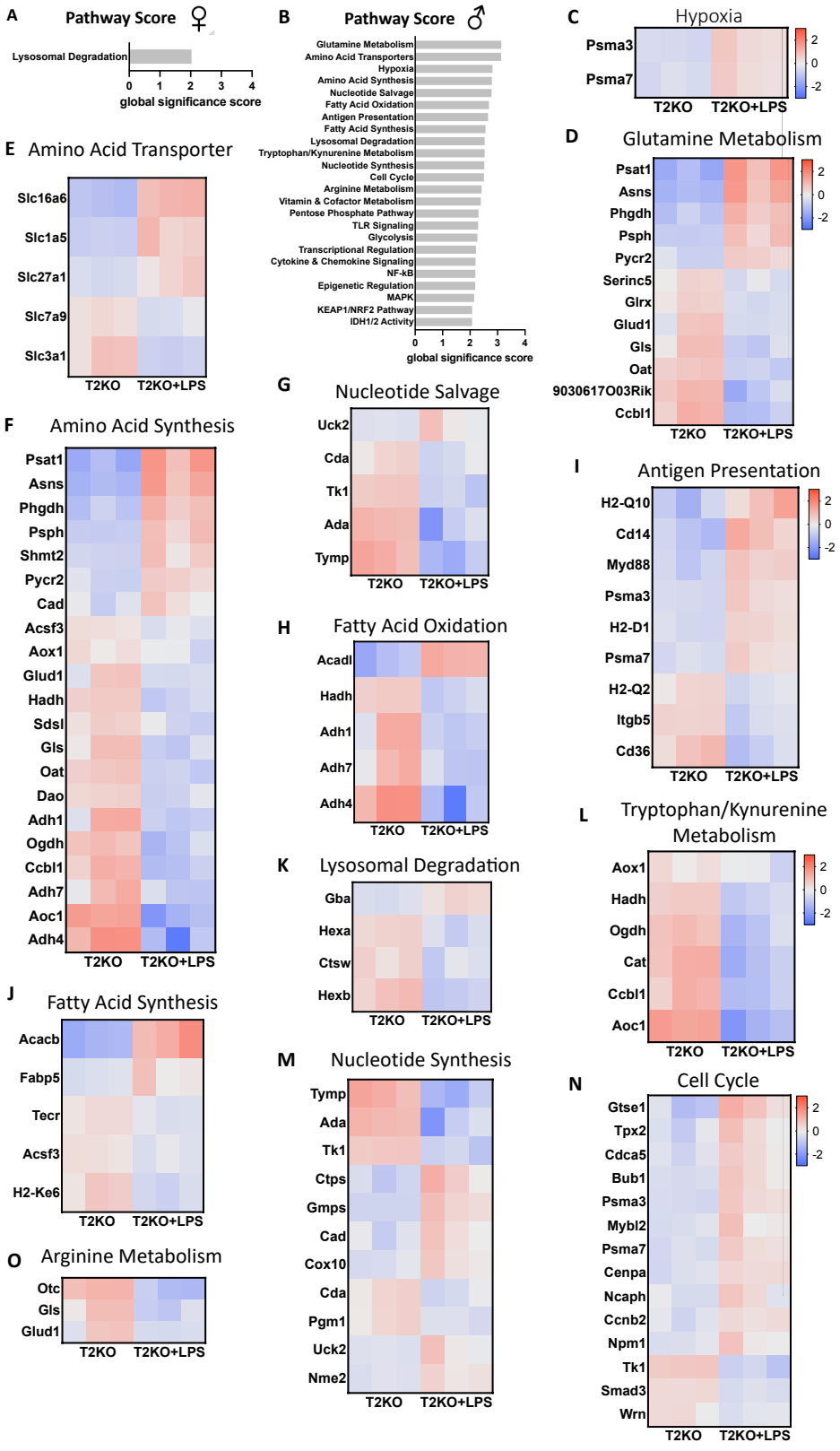
A
Pathway Score ♀
Lysosomal Degradation
0 1 2 3 4
global significance score
B
Pathway Score ♂
Glutamine Metabolism
Amino Acid Transporters
Hypoxia
Amino Acid Synthesis
Nucleotide Salvage
Fatty Acid Oxidation
Antigen Presentation
Fatty Acid Synthesis
Lysosomal Degradation
Tryptophan/Kynurenine Metabolism
Nucleotide Synthesis
Cell Cycle
Arginine Metabolism
Vitamin & Cofactor Metabolism
Pentose Phosphate Pathway
TLR Signaling
Glycolysis
Transcriptional Regulation
Cytokine & Chemokine Signaling
NF-kB
Epigenetic Regulation
MAPK
KEAP1/NRF2 Pathway
IDH1/2 Activity
0 1 2 3 4
global significance score
C
Hypoxia
Psma3
Psma7
T2KO T2KO+LPS
2 0 -2
D
Glutamine Metabolism
Psat1
Asns
Phgdh
Psph
Pycr2
Serinc5
Glrx
Glud1
Gls
Oat
9030617O03Rik
Ccbl1
T2KO T2KO+LPS
2 0 -2
E
Amino Acid Transporter
Slc16a6
Slc1a5
Slc27a1
Slc7a9
Slc3a1
T2KO T2KO+LPS
F
Amino Acid Synthesis
Psat1
Asns
Phgdh
Psph
Shmt2
Pycr2
Cad
Acsf3
Aox1
Glud1
Hadh
Sdsl
Gls
Oat
Dao
Adh1
Ogdh
Ccbl1
Adh7
Aoc1
Adh4
T2KO T2KO+LPS
G
Nucleotide Salvage
Uck2
Cda
Tk1
Ada
Tymp
T2KO T2KO+LPS
H
Fatty Acid Oxidation
Acadl
Hadh
Adh1
Adh7
Adh4
T2KO T2KO+LPS
I
Antigen Presentation
H2-Q10
Cd14
Myd88
Psma3
H2-D1
Psma7
H2-Q2
Itgb5
Cd36
T2KO T2KO+LPS
2 0 -2
J
Fatty Acid Synthesis
Acacb
Fabp5
Tecr
Acsf3
H2-Ke6
T2KO T2KO+LPS
K
Lysosomal Degradation
Gba
Hexa
Ctsw
Hexb
T2KO T2KO+LPS
L
Tryptophan/Kynurenine Metabolism
Aox1
Hadh
Ogdh
Cat
Ccbl1
Aoc1
T2KO T2KO+LPS
2 0 -2
M
Nucleotide Synthesis
Tymp
Ada
Tk1
Ctps
Gmps
Cad
Cox10
Cda
Pgm1
Uck2
Nme2
T2KO T2KO+LPS
N
Cell Cycle
Gtse1
Tpx2
Cdca5
Bub1
Psma3
Mybl2
Psma7
Cenpa
Ncaph
Ccnb2
Npm1
Tk1
Smad3
Wrn
T2KO T2KO+LPS
2 0 -2
O
Arginine Metabolism
Otc
Gls
Glud1
T2KO T2KO+LPS

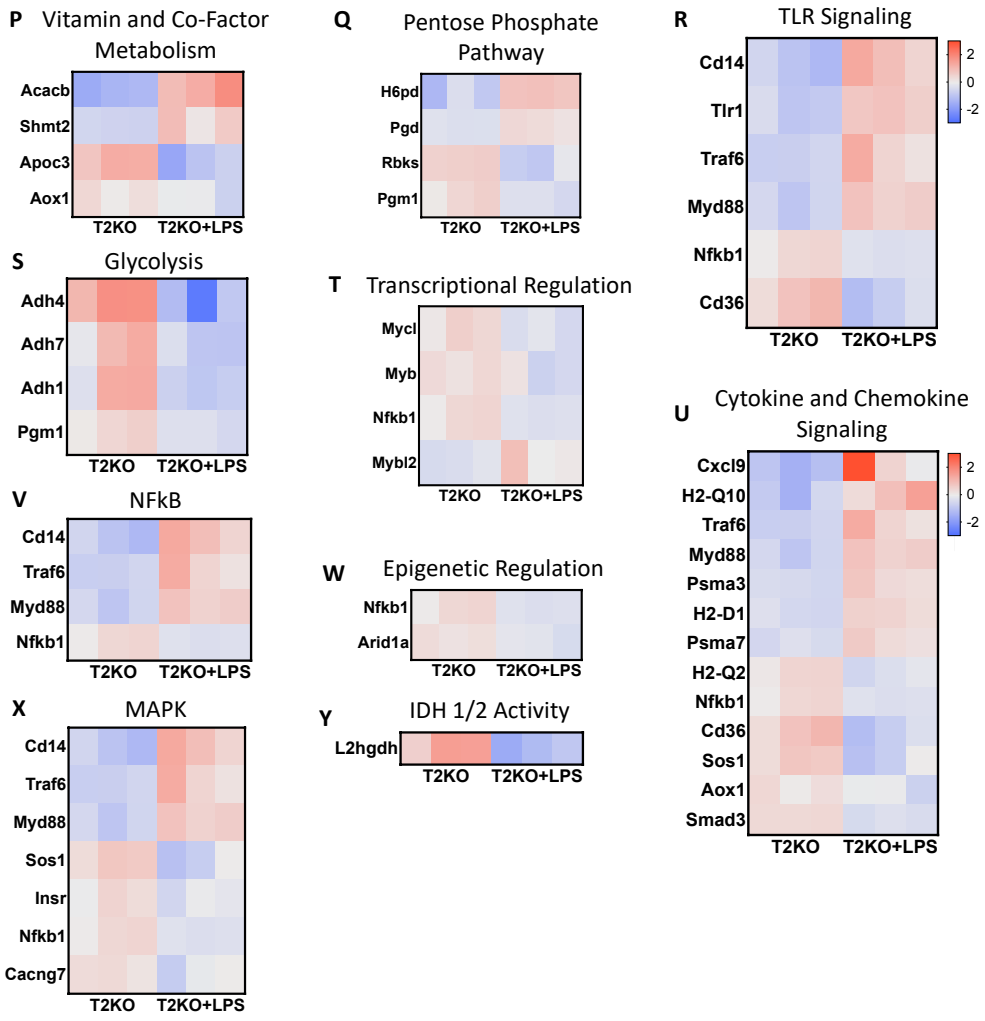
P
Vitamin and Co-Factor Metabolism
Acacb
Shmt2
Apoc3
Aox1
T2KO
T2KO+LPS
Q
Pentose Phosphate Pathway
H6pd
Pgd
Rbks
Pgm1
T2KO
T2KO+LPS
R
TLR Signaling
Cd14
Tlr1
Traf6
Myd88
Nfkb1
Cd36
T2KO
T2KO+LPS
2
0
-2
S
Glycolysis
Adh4
Adh7
Adh1
Pgm1
T2KO
T2KO+LPS
T
Transcriptional Regulation
Mycl
Myb
Nfkb1
Mybl2
T2KO
T2KO+LPS
U
Cytokine and Chemokine Signaling
Cxcl9
H2-Q10
Traf6
Myd88
Psma3
H2-D1
Psma7
H2-Q2
Nfkb1
Cd36
Sos1
Aox1
Smad3
T2KO
T2KO+LPS
2
0
-2
V
NFkB
Cd14
Traf6
Myd88
Nfkb1
T2KO
T2KO+LPS
W
Epigenetic Regulation
Nfkb1
Arid1a
T2KO
T2KO+LPS
X
MAPK
Cd14
Traf6
Myd88
Sos1
Insr
Nfkb1
Cacng7
T2KO
T2KO+LPS
Y
IDH 1/2 Activity
L2hgdh
T2KO
T2KO+LPS

# Chapter 5

## Monocyte recruitment is necessary for jejunal sex-specific response to IP-LPS

### *Introduction*

The intestinal tissue as mentioned previously, is home to a plethora of microorganisms. Their proximity to immune cells is thus a challenge, the microorganisms themselves and their secreted molecules are potential triggers of pro-inflammatory responses. Therefore, the resident population of immune cells must have intricate mechanisms of preventing an exacerbated immune response to keep the organ functioning. Many of the diseases that affect the intestine have dysregulated immune responses: generating an exacerbated inflammation that affects the intestinal epithelium, increase intestinal permeability and impact intestinal function (Ungaro *et al.*, 2017). This is the case for both ulcerative colitis and Crohn's disease.

Both are characterized by immune cell infiltrates, there is increased recruitment of immune cells to the tissue and their retention. Recruited cells, unlike intestinal resident cells, don't have the same mechanisms to prevent the cascade of pro-inflammatory response, thus further contributing to the pathogenesis. The circulation of these immune cells to the gut is a highly regulated mechanism, in which adhesion molecules are expressed in endothelial cells and immune cells weakly interact with it to migrate to their destination.

Mechanism for Immune Cell Recruitment

After an inflammatory response in the tissue, the recruitment of immune cells from outside the tissue use mainly the secretion of soluble molecules known as chemokines. These inflammatory mediators recruit vicinity immune cells to the site of infection and are able to bind the extracellular matrix or remain on the extracellular space, generating a concentration gradient that guides the migration of immune cells toward specific sites. Chemokines are recognized by specific receptors in immune cells to further specialize the tissue needs. For example, CCL2 chemokine expression is recognized by monocyte receptor CCR2, thus increasing the migration of monocytes to a CCL2 rich site.

The first cells recruited during inflammatory responses, including to IP-LPS inflammation are neutrophils. Neutrophils can respond as fast as 4hrs after an initial immune response, peaking usually between 24-48hrs. They are able to migrate from the blood because cytokines secreted in the tissue such as TNFα, affect the expression of adhesion molecules p-selectin and e-cadherin in adjacent blood vessels. Circulating neutrophils recognize adhesion molecules via sialyl-Lewis$^x$ receptor binding, slowing down their progression in blood vessel flow and facilitating stronger interactions with the endothelial cells that culminate with extravasation and transendothelial migration (Fournier and Parkos, 2012). Since neutrophils are very quickly recruited, their interaction with the tissue has implications for directing the immune response. During migration, neutrophils produce ADAM17, an enzyme that cleaves the inactive TNFα into its active form, contributing with the pro-inflammatory response (Cesaro *et al.*, 2009). Neutrophils can also further contribute to inflammation by regulating other cell types. For example, neutrophils

recognize interferon signaling and secrete CXCL9 in response. CXCL9 chemokine is used to recruit CD4+ T cells, which further modulate innate immune responses in a positive feedback loop (Chen *et al.*, 2019).

Mucosal organs, such as the intestine have specialized immune compartments with several adaptive immune cells ready to act in case of an immune response. In the jejunum, this specialized organ is called the Payer's patch. The payer's Patch has a high concentration of T cells, especially regulatory T cells that constantly try to decrease the inflammatory response of the organ. Treg cells constantly produce IL-10 during healthy lamina propria to dimmish innate immunity toward bacterial populations (Denning *et al.*, 2007).

Upon a phagocyte recognition of a PAMP via MHCII molecules, innate immune cells do migrate to payer's patch, but T cell activation at this location is still a matter of debate (Fournier and Parkos, 2012; Bamias, Rivera-Nieves and Grisham, 2018). Most migration has been shown to activate B cells, which interact with the T cell population and recognize a number of cytokines IL-4, IL-5 IL-21 and TGF-β to assist with IgA production from B cells (Bamias, Rivera-Nieves and Grisham, 2018).

Dendritic cells that have recognized PAMPs can also travel via lymphatic vessels toward lymphoid tissues and activate T cell to migrate toward intestinal tissue. This mechanism is time-consuming, as T cells need to be selected by antigen binding and expand their population by clonal expansion, limiting the response to 5-7 days post pathogen invasion and recognition.

During acute inflammatory responses, recruitment of innate immune cells via chemokines is the main mechanism of immune cell recruitment and can contribute to the inflammatory

response via amplification and activation of these innate cells as described (Bamias, Rivera-Nieves and Grisham, 2018).

Monocyte Recruitment is important for physiological and disease states

Monocytes from the bone marrow are attracted to the intestinal tissue via different sets of chemokines CCL8, CCL7 and CCL2. Monocytes recognize CCL2 chemokine via CCR2 and it is an important intestinal mechanism to replenish macrophage populations and induce tissue repair. Bone marrow derived monocyte is not the only mechanism of macrophage recruitment, as peritoneal macrophages also migrate to intestinal tissue during DAMP secretion and contribute to injury repair (Honda *et al.*, 2021).

Once monocytes are attracted to the intestinal tissue, these $CCR2^{+}$ cells are influenced by intestinal microenvironment and differentiate to macrophages or dendritic cells. This process is called monocyte maturation, and is characterized by gene expression modifications, loss of $CCR2^{hi}$ phenotype and increased expression of CX3CR1 to phenotypically acquire resident macrophage characteristics.

In the intestine the resident population of macrophages is heterogenous, and express different types of receptors and are replenished by different progenitors. The lamina propria has the most abundant population of macrophages that require a high level of replenishment from the circulating monocytes. The resident population is characterized by high levels of CX3CR1 and high MHCII, while recruited monocytes are CCR2hi, Ly6Ghi and CX3CR1int (Viola and Boeckxstaens, 2021). Upon arrival, the recruited cells slowly lose their monocyte characteristic by decreasing Ly6G and increasing both CX3CR1 and

MHCII, a process that lasts between 5-6 days. Early in the immune response, when CCR2+ monocytes first arrive in the tissue they differ themselves transcriptionally from the resident population, particularly in terms of complement system pathway, phagocytosis mechanisms and IL-10 (Viola and Boeckxstaens, 2021).

As described in chapter 3, the lamina propria macrophages are highly phagocytic, but unlike other macrophage resident population, upon TLR activation they inhibit the release of reactive oxygen species and nitric oxide. Since the CCR2 newly recruited cells differ in these aspects to their response to PAMPs, during certain intestinal conditions the CCL2-CCR2 axis acts as a pathogenic mechanism that further amplify inflammation in the tissue. During Crohn's disease for example, the microenvironment of a constant increased epithelial permeability drives bacterial molecules to activate TLR receptors. Recruited monocytes to this environment are influenced by mediators to further amplify immune response, contributing to Crohn's pathogenesis. There are high levels of CCL2 chemokine in intestinal tissue and pathogenesis is driven by this axis increasing recruitment of $CD14^{+}$ monocytes to the lamina propria (Martin *et al.*, 2019). Since Crohn's has a higher incidence in women, dissecting the sex-specific mechanisms that contribute to chemokine recruitment is of great importance to understand how sex impacts intestinal diseases that depends on this inflammatory axis.

Thus, here we investigate the role of CCR2 migrating cells in contributing to IP-LPS induced intestinal changes. Since females have a higher ccl2 gene expression in response to IP-LPS we hypothesized CCR2 cells would contribute to female jejunum response, but not male. We show that females increase $CCR2^{+}$ cells, while males do not; a mechanism

dependent on TREM2. Next, we use CCR2KO animals to investigate IP-LPS response and show that CCR2KO reverses changes in intestinal permeability characteristic of female response, but do not impact increased glucose absorption in male jejunum. Collectively, this data suggests female innate immune response in intestine relies on CCL2 in a mechanism that drives changes in permeability, while males do not.

## *Results*

Female recruitment of $CCR2^+$ cells is TREM2 dependent

To further explore the sex-differences observed in the jejunum response to IP-LPS that are controlled by TREM2 we decided to look for immune cell recruitment to the tissue. Females in our data showed an increased expression of ccl2, cxcl9, ccl8 and cxcl10, while males did not, suggesting the recruitment of immune cells to intestinal tissue might be mediating the changes in intestinal permeability. $CCR2^+$ cells recognize ccl2 chemokine and migrate toward target tissue, therefore our initial investigation focused in whether we observed an increased CCR2 recruitment to tissue after IP-LPS.

To investigate this matter, a transgenic mice model expressing RFP under the CCR2 promoter was used. Quantification of RFP cells is a direct measurement of CCR2 cells in intestinal tissue. Female mice increase CCR2 cells in jejunum 24hr after IP-LPS while males do not (Figure 5.1 A,B). The recruitment is TREM2 dependent, since TREM2KO mice fail to upregulate CCR2 cells in jejunum lamina propria (Figure 5.1 A, C).

CCR2 recruitment is necessary and sufficient for changes in intestinal permeability

Because CCR2+ cells migrating to tissue can amplify the initial immune response, we wanted to investigate if this specific cellular population was sufficient to induce changes in intestinal permeability. Animals of both sexes and genotypes were challenged with IP-LPS and cd11b+ population was isolated from spleen 24h later. Spleen cd11b monocytes are rich in CCR2, and do not express TREM2 (Shi & Pamer, 2011). These cells were cultured with confluent T84 cells *in vitro* in transwells. This set up allows cd11b isolated

cells to secrete substances to the media and influence T84 regulation, without the need of physical contact between cells nor the direct recognition of LPS by enterocytes (Fig. 5.2A). LPS activation of cd11b+ cells impacted the T84 cellular response, decreasing TEER in all groups (Fig. 5.2 B-E). There was no sex-specific effect, nor any genotype-specific effect, suggesting CCR2 cells are sufficient to change TEER after IP-LPS activation.

To further understand the requirement of monocyte recruitment via CCR2 to the tissue in developing sex-specific changes in intestinal permeability to IP-LPS we isolated jejunum tissue from CCR2KO male and female mice for ex vivo using chamber analysis. In the absence of CCR2 there was no effect in TEER, 4kDa FITC and IsC generated by IP-LPS in female mice (Fig. 5.2 F-H). Therefore, CCR2 recruitment is necessary for female effect in permeability. On the other hand, CCR2KO had no effect on male increase in glucose absorption 24hr after IP-LPS (Fig. 5.2 G), this result is consistent with our data on the lack of CCR2 recruitment in male jejunum (Figure 5.1).

CCR2KO jejunum fails to recapitulate inflammatory response

Since CCR2 cells seemed to be sufficient to recapitulate changes in jejunum permeability in females after IP-LPS, and necessary for their response we hypothesized gene expression to a pro-inflammatory profile would also be altered in CCR2KO animals.

For this purpose, nCounter Inflammatory gene expression was analyzed in male and female CCR2KO jejunum 24hr after IP-LPS. Again, the CCR2KO jejunum recapitulates a sex-specific response in gene expression even in the absence of changes in intestinal permeability. Female mice up-regulate more genes (Figure 5.3 A, B) than male mice

(Figure 5.3 C). This suggests the sex-specific effects in the gene signature of inflammatory response are not only driven by the recruitment of monocytes from outside the tissue, but rather an inherent resident macrophage or dendritic cell effect.

Regardless of the sex-specific effect, it is very clear that CCR2KO animals (Figure 5.3) respond with less inflammation than the WT female animals (Figure 3.3 A, C, D). The expression profile is characterized by complement proteins *c1qa, c3, c3ar1, c2, c4a* upregulation, a profile associated with a phagocytic role of immune cells, consistent with an intestinal response to LPS (Sina, Kemper and Derer, 2018). Many genes associated with an innate immunity pro-inflammatory response are also upregulated *irf7, ifi44, ifi27l2a*, stat1 all associated with an interferon response (Honda *et al.*, 2005), which are involved with intestinal repair (McElrath *et al.*, 2021) and also in an increased uptake of LPS (Suzuki, Hisamatsu and Podolsky, 2003).

Having already stablished that CCR2 recruitment is necessary for female increased intestinal permeability in response to IP-LPS, the gene expression data further supports that inflammatory up-regulation from resident immune cells is different in function than in the presence of recruited monocytes. Moreover, confirming that female intestinal permeability is dependent on an inflammatory response that needs recruitment of CCR2 cells.

CCR2KO and T2KO jejunum fails to recapitulate inflammatory response

Confirming the profile of gene expression between the different genotypes, we generated a MDS plot to analyze changes in sample variability (Figure 5.4A). The analysis shows

CCR2KO animals to have a completely different response to IP-LPS than TREM2KO and WT females. Surprinsingly, the effect of knocking out CCR2 is more drastic than TREM2. Since none of the volcano plot analysis allow a direct comparison between genotypes we decided to generate counts graphs for this purpose. The genes used in analysis were chosen because of their role in each genotype response: ccl2 in WT, cxcl9 in T2KO and c3 in CCR2 (Figure 5.4 B-G). Only these 3 genes were chosen because since we are not correcting for multiple comparisons, the higher the number of comparisons generated the higher the chance of a false positive finding.

Only females WT significantly increase ccl2 expression, with males and all other genotypes failing to do so (Figure 5.4 B,C). cxcl9 is increased only in WT females, suggesting CCR2KO also affects migration of cells independent of CCR2 response (Figure 5.4D). In male jejunum, cxcl9 is increased only in T2KO jejunum, showing how ablating this receptor affects neutrophil dependent migration in a sex-specific manner.

Lastly, CCR2KO regulated a lot of complement pathway genes, with the highest fold increase in c3. Therefore, we also generated the graph comparing normalized counts for all 3 genotypes and this time we failed to detect any significant changes across groups (Figure 5.4D, E).

Collectivelly, this data shows females IP-LPS response is dependent of CCR2 cell migration that occurs in a TREM2 dependent-manner. Knocking out this receptor in males does not impact their intestinal physiological response to IP-LPS by increasing glucose absorption. However, preventing CCR2 migrating cells to allocate to intestinal tissue we impact both male and female inflammatory gene expression in response to IP-LPS.

## *Discussion*

The intestinal tissue homes the largest number of macrophages in the body; its environment poses a strong challenge for this macrophage population. First, the lumen of the intestine is home to several bacterial molecules that could cause inflammatory responses and disturb intestinal homeostasis. Second, the macrophage population lie in close proximity to a single layer of intestinal epithelial cells at the lamina propria, therefore posing themselves as the first cell type to recognize and respond to DAMPs and PAMPs once breaches of intestinal permeability happen.

Non-surprisingly, because of the position of the macrophage population, a series of adaptations were made to further control the immune response and avoid unnecessary alterations to intestinal function. Resident macrophages phenotype allow them to prevent up-regulation of pro-inflammatory responses, even in the presence of bacterial molecules such as LPS (Nakata *et al.*, 2006). They express low levels of receptors that generate a pro-inflammatory response, including TREM1, TLRs (Hausmann *et al.*, 2002), and CD14 (Nakata *et al.*, 2006). And during development receive IL10 and TGFβ that downregulates both TNFα and NFκB response (Viola and Boeckxstaens, 2021).

Once an inflammatory response takes place, if chemokines are secreted such as ccl2, ccl8 and ccl5, monocytes are recruited to intestinal tissue from the bone marrow. Unlike the resident macrophage population, these CCR2 recruited cells are ready to mount a pro-inflammatory response, after differentiating into either macrophages or dendritic cells in intestinal tissue (Viola and Boeckxstaens, 2021). The $CCR2^{+}$ cells do not have the same

checkpoints to downregulate an inflammatory response and may act as inflammatory amplifiers.

Here, we observe this phenomenon at the 24hr timepoint post IP-LPS. Female mice recruit $CCR2^+$ cells to intestinal tissue at 24hrs, while males do not (Figure 5.1). The increase is TREM2 dependent, since TREM2KO females fail to recruit immune cells to tissue. This suggests an unknown mechanism in which TREM2 signaling is recruiting $CCR2^+$ cells.

To further explore the effect of CCR2 in modulating the immune response, CCR2KO jejunum permeability was measured 24hr after IP-LPS. CCR2 recruitment is necessary for the increased permeability in female jejunum, since CCR2KO females do not change permeability after IP-LPS (Figure 5.2). Suggesting in this case CCR2 recruitment is in fact necessary to amplify the initial immune response, and that is the mechanism of female intestine to generate a change in intestinal permeability and immune response.

Again, this data does not exclude the possibility of a CCR2 dependent effect in males earlier. The effect observed at 24hrs might not be because females have a higher pro-inflammatory response, but rather a different kinetics of response: males respond faster to IP-LPS, change intestinal permeability via $CCR2^+$ cell recruitment and resolve the inflammatory response at the 24hr timepoint while females are still mounting their response. The 24hr time-point is rather early in terms of generating an adaptive immune response, but rather late to detect pro-inflammatory cytokines generated by innate immunity after a single LPS challenge. More experiments are necessary to further understand sex-specific timeline of response.

This becomes even more important to comprehend since the effect of CCR2+ cell recruitment changes from model to model and depends again in the type of inflammatory response and its dependence on other immune cell types that modulate the immune response. In mouse model of inflammatory colitis, blocking CCR2 cell recruitment alleviates the intestinal inflammatory response and ameliorates the histological alterations associated with the disease (Tokuyama *et al.*, 2005). However, in terms of gene expression the same model does not decrease pro-inflammatory cytokine response, only those associated with Th2 and Th1 phenotype (Tokuyama *et al.*, 2005). In models of DSS induced colitis, both T cell and B cell are recruited to tissue since there is a chronic inflammatory response, therefore it is possible the effect we are observing in our model is only there during the initial innate immune response. CCR2KO models have also been shown to reduce expression of pro-inflammatory cytokines IL6 and IL-1β, even though TNFα levels are unchanged. Therefore, the improvement of DSS histological scores and permeability might be associated with these cytokines. In fact, in our model of inflammation, females increase expression of both *il6ra* and *il1rap* in response to IP-LPS (Figure 3.2) but fail to do so in CCR2KO (Figure 5.3) and TREM2KO jejunum (Figure 4.2).

In our model, the gene expression profile of CCR2KO showed other alterations at the 24h timepoint (Figure 5.4). CCR2KO jejunum fail to up-regulate inflammatory response in females and males after IP-LPS. Genes such as *tlr1*, *stat1* and *irf7* are still up-regulated, demonstrating that there is still an innate immune response occurring after IP-LPS in female jejunum, even though it not sufficient to change intestinal permeability (Figure 5.2).

Certain genes associated with complement system are up-regulated in female CCR2KO such as *c2, c1qa, c4a, c3*, so it is likely they are not increasing permeability in jejunum. The complement system is largely associated with phagocytosis by opsonization of molecules (Sina, Kemper and Derer, 2018), so this phagocytic gene signature in response to LPS occurs independent of CCR2 recruitment. In fact, papers that compare the responses of macrophages from intestine to other tissues have shown these cells to be highly phagocytic in nature: even though they have a decreased expression of pro-inflammatory receptors, they are readily to phagocyte antigens and microorganism more effective (Smythies *et al.*, 2005).

In our model, when cd11b+ cells, a population rich in CCR2+, are isolated from spleen and co-culture with intestinal epithelial cells, changes in intestinal permeability are independent of sex- and genotype. This is another proof of concept that the recruitment of cells outside of the intestine seem to be pivotal in the female stronger innate immune response to IP-LPS.

*Figures and Legends*

**Figure 5.1 Females recruit CCR2 cells to jejunum in a TREM2-dependent manner**
**A** - Histological representative sections of 20X jejunum villi of WT and T2KO, naïve and 24h after IP-LPS in females and males. Red represents CCR2-RFP, white arrows represent $CCR2^{+}$ cells, scale bar 30μm.
**B, C** – Number of cells positive for RFP per $\mu m^2$ in villi of both male and female CCR2-RFP +/- (**B**) or T2KO male and female CCR2-RFP +/- (**C**).

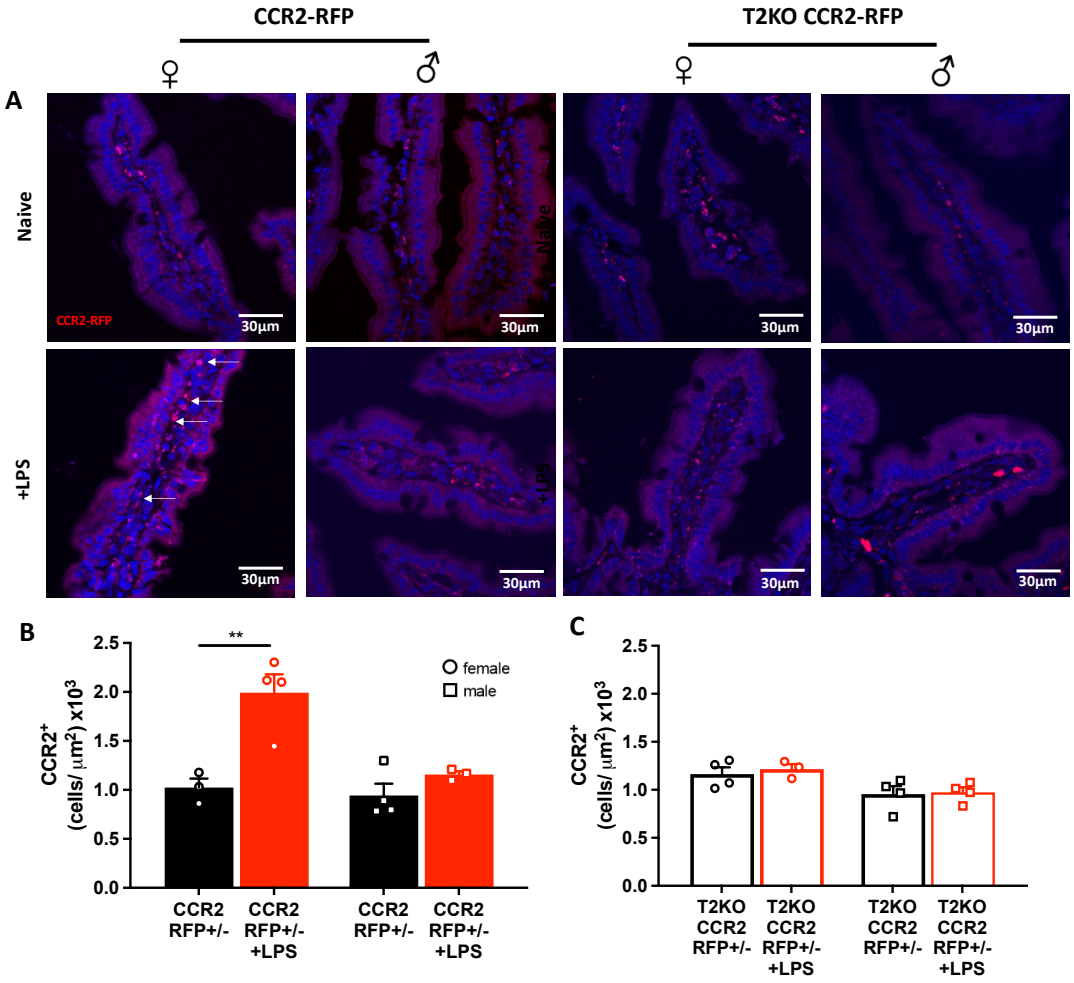
CCR2-RFP
T2KO CCR2-RFP
♀
♂
♀
♂
A
Naive
+LPS
CCR2-RFP
30µm
Naive
+LPS
B
C
**
female
male
CCR2+ (cells/ µm2) x103
2.5
2.0
1.5
1.0
0.5
0.0
CCR2 RFP+/-
CCR2 RFP+/- +LPS
CCR2 RFP+/-
CCR2 RFP+/- +LPS
T2KO CCR2 RFP+/-
T2KO CCR2 RFP+/- +LPS
T2KO CCR2 RFP+/-
T2KO CCR2 RFP+/- +LPS

**Figure 5.2 CCR2 is sufficient and necessary to drive changes in intestinal permeability**
**A** – Schematic figure of experimental design. WT and TREM2KO animals were injected with IP-LPS, 24h later spleen was collected and the cd11b cell population was isolated. The isolated cell population was co-cultured with confluent T84 cells in transwells and TEER was measured at 4, 24 and 48h post co-culture.
**B-E** – Time course of TEER from T84 cells co-cultured with cd11b+ cells isolated from male (**C,E**) and female (**B,D**) mice. Panels B and C represent cells isolated from WT mice naive and 24h after IP-LPS. Panels D and E represent cells isolated from TREM2KO mice naive and 24h after IP-LPS (n=3 independent experiments). Data showed as mean ± SEM, analyzed with two-way ANOVA, *p<0.05, **p<0.01
**F** – Ussing chamber transepithelial resistance (TEER) of jejunum in CCR2KO naive and 24h after IP-LPS in male and female mice (n= CCR2KO F (5), CCR2KO+LPS F(5), CCR2KO M (5), CCR2KO+LPS M(5) mice)).
**G** – 4kDa dextran FITC-conjugated permeability in jejunum of male and female WT naive and 24h after IP-LPS mice (n=3 mice, data represents total jejunum segments).
**H** – Current at rest in jejunum of male and female mice WT naive and 24h after IP-LPS (n= CCR2KO F (5), CCR2KO+LPS F(5), CCR2KO M (5), CCR2KO+LPS M(5)).
**I** – Peak of current after glucose in lumen of male and female jejunum WT naive and 24h after IP-LPS (n= CCR2KO F (5), CCR2KO+LPS F(5), CCR2KO M (5), CCR2KO+LPS M(5), total jejunum segments)
Data showed as mean ± SEM, analyzed with one-way ANOVA, Tukey multiple comparison analysis post-test (**F-I**). **p<0.01, ***p<0.001

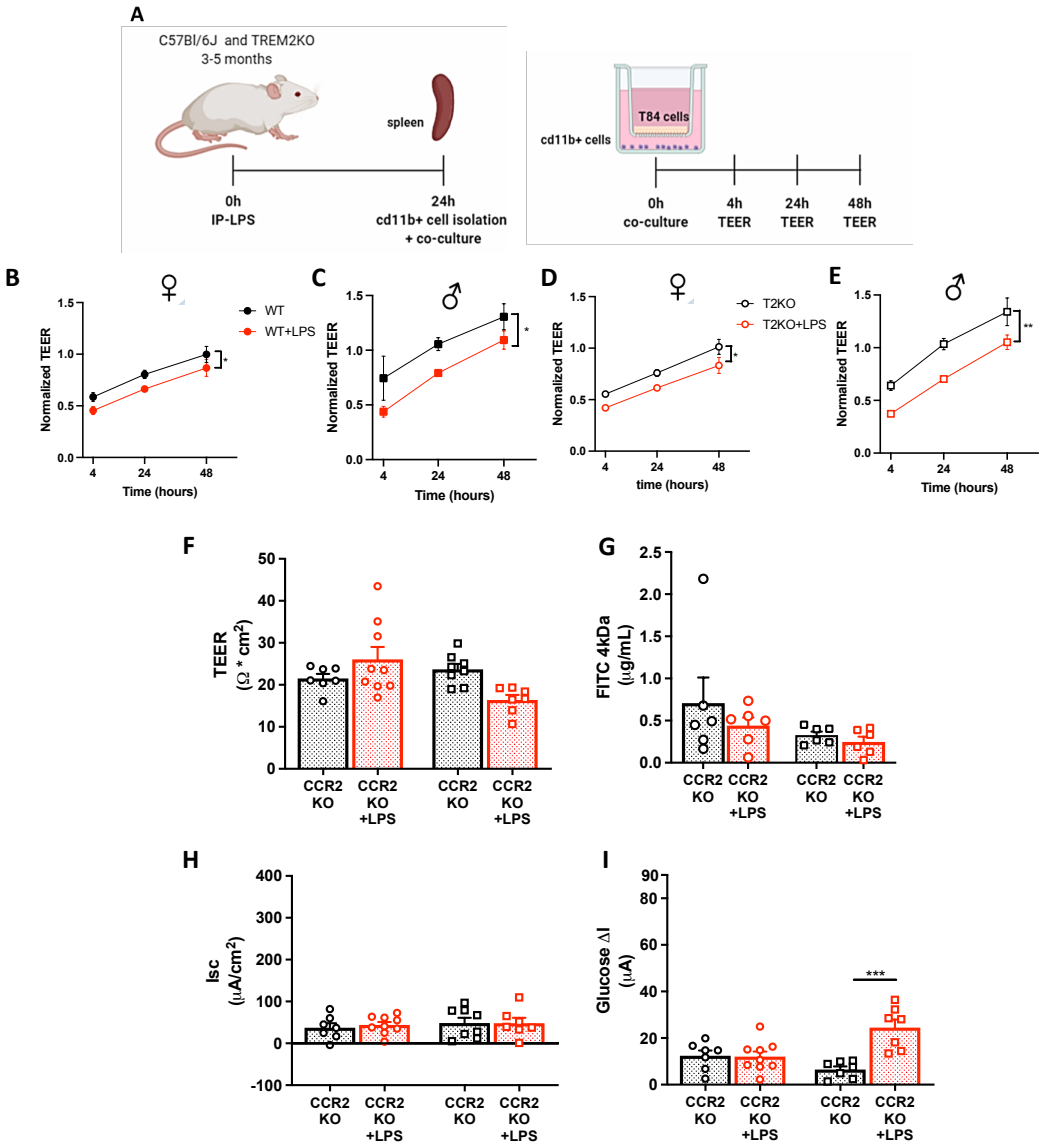
A
C57Bl/6J and TREM2KO
3-5 months
spleen
0h
IP-LPS
24h
cd11b+ cell isolation
+ co-culture
cd11b+ cells
T84 cells
0h
co-culture
4h
TEER
24h
TEER
48h
TEER
B
C
D
E
WT
WT+LPS
T2KO
T2KO+LPS
Normalized TEER
Time (hours)
time (hours)
F
TEER
(Ω * cm²)
G
FITC 4kDa
(µg/mL)
H
Isc
(µA/cm²)
I
Glucose ΔI
(µA)
CCR2 KO
CCR2 KO +LPS

**Figure 5.3 CCR2KO gene expression shows sex-specific response different than WT**

**A,B**– NanoString metabolic panel volcano plot analysis by Rosalind Software of differentially regulated gene expression in response to inflammation in T2KO females (**A**) and males (**B**). Red represents significantly upregulated genes and blue represents significantly downregulated genes with p-value adjusted to multiple comparisons by Benjamin-Yekutieli method. n=3 animals per group

**C** – Fold change and adj.p-value of genes from volcano plot analysis in females.

**D** – List of Pathway Global Significance Scores in NanoString Metabolic cartridge panel. Only pathways with a higher score than 2 are included in analysis. Global significance scores are calculated based on the sum of the combined t-tests of differentially expressed genes in each pathway. N=3 per group

**E** – Heatmap expression with significantly regulated genes from volcano plots for females.

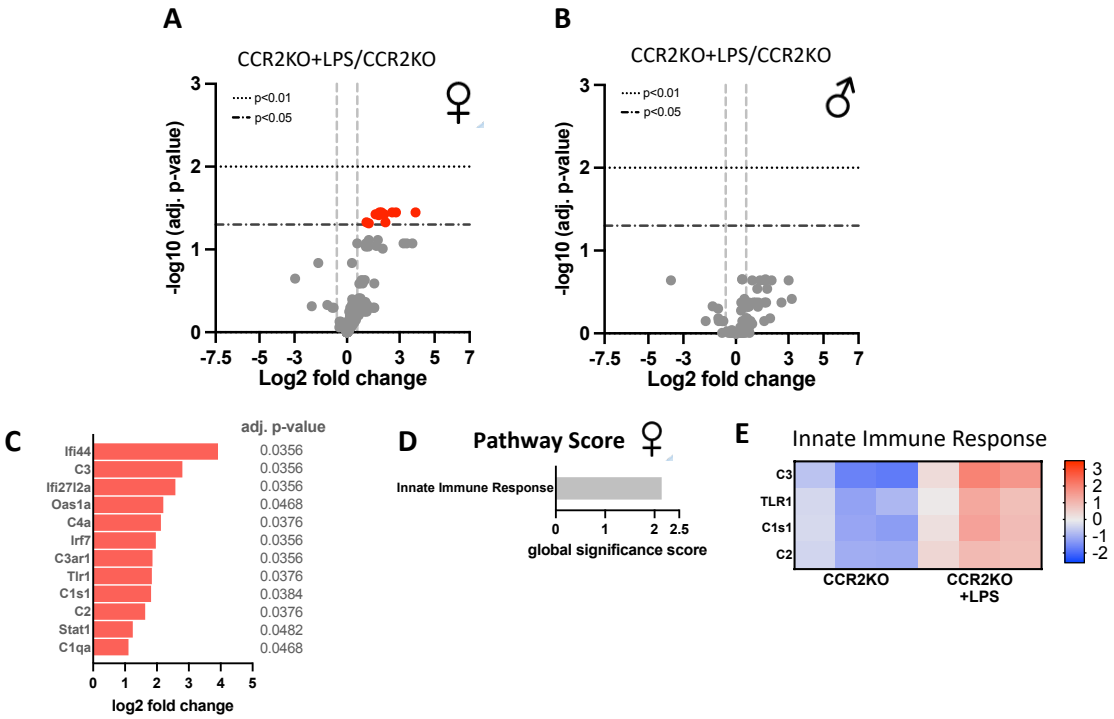
A
CCR2KO+LPS/CCR2KO
p<0.01
p<0.05
-log10 (adj. p-value)
Log2 fold change
B
CCR2KO+LPS/CCR2KO
p<0.01
p<0.05
-log10 (adj. p-value)
Log2 fold change
C
adj. p-value
Ifi44 0.0356
C3 0.0356
Ifi27l2a 0.0356
Oas1a 0.0468
C4a 0.0376
Irf7 0.0356
C3ar1 0.0356
Tlr1 0.0376
C1s1 0.0384
C2 0.0376
Stat1 0.0482
C1qa 0.0468
log2 fold change
D
Pathway Score
Innate Immune Response
global significance score
E
Innate Immune Response
C3
TLR1
C1s1
C2
CCR2KO
CCR2KO +LPS

**Figure 5.4 Comparison of CCR2KO with TREM2KO and WT jejunum**

**A** – Multidimensional Scaling Plot generated by Rosalind Software of sample clustering according to similarities in gene expression

**B-G** – Graphs generated from normalized counts of each analysis for comparison between different genotypes for females (**B, D, F**) and males (**C, E, G**). The following genes were analyzed: ccl2 (**B, D**), cxcl9 (**E, F**), c3 (**G, H**). N=3-5 per group.

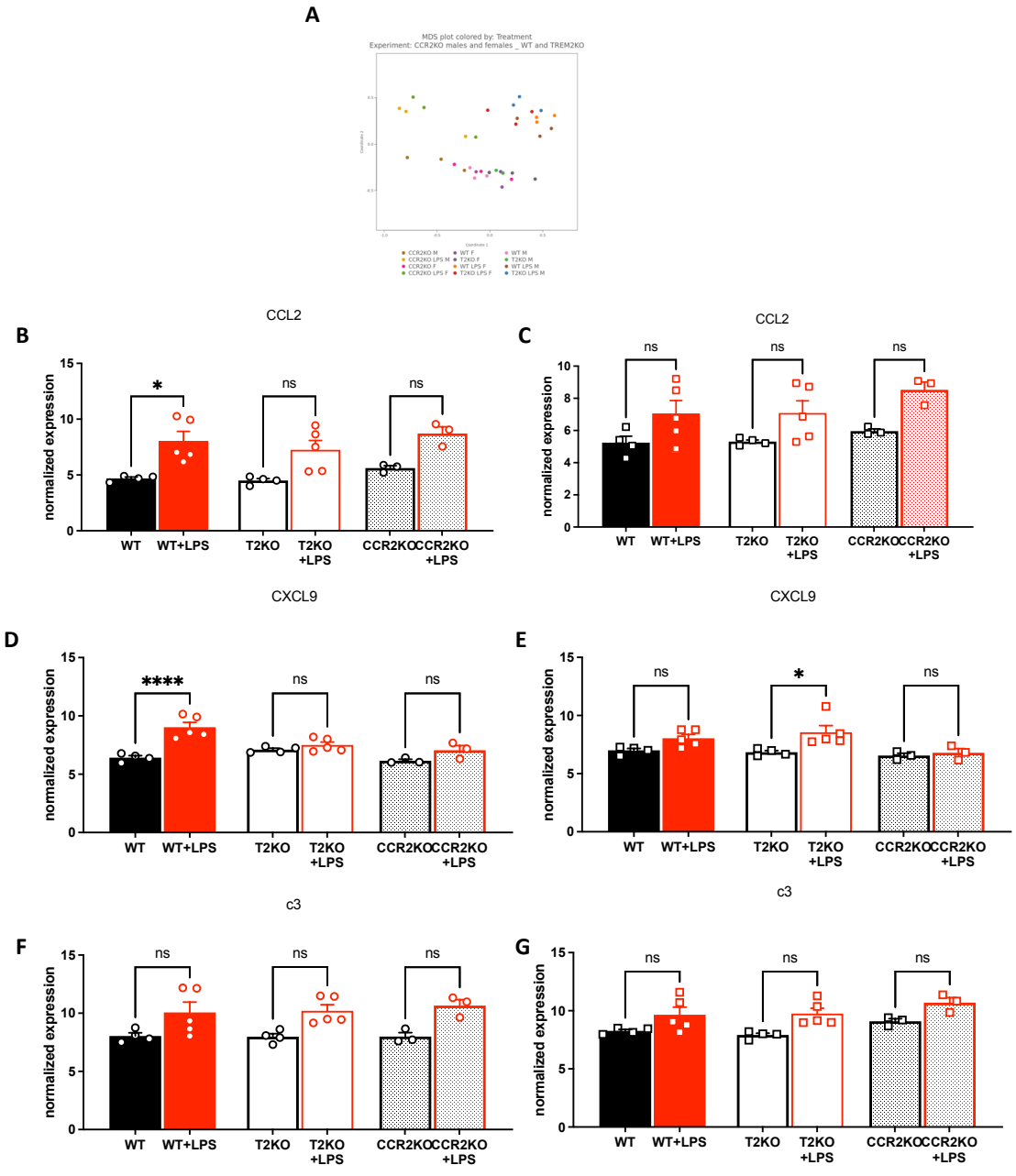
A
MDS plot colored by: Treatment
Experiment: CCR2KO males and females _ WT and TREM2KO
B
CCL2
normalized expression
*
ns
ns
WT
WT+LPS
T2KO
T2KO +LPS
CCR2KO
CCR2KO +LPS
C
CCL2
ns
ns
ns
D
CXCL9
****
E
CXCL9
*
F
c3
G
c3

# Chapter 6

## Allergic lung Inflammation produces sex-specific brain alterations

### *Introduction*

This chapter will now explore a second model for the investigation of sex-specific responses to inflammation, this time focusing on the lung-brain axis. The introduction first sub-section will explain the model we use to induce lung inflammation and its consequence to lung function. The second sub-section will focus on the fibers that conduct the information from lung to brain. The third and last sub-section focuses on how the brian impacts lung function.

#### Lung allergic Inflammation and Alternaria

*Alternaria alternata* is a fungus known to infect plants, including fruits, vegetables and grass and is recognized by the presence of dark black spots (Thomma, 2003). Although extremely common in outdoor environments, *Alternaria alternata* can also grow in indoor humid environments (Abbott, 2003). Its spores are released in dry air and can survive for a wide range of temperatures including -5 to 35$^{o}$C (Hernandez-Ramirez *et al.*, 2021). Because of its ability to adapt well, *Alternaria alternata* is the most prevalent fungi in the United States, known to grow indoors and outdoors (Hernandez-Ramirez *et al.*, 2021); as well be found throughout other countries of Europe, China, Canada, and Australia (Zureik *et al.*, 2002; Guan *et al.*, 2019).

*Alternaria alternata* has more than fifteen different allergens that induce a hyperreactivity of the immune system and is clinically associated to asthma development (Bush and Prochnau, 2004). Upon breathing Alternaria into the lung, both lung epithelial cells and resident innate immune cells are capable of recognizing Alternaria particles via TLR2 and TLR4 receptors (Hayes *et al.*, 2018). Since extracts of Alternaria are composed of a mixture of substances that act as allergens, it is unclear which particles elicit the responses, non-surprinsingly, TLR2/4 are not the only receptors known to be associated with Alternaria alternata inflammation.

During a regular immune response of the lung, PAMPs are recognized and innate immune cells respond with an inflammatory reaction that is acute. Adaptive immune cells can be recruited and pathogen is eliminated, as described during the introductory chapter of this dissertation.

Sometimes non-pathogenic stimuli are recognized by the immune system, generating a series of alterations in the immune response known as hypersensitivity. This happens because during recognition of the molecule by the immune system, non-classical cytokines IL-33, IL-25 IL-4 and IL-13 are produced (Hernandez-Ramirez *et al.*, 2021), as it happens during *Alternaria alternata* recognition (Figure 6.1). These cytokines recruit eosinophils, a population of cells that are characteristic of allergic inflammation; change B cell antibody toward IgE; and activate mast cells to release histamine and other granules that will contribute to allergic symptoms.

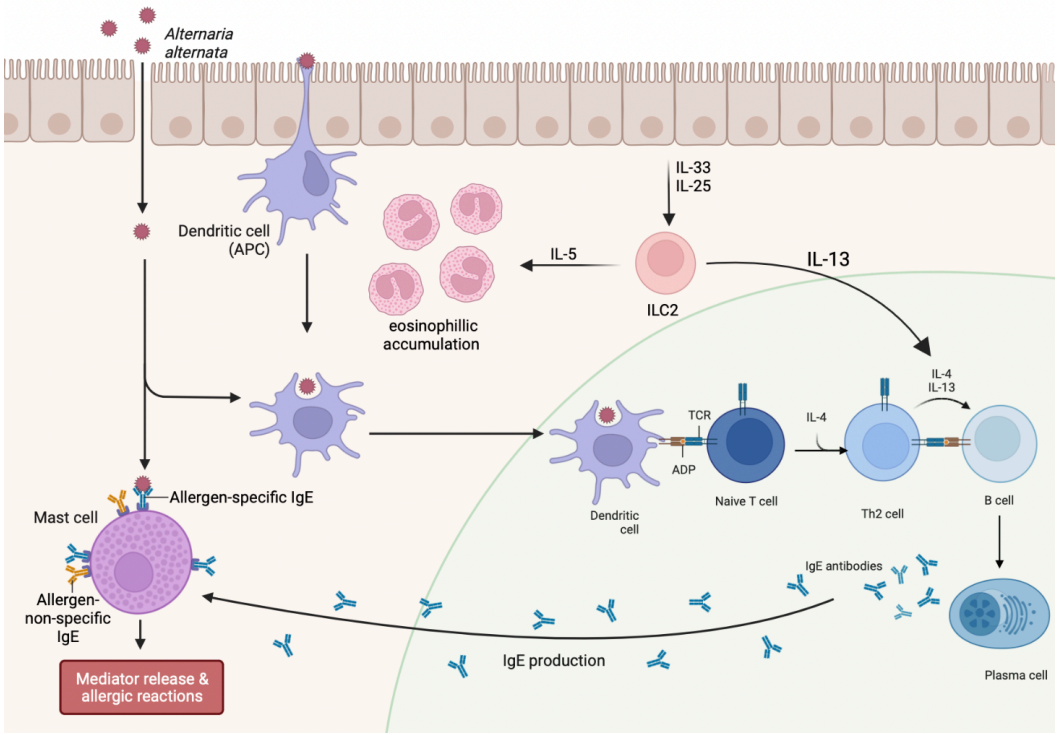


**Figure 6.1. Immune response to allergens.** *Alternaria alternata* is recognized by dendritic cells and alveoli epithelial cells via TLRs. Dendritic cells present the antigen derived peptide (ADP) to T cells, which activate, expand clonally and give rise to Th2 cells. T cells than will activate B cells into plasma cells. One major player in the allergic immune response is the group 2 innate lymphoid cell (ILC2). It recognizes IL-33 and IL-25 released by the epithelium and in turn secretes IL-13, which induces a class switch of B cell antibody toward IgE; and IL-5, which induces the accumulation of eosinophils.

The allergic immune response is responsible for inducing bronchoconstriction in a mechanism dependent of mast cells. IgE antibodies are recognized by mast cells upon contact with allergen and lead to degranulation. Among the active substances released the most notorious in asthma pathophysiology is histamine. Histamine is capable of producing bronchoconstriction and vasodilation, which both increases fluid accumulation in lung, facilitates immune cell infiltration and hinder oxygen and carbon dioxide exchange (Fanelli *et al.*, 1994). In animal models of the disease, breathing Alternaria continuously for a

period of 5 days (1500μg/$m^3$) is sufficient to induce the migration of neutrophils, eosinophils, B cells and T cells to lung (Peng *et al.*, 2018).

Given the theme of sex-specific differences within this dissertation, it is worth mentioning that allergic diseases have a very big sex divergence. Allergic diseases such as asthma affect more women than men (Chowdhury *et al.*, 2021), and symptomatic presentation of disease is more severe in woman than man (Chowdhury *et al.*, 2021). In fact, symptoms of allergy such as bronchoconstriction have been shown to be more responsive in females in both human and animal data regardless of inflammation (Langdeau *et al.*, 2000). Mechanistically explanations for the sex-effect in asthma haven't been throughouly explored in the literature, although smaller anatomical size of bronchi correlates with increased female bronchoconstriction response (Langdeau *et al.*, 2000).

From lung to brain communication

The lungs are innervated by fibers that sense alterations in lung environment and respond with specificity depending on stimuli. And this is also the case for allergic lung responses. These fibers have differences in molecular markers, conduction velocity and transduction of information. These classifications overlap with each other, making it hard sometimes to isolate a specific type of sensory fiber. To tackle this issue, the dissertation will focus on conduction velocity, explaining the overlap of the other classifications when necessary. There are two main types of conduction velocity fibers: A-fibers, that conduct very fast action potentials when activated and are myelinated; and C-fibers, that are unmyelinated slow responsive fibers.

A-fibers express voltage-gated sodium channels 1.1 (Nav1.1) and Nav 1.6 to generate a response to sensory information. Most A-fibers transduce mechanical stretching of internal organs including the lung (Kollarik, Ru and Brozmanova, 2010) and are named mechanosensory fibers. The capability to adapt to mechanical stimulation further classify A-fibers into fast-adapting receptors or slow adapting receptors (Kubin *et al.*, 2006).

Slow adapting pulmonary A-fibers have stretch receptors that respond to mechanical stimuli. They innervate smooth muscle located at the submucosa of central airways (Bartlett and Sant'ambrogio, 1976) and are activated by lung inflation during inspiration in normal breathing and by very low levels of CO2 (Peterson *et al.*, 1981). When activated they inhibit inspiratory activity (Motoyama and Finder, 2011).

Rapid Adapting Receptors are another class of mechanosensory A-fibers that respond to a wide range of stimuli. They are capable of firing during lung collapse, or lung inflation and sense changes in the physical lung environment: changes in interstitial or luminal pressure, changes in diameter, bronchoconstriction, among others. These fibers are thought to play a role in the initiation of cough. Molecular analysis has suggested Piezo2 to transduce mechanosensory information in these rapid adapting A-fibers (Nonomura *et al.*, 2017).

Even though most A-fibers are mechanosensors, a portion of them is capable of transducing cold temperature sensory information. These fibers express TRPM8, a receptor that opens in response to decreases in temperature (McKemy, Neuhausser and Julius, 2002).

The second type of fibers that are present in lung innervation are C-fibers, the most abundant type of sensory fibers innervating the lung and are classified based on their slow response to stimuli. These are unmyelinated fibers with free nerve endings that sense

noxious stimuli including pain and heat and express voltage gated sodium channels 1.7 (Nav1.7), Nav1.9 and Nav 1.8.

C-fibers sense noxious stimuli through a variety of different channels: TRPV1 channels are capsaicin responding channels that transduce changes in heat and are responsible for noxious hyperalgesia behavior (Shuba, 2020). TRPA1 expression drives the translation of cold and stretch irritants (Talavera *et al.*, 2020). TRPC3 and TRPC6 are channels that sense mechanosensory information and are expressed within a subset of C-fibers. These receptors overlap in expression, therefore TRPV1 noxious heat sensing fibers can also express TRPC3 and sense mechanosensory information, although uncommon (Mickle, Shepherd and Mohapatra, 2016). Because of the polymodal nature of sensory fibers, inflammatory stimuli can affect a variety of different subsets of sensory information. For example, eosinophil granules activate C-fibers and enhance their mechanical and chemical sensitivities (Dempsey, 2015).

Inflammatory mediators are known to activate nociceptor C-fibers. This is due in part to their expression of receptors that sense inflammation. They express a variety of toll-like receptors (Diogenes *et al.*, 2011), cytokine receptors (Ferreira *et al.*, 1988), and prostaglandin receptors (Tavares-Ferreira *et al.*, 2022), and have been implicated in the pathophysiology of asthma. In animal models, deletion of nociception fibers during allergic inflammation reduces immune cell infiltration in lung (Talbot *et al.*, 2015). Moreover, nociceptor fibers promote B cell antibody class switch toward IgE, contributing to allergic reactions (Mathur *et al.*, 2021). Allergy is capable of modifying the transcriptional landscape of nociceptor fibers, increasing cytokine expression and neuropeptide release

(Crosson *et al.*, 2023). Despite the strong sex interaction and influence in asthma, and the role of nociceptor in contributing to pathology, there are limited investigations toward sex specific differences in nociceptor regulatory mechanisms. One study does suggest sex regulation is involved: nociceptor fibers express more prostaglandin receptors at baseline in females than males (Tavares-Ferreira *et al.*, 2022), and female nociceptors secrete more neuropeptides that regulate the immune response than males (Crosson *et al.*, 2023).

All nociceptive fibers express the voltage-gated sodium channel 1.8 (Nav1.8), allowing for the genetic targeting of this population. One strategy to eliminate nociceptive information from arriving into the brain is to use an animal model with cre expression driven by Nav1.8 and diphterin toxin A (DTA) expression with a STOP locus between two loxp sites (Nassar *et al.*, 2004; Voehringer, Liang and Locksley, 2008). This model has been extensively characterized in the literature since 2008 (Abrahamsen *et al.*, 2008).

Nav1.8 selective ablation via Nav1.8 x DTA affects 80% of C-fibers, with little impact on A-fibers. Therefore, there is a decrease in TRPV1, TRPC3, TRPC6 and TRPA1 expression, C-fiber markers, without changing levels of TRPM8 (Abrahamsen *et al.*, 2008), an A-fiber marker. Behavior analysis of Nav1.8x DTA mice has shown that inflammatory thermal hyperalgesia detection is impaired (Abrahamsen *et al.*, 2008), a classically described TRPV1 behavior. Moreover, close to 96% of TRPV1+ fibers are deleted upon Nav1.8xDTA ablation. This provides a very useful tool to investigate the role of these fibers in allergic responses.

Sensory fibers from the lung have cell bodies in nodose and jugular ganglion before arriving with the information in the medulla region of the brainstem (Hiroki *et al.*, 2021),

into the nuclei of the solitary tract (NTS). These brain regions are capable of communicating with many centers within the brainstem that regulate breathing patterns, cardiovascular functions and further promote feedback to peripheral organs based on the received information.

From brain to lung communication

The literature provides very strong evidence that fibers innervating internal organs including the lung are collecting information about their inflammatory milieu. Once the information from lung and other internal organs reach the NTS, the NTS contacts a variety of brain regions to regulate many relevant functions of lung response during allergic reactions. These include: breathing rhythms, bronchoconstriction and lung immune cell infiltration.

Breathing rhythms are regulated by a variety of interactions within different parts of the medulla. Two different regions are thought of as the breathing pattern generators of the brain: The BötC and the pre BötC (Yackle, 2023). The pre BötC sends projections to the rostral ventral respiratory group mediating motorneuron innervation of the diaphragm. Activation of pre BötC drives inspiration by contracting the diaphragm. Expiratory phase of breathing is thought to be rather passive, and is mediated by the BötC inhibitory influence on pre BötC neurons (Yackle, 2023). The NTS comes into play by affecting these breathing patterns and contacting BötC, preBötC and ventral respiratory group with information from lung environment to modulate breathing. Given the different number of regions involved in breathing rhythmns, there are a series of described neuronal diversity

within the NTS that mediates the control of this response. Phox2b$^{+}$ neurons within the NTS contact all 3 regions and mediate an increase in breathing patterns when activated (Fu *et al.*, 2019). In fact, activation of fibers arriving at the NTS is sufficient to induce changes in breathing patterns, even in fibers in which the medullary contacting regions haven't been described. For example, activation of p2ry1$^{+}$ fibers that arrive within the NTS is sufficient to induce apnea and alter normal breathing patterns. At the same time, activation of npy2r$^{+}$ fibers that arrive within the NTS is sufficient to induce a rapid and shallow breathing pattern (Chang *et al.*, 2015). These studies point to the NTS as a major regulator of breathing rhythms and show how much lung environment and lung inflammation influence this response.

For bronchoconstriction, the circuitry has recently been characterized in a pre-print work. The NTS has a population of fibers dbh$^{+}$, phox2b$^{+}$ that are mainly responsible for relaying the information to the nucleus ambiguous by an increase in their firing rate. The nucleus ambiguous has a high density of cholinergic fibers that synapse back into the lung and generate bronchoconstriction via acetylcholine release (Su *et al.*, 2023). Lung allergic response increase the activation of bronchoconstriction fibers, inducing a pathway for brain mediated bronchoconstriction during allergy.

The control of the inflammatory response by the NTS is still a matter of growing research. The dorsomotor nucleus of the vagus (DMV) is responsible to carry out the information from the brain that arrived via the NTS and its release of acetylcholine modulates T cell, B cell and innate immune infiltration in a variety of models (Borovikova *et al.*, 2000; Pavlov *et al.*, 2006). During allergic inflammation, ablation of the nociceptor fibers that arrive

from the lung into the NTS is capable of downregulating the migration of eosinophils, macrophages, T cells and B cells into lung (Talbot *et al.*, 2015) and modulating T cell response in non-allergic models (Baral *et al.*, 2018). These models propose neuropeptide direct release from nociceptor fibers as the mechanism for this response. Whether this information is also central nervous system dependent or mediated solely by peripheral fibers remains to be investigated.

Given the role of the NTS in modulating a series of lung functions; synaptic plasticity and alterations within the NTS region have a dramatic effect in peripheral organs. Given the sex-specific alterations in allergic inflammatory responses and nociceptive fibers that arrive within the NTS, we wanted to investigate their role in mediating sex-specific alterations in allergy. Here, we demonstrate nociceptor fibers have a sex-specific synaptic plasticity response within the NTS that is driven by lung inflammation. The effect shows females to be more responsive regardless of the type of lung inflammation, but directionally of NTS response is both dose- and type-dependent. This study provides an insight into sex-specific mechanisms of lung disease.

## *Results*

Airborne Alternaria extract exposure for one week triggers lung inflammation that is reversible after cessation of exposure

*Alternaria alternata* has been shown to elicit an allergic immune response in the lung with the migration of both innate and adaptive immune cells to the tissue (Peng *et al.*, 2018). To characterize the sex-specific lung inflammatory response to *Alternaria alternata*, we exposed mice for 7 days to either non-infectious *Alternaria alternata* extract particles or filtered air (Figure 6.2 A). Afterwards, the lung was flushed with PBS for the collection of immune cells in bronchoalveolar fluid (BALF) as previously described (Biddle *et al.*, 2023). Both males and females show an overall increase in immune cell infiltration $CD45^+$ to lung (Figure 6.2 C, D). Since the data is expressed in number of magnitude, one interesting effect is that males have an overall larger $CD45^+$ cell migration than what females do (Figure 6.2 B, C).

Next, gates were selected to isolate specific populations of innate immune cells: $CD45^+/CD11c^+/SingleF^+$ alveolar macrophages, $CD45^+/CD11c^-/CD11b^+/SinglecF^+$ eosinophils and $CD45^+/CD11c^-/CD11b^+/Ly6G^+$ neutrophils (Figure 6.2 D). The Alternaria effect is consistent for both sexes in almost all cell types investigated. Neutrophils are increased in both males and females after *Alternaria alternata* exposure, with a trend for the eosinophilic population (Figure 6.2 G-N). Eosinophils characterize the response as allergic, corroborating with previous exposures of Alternaria (Biddle *et al.*, 2023). Macrophages are the only cell type investigated that do not change in number after *Alternaria alternata* exposure (Figure 6.2 E,F), again in both sexes.

To understand how long-lasting these effects were, mice exposed to 1 week of *Alternaria alternata* were transferred to an air chamber for another week and had their bronchoalveolar lavage fluid (BALF) collected for analysis (Rev group). Despite the increase in lung immune cells, 7 days of filtered air is sufficient to reverse immune cell infiltration in both males and females (Figure 6.2 C-N).

Adaptive immune cells recruitment to the lung increase in both males and females after *Alternaria alternata* exposure, and effect is reversed after breathing filtered air for 1 week

Same experimental design is used to investigate lung infiltration of adaptive immune cells (Figure 6.3 A). Cells are gated by size, and expression of CD19 and CD3 markers are used to selectively quantify B and T cell infiltration (Figure 6.3 B). Same pattern observed for innate immunity is shown here. Both males and females increase adaptive immune cell migration to tissue (Figure 6.3 C-F), that is fully reversed after 1 week of filtered air. Magnitude of response is higher for males in both cell types.

Collectively data suggests *Alternaria alternata* does not elicit a sex-specific response to lung immune cell infiltration in terms of cell types infiltrating and tissue recovery. But does suggest magnitude of response is higher in males, although direct comparison experiments are necessary to draw more conclusions.

Medulla has sex-specific alterations in excitatory synaptic numbers after *Alternaria alternata* exposure

Lung sensory information, including changes in the inflammatory milieu, are sent to the medulla in the NTS region. To investigate the effects of allergic lung inflammation in this region, we collected the medulla from male and female mice 7 days after *Alternaria alternata* exposure (Alt group). Females had a reduced amount of excitatory synaptic markers vglut2 and PSD-95 (Figure 6.4 A-C) when compared to a matched filtered air breathing control. Overall pre-synaptic proteins are not affected (Figure 6.4 D).

In males, no changes are detected in protein expression of synaptic markers in the medulla (Figure 6.4 E-H). This data suggests a sex-specific modulation of the lung information arriving at the medullary center, even in the event of a similar lung immune response (Figure 6.2).

BötC or pre- BötC breathing regions are not impacted by changes in synaptic numbers

The medulla comprises many different regions that are responsible for a variety of lung functions. Most notably, the respiratory centers of the brain that regulate breathing patterns are localized to medulla and pons within the brainstem (Yackle, 2023). To understand if the decreased excitatory protein levels within female brainstem were localized to breathing regions Bötc and preBötc (Figure 6.5 A, E) we measured pre-synaptic puncta numbers in both centers (Figure 6.5 B, F).

Co-localized vglut2 and synaptophysin are used to determine changes in excitatory synaptic levels (Herzog *et al.*, 2006). Here, no changes were observed in males nor females

within these regions (Figure 6.5 C,D,G,H), the n is small, so more animals need to be added before drawing conclusions on effect in Bötc and preBötc.

Sex-specific alterations in excitatory synapses are localized to NTS region

Sensory information is known to be plastic and interoception neurons respond to lung inflammatory mediators synapsing into NTS (Hiroki *et al.*, 2021). Therefore, we next investigated if the NTS would have changes in vglut2 synaptic protein levels after *Alternaria alternata* exposure. Again, to avoid measuring vglut2 not localized to synaptic terminals, we co-localized vglut2 and synaptophysin and measured co-localized synaptic puncta (Figure 6.6 A,B).

The NTS shows a decreased number of excitatory co-localized puncta in females, but not males (Figure 6.6 A, C,D). This data suggests the alterations within medulla are localized to the NTS region, that receives lung sensory information. Once again, to understand how long-lasting NTS effects are, reversal mice had their synaptic puncta quantified after 1 week breathing filtered air. During this time-point, all the infiltration of immune cells have already returned to baseline (Figure 6.2).

Reversal group shows complete reversal of effect in female NTS puncta (Figure 6.6 C) and no change in male NTS (Figure 6.6 D).

GeoMx shows differing cell signaling activation in male and female NTS without changes in inflammatory markers of glial cells

Next, we wanted to explore the mechanisms within the NTS that would explain the differences in males and females after *Alternaria alternata* exposure. For this purpose, we used GeoMx spatial protein quantification, in which using antibody binding we are able to quantify within a specific region, the amount of protein associated with a biological function. Tyrosine hydroxylase antibody was used as a marker of the NTS region (Figure 6.7 A), as NTS sends adrenergic fibers to other brain regions and is characterized by a high density of these fibers as previously described (Carrettiero, Ferrari and Fior-Chadi, 2012). We selected a portion of the NTS known to be enriched with lung interoception fibers (Zhao *et al.*, 2022) for collection (Figure 6.5 B).

The region of interest collected has the information of protein expression associated with neuronal markers, glial markers, autophagy associated markers, PI3K/AKT signaling and MAPK signaling, a list of proteins are provided in the methods section of this document (Figure 2.2).

Volcano plots generated with the significant changes in protein expression show a strikingly difference between males and females in proteins associated with signaling cascades from MAPK and PI3K/AKT. Females downregulate p-S6, a protein activated by c-fos and used as a proxy for neuronal activation (Knight *et al.*, 2012), corroborating with our decreased excitatory puncta in females only. Females also upregulate p-GSK3β and in pan-RAS protein in response to *Alternaria alternata* exposure (Figure 6.7 C).

Males on the other hand only up-regulate molecules associated with MAPK and PI3K signaling cascades: p-JNK and p-AMPK (Figure 6.7 D). This suggests a difference in signaling cascades being activated in response to *Alternaria alternata* in males and females.

An important consequence of this data is that none of the stress markers of autophagy, nor proteins associated with glial reactivity: IBA1, cd11b, MHCII, CD68, TMEM119, GFAP, S100B show any alteration in our model. This suggests the changes in synaptic numbers are not occurring because of glial reactivity or neuronal stress, and are more likely a synaptic plasticity response to lung allergic inflammation in female NTS, not shared by males.

To understand how long-lasting the Alternaria changes to the NTS would be, we next investigated GeoMx protein alterations in Reversal animals. Both male and female NTS protein changes return to baseline levels after 1 week breathing air (Figure 6.7 E,F).

Glial cells play a role in synaptic plasticity in the absence of reactivity markers

Glial cells play important roles in supporting neuronal function in the absence of neuroinflammation and glial reactivity. Microglial cells regulate synaptic numbers and neuronal activity in normal brain (Badimon *et al.*, 2020), while astrocytic cells regulate metabolic changes and neurotransmitter availability in neurons (Su *et al.*, 2003). We next sought to understand if the alterations in males and females were associated with glial function alterations.

Females decrease astrocytic glutamate transporter EAAT2 after *Alternaria alternata* exposure (Figure 6.8 A,B). Males do not change EAAT2 expression (Figure 6.8 A,C). Since EAAT2 uptake glutamate and contribute to glutamate availability at synapse it is possible effect is decreased because less excitatory synapses are present.

As predicted by GeoMx analysis, neither IBA1 expression nor cell numbers are changed in microglia within the NTS in males or females (Figure 6.8 D-H).

Genetic ablation of nociception neurons prevents alterations in NTS excitatory puncta

To further investigate which component of our immune response in the lung was causing the NTS alterations in females, we decided to selectively ablate nociceptor fibers. For this purpose, Nav1.8$^{+/-}$ cre DTA flox $^{+/-}$ are used. These animals express the diphterin toxin A under the Nav1.8 cre promoter, selectively ablating Nav1.8$^{+}$ fibers, or nociceptors as previously described (Abrahamsen *et al.*, 2008). In these animals, male and female mice exposed to *Alternaria alternata* for 1 week show no effects in excitatory synaptic puncta numbers (Figure 6.9 A-C). This data shows that nociception communication into the NTS is necessary for the synaptic puncta alterations in females: the effect is driven by nociception synaptic plasticity. This data allows us to conclude two things: (1) a very limited effect of mechanosensory or other innervating fibers are taking place in the synaptic plasticity observed in females, since deleting nociceptors was sufficient to prevent decrease in excitatory synapses. And (2) a definitive proof that circulating pro-inflammatory mediators are not driving changes in synaptic numbers; since if neuroinflammation was playing a role, we would still see a decrease in synaptic numbers, which we don't.

Female do not change immune cell infiltration in Nav1.8$^{+/-}$ cre DTA flox $^{+/-}$ mice

The NTS is capable of modulating many different roles of lung function: bronchoconstriction (Su *et al.*, 2023), breathing patterns (Chang *et al.*, 2015) and immune cell infiltration (Talbot *et al.*, 2015). To understand if the synaptic plasticity observed within the NTS was directly impacting lung function we decided to investigate the immune cell infiltration in our model. As previously described, neuronal efferents exiting the dorsal motor nucleus of the vagus (DMV) negatively regulates the immune cell infiltration of peripheral organs (Borovikova *et al.*, 2000) , and they are modulated by NTS activity (Davis *et al.*, 2004). And the afferent fibers Nav1.8$^{+}$ when ablated, decrease the immune cell infiltration of lung tissue in response to allergic stimuli (Talbot *et al.*, 2015).

Here, we show that females do not significantly change the number or composition of immune cells in the lung bronchoalveolar fluid (BALF) (Figure 6.10 A). Alternaria exposure affects numbers of immune cells in a similar fashion in Nav$^{+/-}$DTA$^{+/-}$ and WT mice. And cell number confirms data as female Nav$^{+/-}$DTA$^{+/-}$ have a similar increase of CD45$^{+}$ cells, eosinophils, neutrophils, T and B cell (Figure 6.10 B-G) in response to alternaria. Macrophages are the only cell type that seem to have a change in response to *Alternaria alternata* inhalation. Females Nav1.8$^{+/-}$DTA$^{+/-}$ increase alveolar macrophage population (Figure 6.10 G).

Males do not change the immune cell response to Alternaria in $Nav^{+/-}DTA^{+/-}$ mice

The same investigation of BALF immune cell infiltration was performed in male animals to continue investigation of sex-specific effects. There was not a major shift in immune cell content after *Alternaria alternata* exposure to male mice (Figure 6.11 A). Alternaria significantly increases the percentage of T cells from 0.75% in air exposed to 25.60% in Alternaria exposed $Nav^{+/-}DTA^{+/-}$ mice, while WT animals change percentage from 0.74% to 15.20%. This percentage increase in the T cell population is reflected in cell number, as the T cell increase after Alternaria exposure (Figure 6.11 G) is almost two-fold what WT mice had previously shown (Figure 6.3). This could suggest a T cell control of nociceptor fiber as previously reported (Baral *et al.*, 2018), although more experiments are necessary to draw conclusions.

Regardless of T cell alteration, most immune cell types remain relatively close to WT levels, and overall Alternaria exposure increase eosinophils, B cells, CD45+ and neutrophil infiltration in BALF, without an effect in macrophages.

Collectively the data suggests nociceptor fibers do not change immune cell infiltration in males nor females, and NTS sex-specific synaptic plasticity response is mediating other functional aspects of lung.

NTS sex-specific response is not exclusive to Alternaria exposure

To investigate if the sex-effect observed was exclusive for allergic inflammation we next used a well characterized innate immune inducer LPS to drive lung inflammation. As described in other chapters of this dissertation, LPS is a lipopolysaccharide that is

classically described as a TLR-4 agonist and promotes innate immune response. Animals were exposed to LPS inhalation in two different concentrations: 1μg/m3 and 15μg/m3. Lung immune responses to 1μg LPS were characterized in Biddle et al showing a strong neutrophilic infiltration at 48hr that is almost reverted back at 7day timepoint (Biddle *et al.*, 2023). LPS inhalation showed a very specific sex-effect with a higher vglut2 and synaptophysin co-localized puncta in females exposed to 15μg of LPS, but not in males nor smaller doses (Figure 6.12 A-C). This suggests the NTS response is dose-dependent and very sex-specific, although nature of inflammation differentially modulate vglut2 effect.

GeoMx analysis shows sex-specific and stimuli specific alterations within the NTS

To further verify alterations within NTS inflammatory, neuronal stress markers and secondary messenger signaling cascades we used GeoMx technologies in both 1μg and 15μg LPS exposed animals.

We observe males to be more responsive to 1μg of LPS exposure, with changes in protein 100SB associated with astrocytic reactivity (Figure 6.13 A,B). At the higher dose administration, 15μg of LPS elicit now a strong female response decreasing ITGAX and MEK1, again associated with glial reactivity (Figure 6.13 C,D).

Collectively the data shows a strong sex-specific effect to lung inflammation that is dependent on the type of lung immune response. More experiments are necessary to determine which NTS controlled lung function the female NTS synaptic plasticity is modulating.

## *Discussion*

Lungs are innervated by nociceptive fibers that sense changes within the environment and send the information to the medulla to control bronchoconstriction, immune cell infiltration and breathing rhythmns. All of which are affected during lung allergic reactions. This provides the possibility that changes within lung environment are sensed and modulated by the central nervous system, idea that has recently been explored by different papers (Chang *et al.*, 2015; Talbot *et al.*, 2015; Nonomura *et al.*, 2017).

Sex is a major factor that influences the immune response during lung allergic inflammation. Females have more severe symptoms associated with asthma and are more affected by asthma and related allergic disorders (Chowdhury *et al.*, 2021), but mechanisms of pathophysiology that involve sex susceptibility of disease have not been uncovered. Moreover, the same CNS controlled aspects of allergic reactions have themselves a female increased susceptibility: women respond with more bronchoconstriction than men (Langdeau *et al.*, 2000), and women adapt breathing rhythmns to changes in lung environment more readily than men (Horiuchi *et al.*, 2019).

Here, we sought to investigate the sex-specific allergic lung responses and the involvement of central nervous system alterations via sensory fibers. We show females seem more responsive in the NTS to two different types of lung inflammatory challenges an allergic *Alternaria alternata* and a non-allergic LPS mediated.

*Alternaria alternata* lung inflammation recruits allergic immune cells eosinophils, adaptive immune cells T cells and B cells and innate immune cells neutrophils in both males and females. Regardless of the seemingly identical lung immune response, the mediated

medullary effect is drastically sex-specific. Lung allergic sex-specific effects vary from model to model, depending on strain or immune challenge. For example, a comparison between C57Bl/6NJ and BALB/c mice shows females have increased immune cell infiltrates to the lung than males in BALB/c, but males have increased eosinophilic infiltrations in lung in C57Bl/6NJ (Mostafa *et al.*, 2022). To avoid misinterpretation of our findings, direct comparisons between male and female mice were not performed. We were instead interested in the mechanism in males and females that are dictated by *Alternaria alternata* exposure.

Even with similar immune responses, males and females presented differences in their central nervous system alterations. Females decrease vglut2 and PSD95 excitatory synapses, while males do not. Changes in excitatory synapses within the brain after systemic inflammation are well described in the literature, but usually as a consequence of neuronal inflammation, microglial reactivity or active engulfment of synapses by microglia (Schafer *et al.*, 2012). These responses have been described in animal models of lung allergic inflammation as well. Ovalbumin use for lung allergic sensitization was sufficient to increase the response of lung sensory fibers to capsaicin, an agonist of TRPV1 channels. This sensitized increased response correlated with an increased in microglial and astroglial numbers within the NTS region (Spaziano *et al.*, 2015). In systemic administration of LPS i.v., once again NTS seems to increase IBA1+ cells in number, correlating with a decreased in branch length of NTS neuronal fibers (Amorim *et al.*, 2019). However, this well described mechanism does not seem to be necessary for the alterations seen in our model. Both Iba1 quantification in NTS region by immunofluorescence, and the GeoMx

quantification of proteins associated with microglial and astroglial reactivity do not change after lung Alternaria exposure in neither males nor females.

Regardless of the absence of reactivity, glial cells play important roles in supporting and influencing neuronal activity (Su *et al.*, 2003; Badimon *et al.*, 2020). Astrocytes particularly change EAAT2 levels to modulate glutamate availability at the synaptic cleft. Inhibition of EAAT2 is sufficient to induce an increase in NTS neuronal activity (Matott, Kline and Hasser, 2017). This provides us with a mechanism in which astrocytes may counterbalance the decreased excitatory synapses in females only. And thus, suggests 7 day Alternaria exposure is a turning point in synaptic regulation, although temporal experiments of effect are necessary for further conclusions.

GeoMx data into female response also suggests this turning point. Activation of GSK-3β happens via phosphorylation of threonine residues, while its inactivation is obtained by phosphorylation of serine residue 9 (Beurel, Grieco and Jope, 2015). Females show an increased inactivation of GSK-3β, a protein in which activation suppresses exocytosis of vglut2 in other brain regions (Zhu *et al.*, 2010). This also suggests an effort at the protein level to counterbalance the decrease in vglut2 observed in female NTS.

Alternatively, GSK-3β has many different roles and its inactivation could potentially mediate a myriad of functions. Inactivation of GSK-3β decreases c-fos and NFκB activation (Ko *et al.*, 2015) and alters cellular metabolism in hypoxia (Beurel, Grieco and Jope, 2015); all of which are candidates to affect NTS neurons in our model and a closer investigation into its functional roles are necessary. Regardless of its function, females

NTS excitatory synaptic decrease is associated with a decrease of GSK-3β activity, a regulation not present in male NTS.

Females GeoMx also show changes in 2 different proteins in NTS region: pan-RAS augmentation and p-S6 decrease. p-S6 is a ribosomal protein associated with protein synthesis (Bohlen, Roiuk and Teleman, 2021), it is known to be activated by c-fos, correlating with neuronal activity (Knight *et al.*, 2012). A decrease in p-S6 corroborates our findings of an overall decrease in female neuronal activation.

Excessive glutamate release by synaptic activity can become toxic, a process known by excitotoxicity. An increase in response would either have to be counter balanced by a decrease of neuronal activity, otherwise can lead to neuronal stress and cellular death if activity is not reduced. However, no proteins associated with stress nor autophagy are changing within the NTS as investigated by GeoMx, suggesting this modulation is not happening in our model.

Males undergo specific protein alterations within the NTS, that are once again associated with signaling cascades. Both p-AMPK and p-JNK can modulate a series of cellular function including synaptic plasticity and neuroinflammation (Kristiansen and Edvinsson, 2010; Evans and Hardie, 2020), and more experiments are necessary to address function. Within brainstem, p-AMPK is increased in neurons during lung hypoxia, and facilitates increases in synaptic activity that drive changes in breathing rhythmns (MacMillan and Evans, 2023). Moreover, p-JNK is associated with downregulation of synaptic plasticity by decreasing glutamate NMDAR in membrane within the hippocampus (Morel *et al.*, 2018). Contributing to an interpretation that males could be changing synaptic plasticity at

the post-synaptic terminal, which in terms of neurotransmitter receptors was not investigated in our model.

The sex-effect was not exclusive to Alternaria, since LPS elicited a dose dependent sex-effect within the NTS. Females responded with an increased excitatory synaptic puncta in response to 15μg LPS, while males did not.

Given the sex-specific effects observed and the lack of neuroinflammation effects within the NTS we decided to investigate which lung sensory fibers could mediate female NTS synaptic plasticity. Nociceptive fibers are the majority of fibers that innervate lung arriving at NTS and are molecularly identified by the expression of Nav1.8 (Abrahamsen *et al.*, 2008). Ablation of nociception fibers reverses NTS alterations in our model and suggest nociceptive fibers are the ones driving the effect in females. There is a disadvantage to this model. Nav1.8 is also expressed by testes, heart and placental tissue (*Scn10a Gene Expression Tissue Summary - GXD*, no date). In the heart, it has been shown to impact heartbeat during extreme conditions, but not normal response (Stroud *et al.*, no date). It is possible this has an effect in our model, since lung and heart regulation are affected by similar stimulus.

Among all the NTS characterized regulations in lung function, we decided to investigate the role of immune cell infiltration that has been shown to be sex-modulated (Crosson *et al.*, 2023). The animals do seem to lose tight regulation of immune infiltration control, as both female and male variability increases with ablation of Nav1.8$^{+}$ fibers. This is in contrast with data obtained from Talbot group: They show a decrease in immune cell infiltration by total numbers CD45+ cells and also an allergic immune type eosinophil after

ablation of the same fibers Nav1.8$^{+}$ (Talbot *et al.*, 2015). This drastic response might be an effect of our model of continuous exposure for 7 days. In fact, a model of active infection by bacterial particles within lung shows that ablation of TRPV1 fibers is responsible for increasing T cell migration only (Baral *et al.*, 2018), corroborating with our allergic data. Collectively the data suggests lung inflammation to drive synaptic plasticity changes within the NTS via nociceptors, that are dependent upon the type of inflammatory response of the lung. And provide a mechanism for sex-specific NTS driven changes in lung function.

## *Figures and Legends*

**Figure 6.2 Males and females increase migration of innate immune cells after Alternaria exposure that is reversed after 1 week of filtered air exposure**

**A.** Schematic representation of experimental design. Males and females remain in home cage and are transferred to a chamber that allows them to naturally breath *Alternaria alternata* particles for 7 days. Another group is transferred to a filtered air chamber after 1 week to investigate reversal effects (reversal group).

**B,C.** Flow cytometry generated graphs from total immune cells infiltrated in BALF, characterized by $CD45^+$, in females (**B)** and males (**C**).

(**D**) Gating strategy used for isolating the different types of immune cells measured from percent $CD45^+$ cells.

**E-J.** Graphs generated from cell count of gates in flow cytometry. Alveolar macrophages are defined as $CD45^+CD11c^+SinglecF^+$ and shown in females (**E**) and males (**F)**. Eosinophils were defined as $CD45^+CD11b^+SiglecF^+CD11c^-$ in females (**F**) and males (**I)**. Neutrophils were defined as $CD45^+CD11b^+Ly6G^+SiglecF^-CD11c^-$ in females (**G**) and males (**J**).

Data showed as mean ± SEM, analyzed with one-way ANOVA, Tukey multiple comparison analysis post-test. ***$p<0.001$ ****$p<0.0001$.

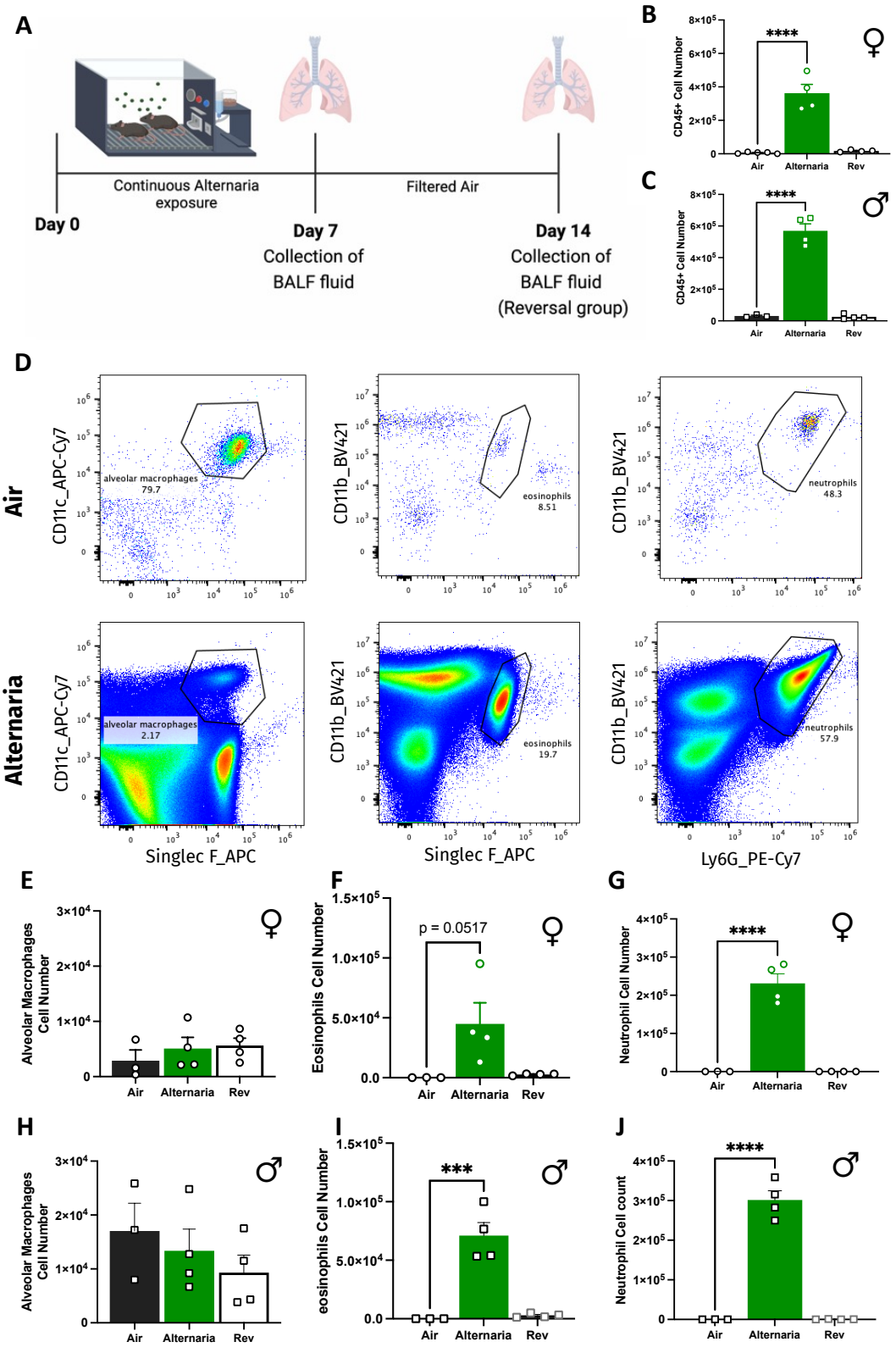
A
Continuous Alternaria exposure
Filtered Air
Day 0
Day 7
Collection of BALF fluid
Day 14
Collection of BALF fluid (Reversal group)
B
CD45+ Cell Number
****
Air
Alternaria
Rev
C
CD45+ Cell Number
****
Air
Alternaria
Rev
D
Air
Alternaria
CD11c_APC-Cy7
alveolar macrophages
79.7
CD11b_BV421
eosinophils
8.51
neutrophils
48.3
alveolar macrophages
2.17
eosinophils
19.7
neutrophils
57.9
Singlec F_APC
Ly6G_PE-Cy7
E
Alveolar Macrophages Cell Number
Air
Alternaria
Rev
F
Eosinophils Cell Number
p = 0.0517
G
Neutrophil Cell Number
****
H
Alveolar Macrophages Cell Number
I
eosinophils Cell Number
***
J
Neutrophil Cell count
****

**Figure 6.3 Males and females increase migration of adaptive immune cells after Alternaria exposure that is reversed after 1 week of filtered air exposure**

**A.** Schematic representation of experimental design. Males and females remain in home cage and are transferred to a chamber that allows them to naturally breath *Alternaria alternata* particles for 7 days. Another group is transferred to a filtered air chamber after 1 week to investigate reversal effects (reversal group).

**B.** Gating strategy used for isolating the B and T cell counts measured from $CD45^+$ cells.

**C-F**. Graphs generated from gates defined by flow cytometry. T cells are defined by $CD45^+CD3^+CD19^-$ in females (**C**) and males (**E**). B cells are defined by $CD45^+CD3^-CD19^+$ in females (**D**) and males (**F**).

Data showed as mean ± SEM, analyzed with one-way ANOVA, Tukey multiple comparison analysis post-test. **p<0.01, ***p<0.001 ****p<0.0001.

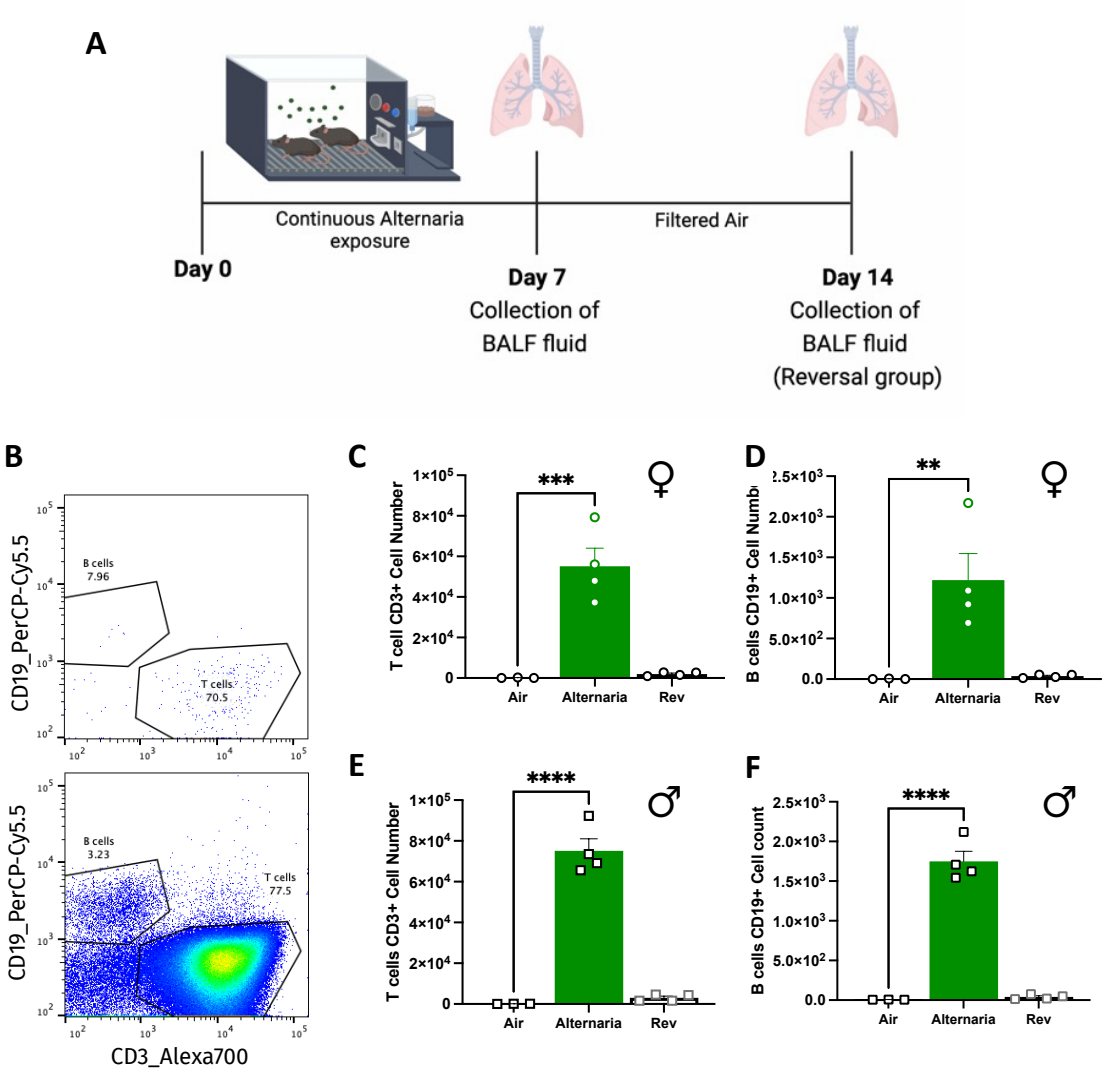
A
Continuous Alternaria exposure
Filtered Air
Day 0
Day 7
Collection of BALF fluid
Day 14
Collection of BALF fluid (Reversal group)
B
CD19_PerCP-Cy5.5
B cells 7.96
T cells 70.5
B cells 3.23
T cells 77.5
CD3_Alexa700
C
T cell CD3+ Cell Number
***
Air
Alternaria
Rev
D
B cells CD19+ Cell Numb
**
E
T cells CD3+ Cell Number
****
F
B cells CD19+ Cell count

**Figure 6.4 Medulla decrease synaptic proteins in females after Alternaria exposure, but not in males**

**A.** Representative image of medulla western blotting of females vglut2, PSD95, synaptophysin (SYN) and total protein stain (TPS) in air and Alternaria exposed.

**B-D** Graphical analysis of western blotting for female medulla of vglut2 (**B**), PSD-95 (**C**) and synaptophysin (**D**).

**E**. Representative image of medulla western blotting of males vglut2, PSD95, synaptophysin (SYN) and total protein stain (TPS) in air and Alternaria exposed.

**F-H.** Graphical analysis of western blotting for female medulla of vglut2 (**F**), PSD-95 (**G**) and synaptophysin (**H**).

Data showed as mean ± SEM, analyzed with unpaired two-tailed t-test. *$p<0.05$

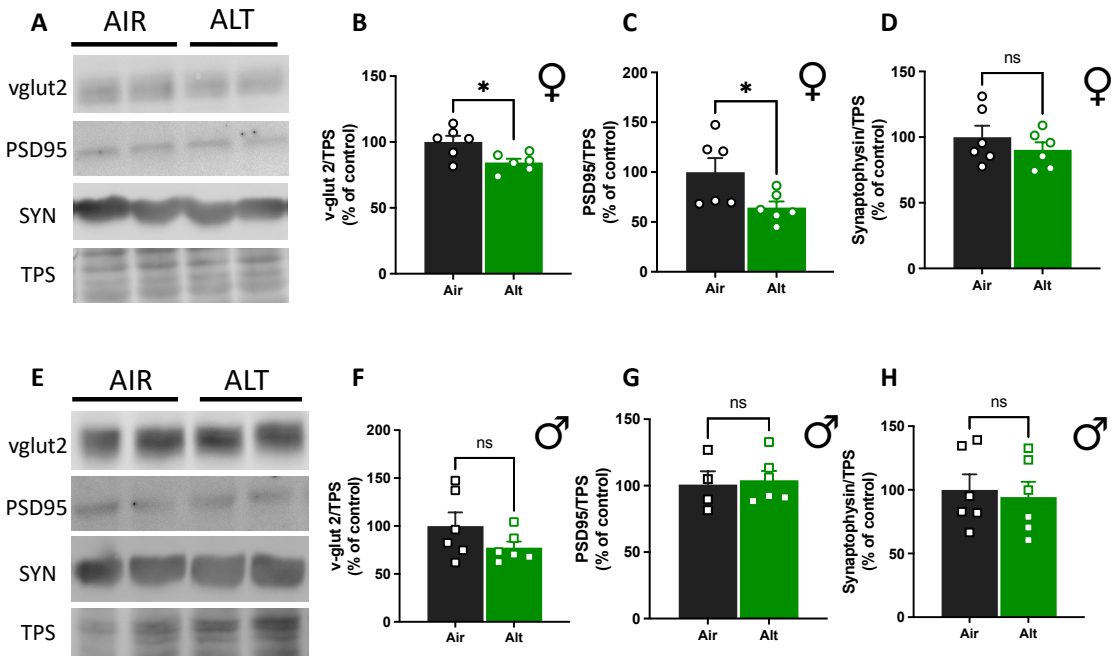
A
AIR
ALT
vglut2
PSD95
SYN
TPS
B
v-glut 2/TPS (% of control)
Air
Alt
C
PSD95/TPS (% of control)
D
Synaptophysin/TPS (% of control)
ns
E
F
G
H

**Figure 6.5 BotC or pre-Botc breathing reagions are not impacted by changes in synaptic numbers**

**A.** drawing of analyzed section within the medulla in bregma -6.64mm. BötC region is shadowed in grey to represent quantificated region.

**B**. Representative images of puncta quantification in air and Alternaria exposed BötC. Images were taken at 63X and magnified view of images are displayed. In blue DAPI staining, in red vglut2 and green synaptophysin (syn). Scale bar = 10μm.

**C, D**. Graphical quantification of puncta from BötC region in females (**C**) and males (**D**).

**E.** drawing of analyzed section within the medulla in bregma -7.08mm. preBötC region is shadowed in grey to represent quantificated region.

**F**. Representative images of puncta quantification in air and Alternaria exposed preBötC. Images were taken at 63X and magnified view of images are displayed. In blue DAPI staining, in red vglut2 and green synaptophysin (syn). Scale bar = 10μm.

**G, H**. Graphical quantification of puncta from BotC region in females (**G**) and males (**H**).

Data showed as mean ± SEM, analyzed with unpaired two-tailed t-test.

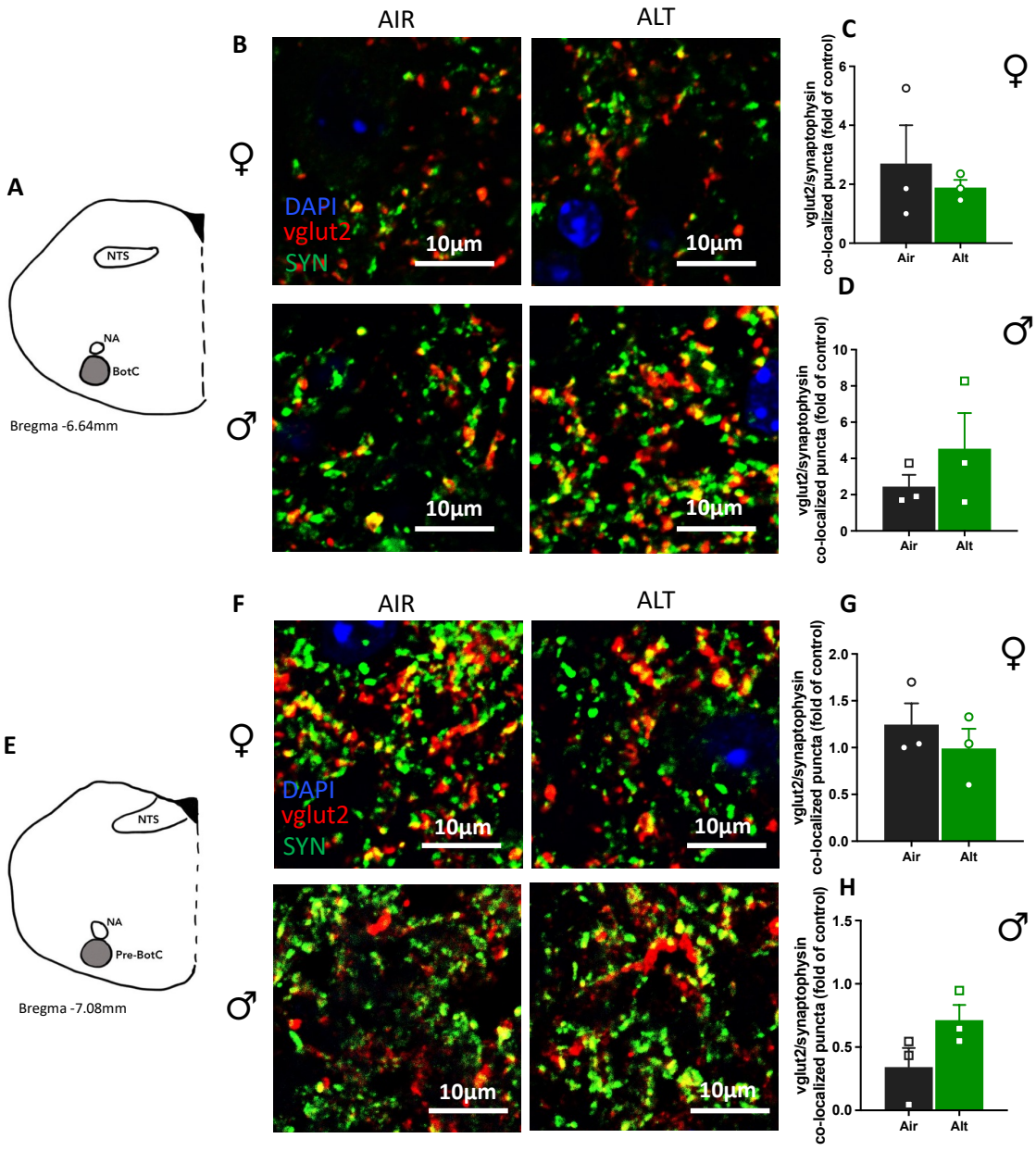
A
NTS
NA
BotC
Bregma -6.64mm
B
AIR
ALT
♀
♂
DAPI
vglut2
SYN
10µm
C
D
vglut2/synaptophysin
co-localized puncta (fold of control)
Air
Alt
E
Pre-BotC
Bregma -7.08mm
F
G
H

**Figure 6.6 Sex-specific alterations in synaptic proteins are localized to NTS region**
**A.** Representative images of puncta quantification in air and Alternaria exposed NTS. Images were taken at 63X and magnified view of images are displayed. In blue DAPI staining, in red vglut2 and green synaptophysin (syn). Scale bar = 10μm.
**B**. Drawing of analyzed section within the medulla in bregma -7.56mm. NTS region is shadowed in grey to represent region quantified.
**C, D**. Graphical quantification of puncta from NTS region in females (**C**) and males (**D**).
Data showed as mean ± SEM, analyzed with one-way ANOVA, Tikey multiple comparisons analysis post-test.

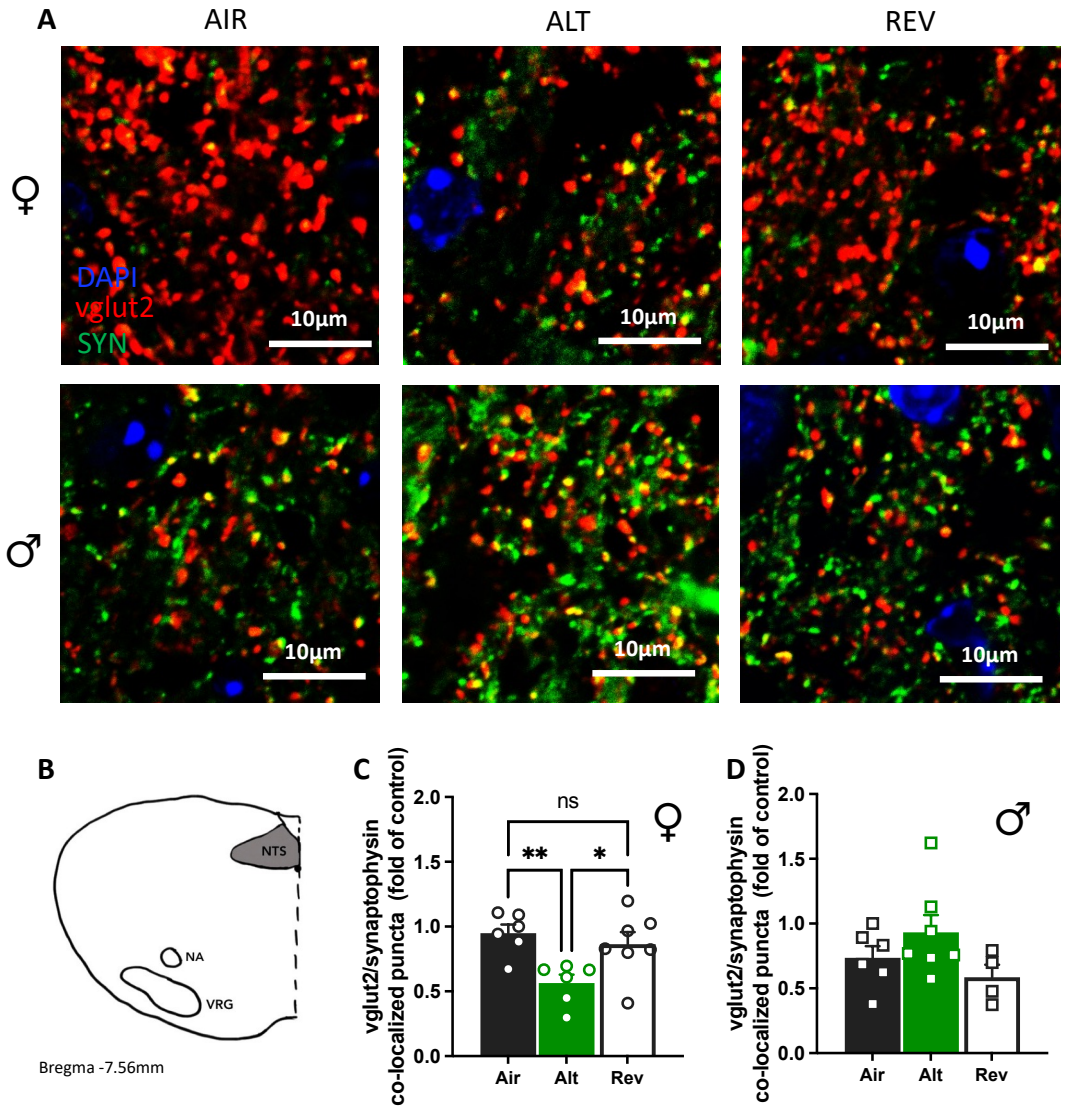
A
AIR
ALT
REV
♀
♂
DAPI
vglut2
SYN
10µm
B
NTS
NA
VRG
Bregma -7.56mm
C
D
vglut2/synaptophysin
co-localized puncta (fold of control)
2.0
1.5
1.0
0.5
0.0
ns
**
*
Air
Alt
Rev

**Figure 6.7 GeoMx shows differing cell signaling activation in male and female NTS without changes in inflammatory markers of glial cells**

**A**. GeoMx representative image of NTS section in air and Alternaria exposed male and female mice. In blue syto13 nuclei staining, in yellow TH staining.

**B.** zoom image of NTS region showing ROI collected for analysis.

**C-F**. Volcano plots generated from data of males and females NTS. Red represents significantly up-regulated proteins, blue represents significantly downregulated proteins between treatment and air control in females (**C, E**) and males (**D, F**)

Data analyzed by linear mixed model, p-test corrected by Benjamini and Hochberg method.

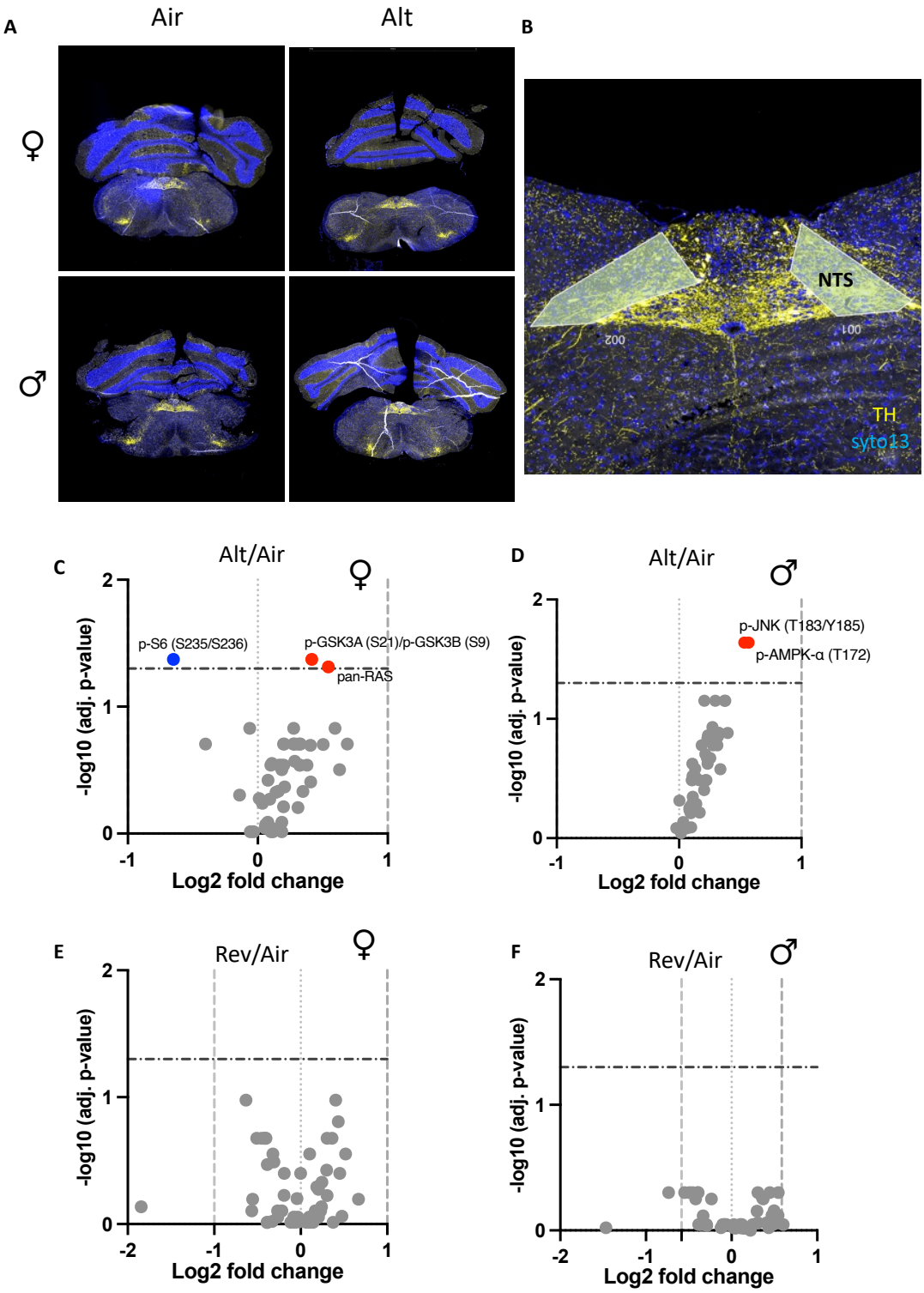
A
Air
Alt
♀
♂
B
NTS
TH
syto13
C
Alt/Air
♀
p-S6 (S235/S236)
p-GSK3A (S21)/p-GSK3B (S9)
pan-RAS
-log10 (adj. p-value)
Log2 fold change
D
Alt/Air
♂
p-JNK (T183/Y185)
p-AMPK-α (T172)
-log10 (adj. p-value)
Log2 fold change
E
Rev/Air
♀
-log10 (adj. p-value)
Log2 fold change
F
Rev/Air
♂
-log10 (adj. p-value)
Log2 fold change

**Figure 6.8 Glial cells play a role in synaptic plasticity in the absence of reactivity markers**
**A**. Representative image of medulla western blotting of females EAAT2 and total protein stain (TPS) in air and Alternaria exposed.
**B,C** Graphical analysis of western blotting for EAAT2 in female (**B**) and male (**C**) medulla.
**D**. Representative images of IBA1 quantification in air and Alternaria exposed NTS. Images were taken at 20X. In blue DAPI staining, and green IBA1. Scale bar = 50μm.
**C, D**. Graphical quantification of IBA1 from NTS region in females. Mean fluorescence intensity of IBA1 is represented in (**C**) and $IBA1^+$ cells/$mm^2$ in (**D**).
**E, F**. Graphical quantification of IBA1 from NTS region in males. Mean fluorescence intensity of IBA1 is represented in (**E)** and $IBA1^+$ cells/$mm^2$ in (**F**).
Data showed as mean ± SEM, analyzed with unpaired two-tailed t-test. *$p<0.05$

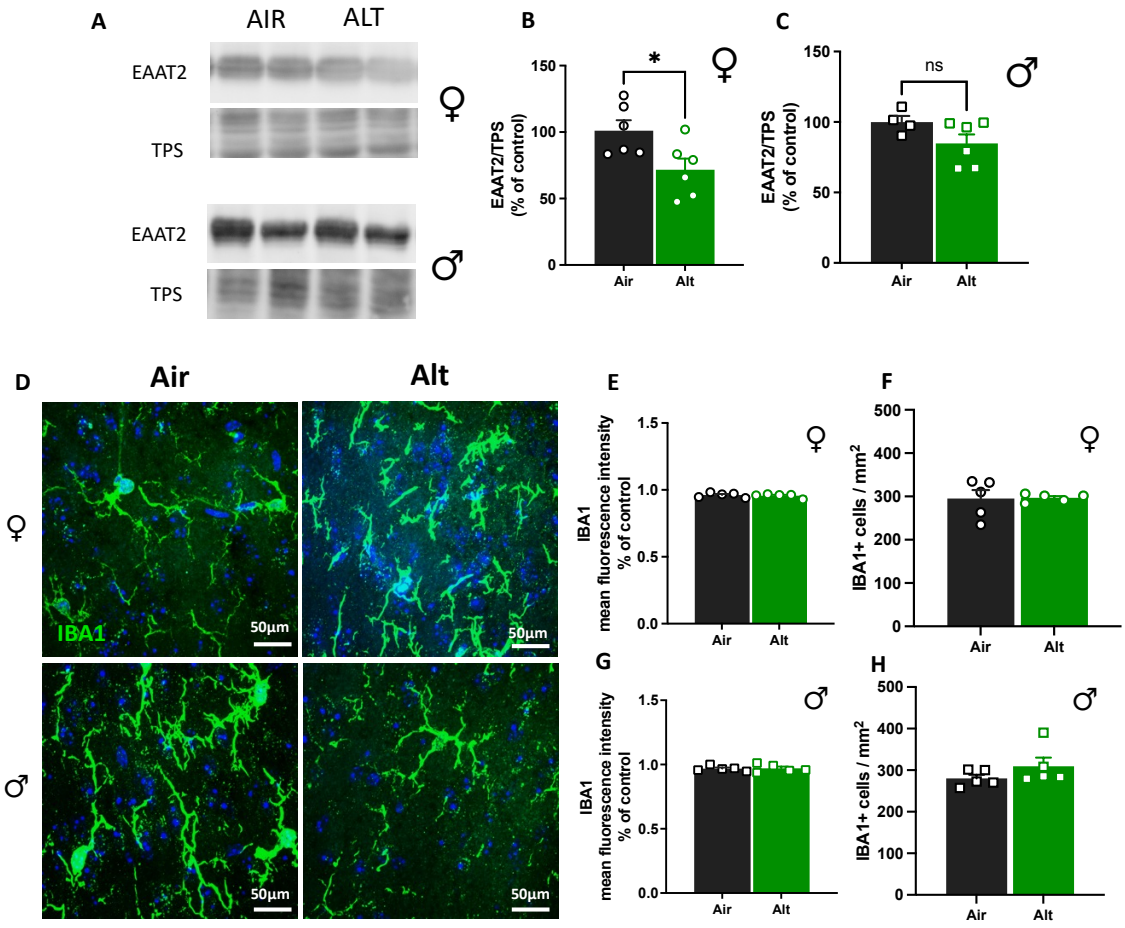
A
AIR
ALT
EAAT2
TPS
EAAT2
TPS
B
EAAT2/TPS (% of control)
Air
Alt
C
ns
EAAT2/TPS (% of control)
Air
Alt
D
Air
Alt
IBA1
50µm
E
IBA1 mean fluorescence intensity % of control
Air
Alt
F
IBA1+ cells / mm2
Air
Alt
G
IBA1 mean fluorescence intensity % of control
Air
Alt
H
IBA1+ cells / mm2
Air
Alt

**Figure 6.9 Nav1.8 is used to investigate nociceptor influence in NTS synaptic plasticity**
**A, C.** Representative images of puncta quantification in air and Alternaria $Nav^{+/-}DTA^{+/-}$ female (**A**) and male (**C**) NTS. Images were taken at 63X and magnified view of images are displayed. In blue DAPI staining, in red vglut2 and green synaptophysin (syn). Scale bar = 10μm.
**B, D**. Graphical quantification of puncta from NTS region in females (**B**) and males (**D**).
Data showed as mean ± SEM, analyzed with unpaired one-tail t-test.

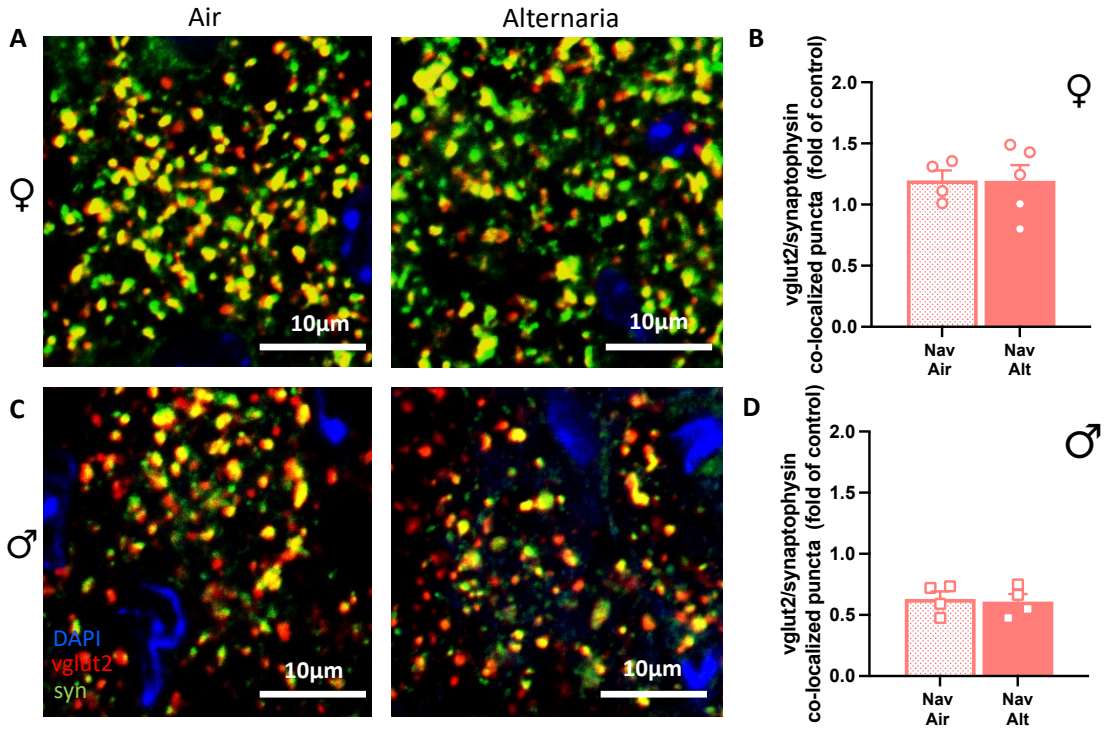
A
Air
Alternaria
♀
10µm
10µm
C
♂
DAPI
vglut2
syn
10µm
10µm
B
vglut2/synaptophysin
co-localized puncta (fold of control)
2.0
1.5
1.0
0.5
0.0
Nav
Air
Nav
Alt
D
♂

**Figure 6.10 Absence of nociceptors do not impact female BALF immune cell infiltration**
**A.** Graphs represent percent immune cells from $CD45^+$ population in WT and $Nav^{+/-}DTA^{+/-}$ female.
**B.** $CD45^+$ cell counts for both $Nav^{+/-}DTA^{+/-}$ air and Alternaria exposed females
**C-G**. Graphs generated from gates defined by flow cytometry from $CD45^+$ population. Alveolar macrophages are defined as $CD45^+CD11c^+SinglecF^+$ (**C**). Neutrophils were defined as $CD45^+CD11b^+Ly6G^+SiglecF^-CD11c^-$ in (**D)**. Eosinophils were defined as $CD45^+CD11b^+SiglecF^+CD11c^-$ in (**E**). B cells are defined by $CD45^+CD3^-CD19^+$ (**F**). T cells are defined by $CD45^+CD3^+CD19^-$ in (**G**).
Data showed as mean ± SEM, analyzed with unpaired two-tail t-test. *p<0.05, ***p<0.001 ****p<0.0001.

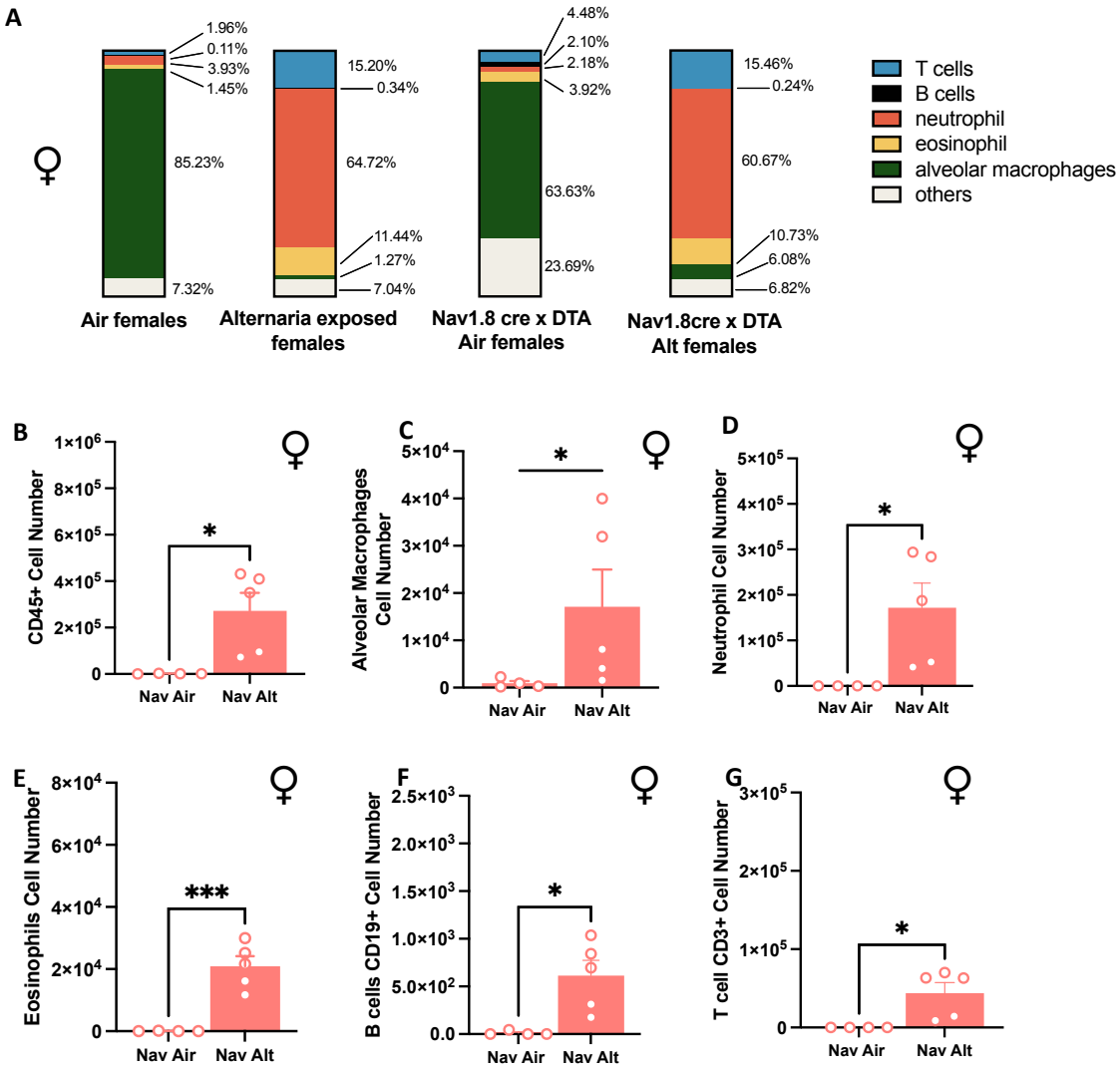
A
1.96%
0.11%
3.93%
1.45%
85.23%
7.32%
15.20%
0.34%
64.72%
11.44%
1.27%
7.04%
4.48%
2.10%
2.18%
3.92%
63.63%
23.69%
15.46%
0.24%
60.67%
10.73%
6.08%
6.82%
T cells
B cells
neutrophil
eosinophil
alveolar macrophages
others
Air females
Alternaria exposed females
Nav1.8 cre x DTA Air females
Nav1.8cre x DTA Alt females
B
CD45+ Cell Number
C
Alveolar Macrophages Cell Number
D
Neutrophil Cell Number
E
Eosinophils Cell Number
F
B cells CD19+ Cell Number
G
T cell CD3+ Cell Number
Nav Air
Nav Alt

**Figure 6.11 Absence of nociceptors affect T cell in male BALF**

**A.** Graphs represent percent immune cells from $CD45^+$ population in WT and $Nav^{+/-}DTA^{+/-}$ male.

**B.** $CD45^+$ cell counts for both $Nav^{+/-}DTA^{+/-}$ air and Alternaria exposed males

**C-G**. Graphs generated from gates defined by flow cytometry from $CD45^+$ population. Alveolar macrophages are defined as $CD45^+CD11c^+SinglecF^+$ (**C**). Neutrophils were defined as $CD45^+CD11b^+Ly6G^+SiglecF^-CD11c^-$ in (**D)**. Eosinophils were defined as $CD45^+CD11b^+SiglecF^+CD11c^-$ in (**E**). B cells are defined by $CD45^+CD3^-CD19^+$ (**F**). T cells are defined by $CD45^+CD3^+CD19^-$ in (**G**).

Data showed as mean ± SEM, analyzed with unpaired two-tail t-test. *p<0.05, **p<0.01, ***p<0.001, ****p<0.0001

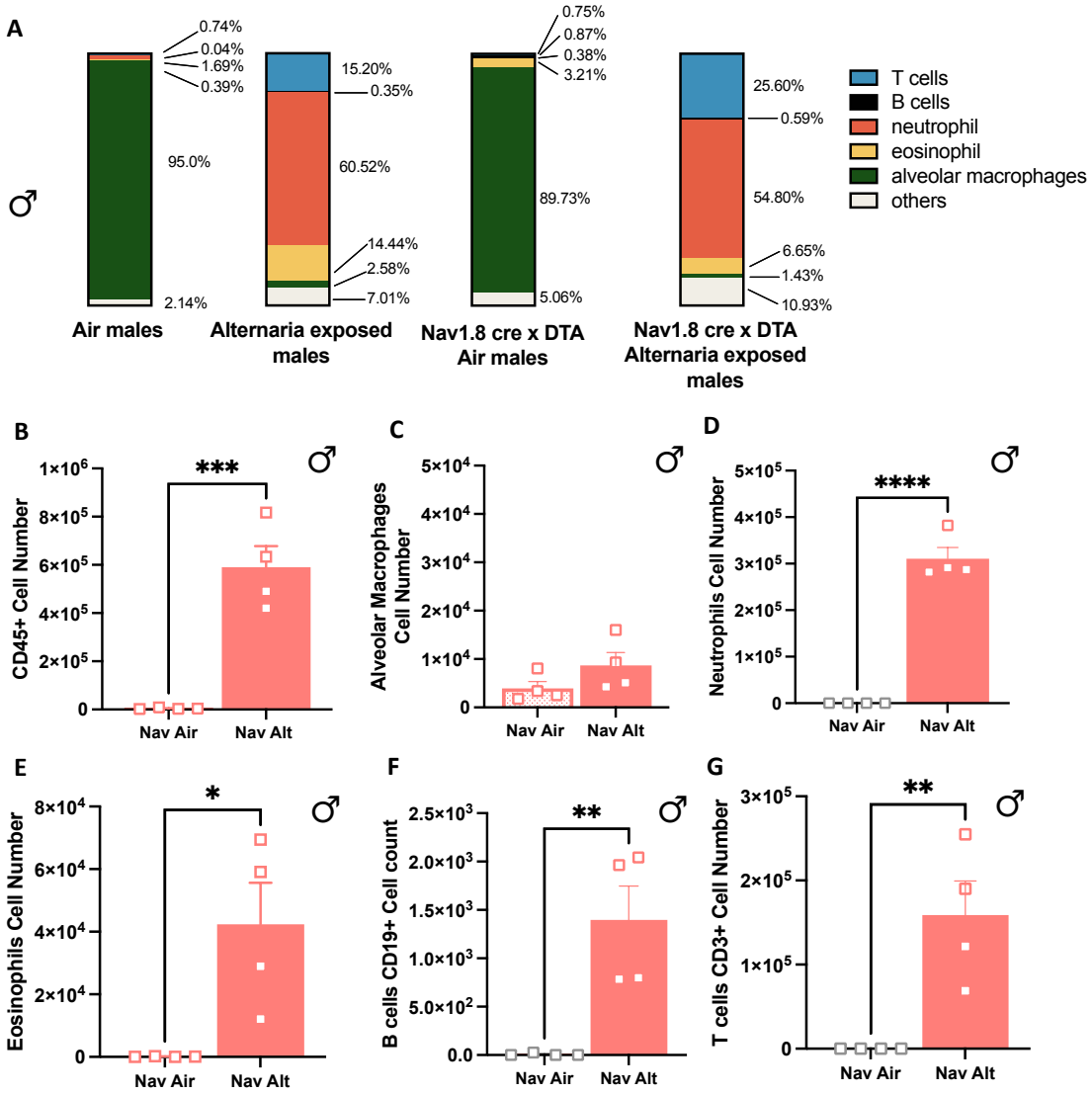
A
♂
0.74%
0.04%
1.69%
0.39%
95.0%
2.14%
15.20%
0.35%
60.52%
14.44%
2.58%
7.01%
0.75%
0.87%
0.38%
3.21%
89.73%
5.06%
25.60%
0.59%
54.80%
6.65%
1.43%
10.93%
T cells
B cells
neutrophil
eosinophil
alveolar macrophages
others
Air males
Alternaria exposed males
Nav1.8 cre x DTA Air males
Nav1.8 cre x DTA Alternaria exposed males
B
CD45+ Cell Number
1×10^6
8×10^5
6×10^5
4×10^5
2×10^5
0
***
Nav Air
Nav Alt
C
Alveolar Macrophages Cell Number
5×10^4
4×10^4
3×10^4
2×10^4
1×10^4
0
Nav Air
Nav Alt
D
Neutrophils Cell Number
5×10^5
4×10^5
3×10^5
2×10^5
1×10^5
0
****
Nav Air
Nav Alt
E
Eosinophils Cell Number
8×10^4
6×10^4
4×10^4
2×10^4
0
*
Nav Air
Nav Alt
F
B cells CD19+ Cell count
2.5×10^3
2.0×10^3
1.5×10^3
1.0×10^3
5.0×10^2
0.0
**
Nav Air
Nav Alt
G
T cells CD3+ Cell Number
3×10^5
2×10^5
1×10^5
0
**
Nav Air
Nav Alt

**Figure 6.12 LPS lung inhalation elicits sex-specific modulation of NTS response**

**A.** Representative images of puncta quantification in air and LPS exposed NTS (1μg and 15μg). Images were taken at 63X and magnified view of images are displayed. In blue DAPI staining, in red vglut2 and green synaptophysin (syn). Scale bar = 10μm.

**B**, **C**. Graphical quantification of puncta from NTS region in females (**B**) and males (**C**).

Data showed as mean ± SEM, analyzed with one-way ANOVA, Tukey multiple comparisons analysis post-test. **p<0.01.

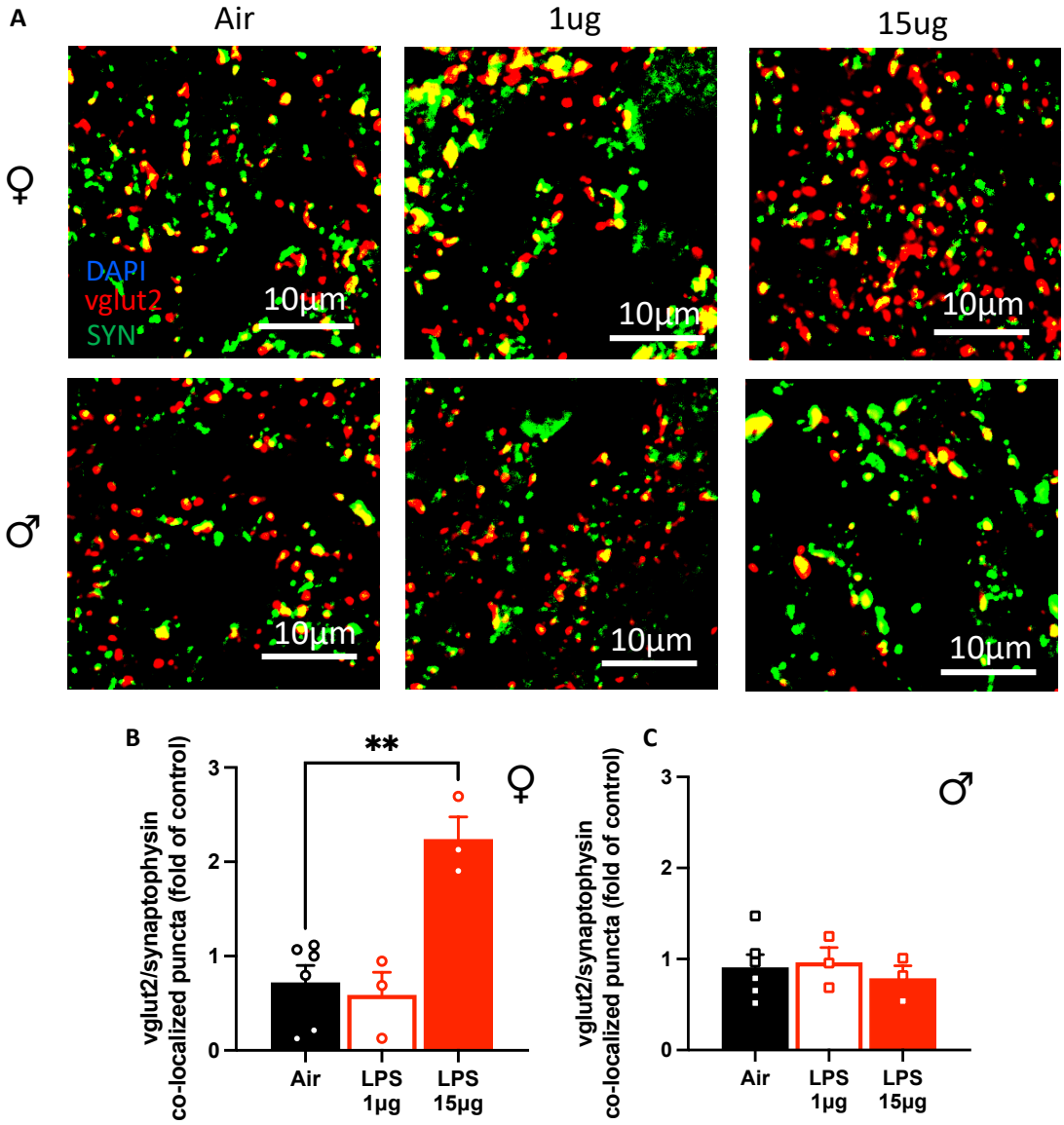
A
Air
1ug
15ug
♀
♂
DAPI
vglut2
SYN
10μm
B
C
**
vglut2/synaptophysin
co-localized puncta (fold of control)
Air
LPS
1μg
LPS
15μg

**Figure 6.13 GeoMx Analysis of NTS shows dose- and sex-dependent protein alterations**

**A-D**. Volcano plots generated from GeoMx data of males and females NTS. Red represents significantly up-regulated proteins, blue represents significantly downregulated proteins between treatment and air control in females (**A,C**) and males (**B,D**)

Data analyzed by linear mixed model, p-test corrected by Benjamini and Hochberg method.

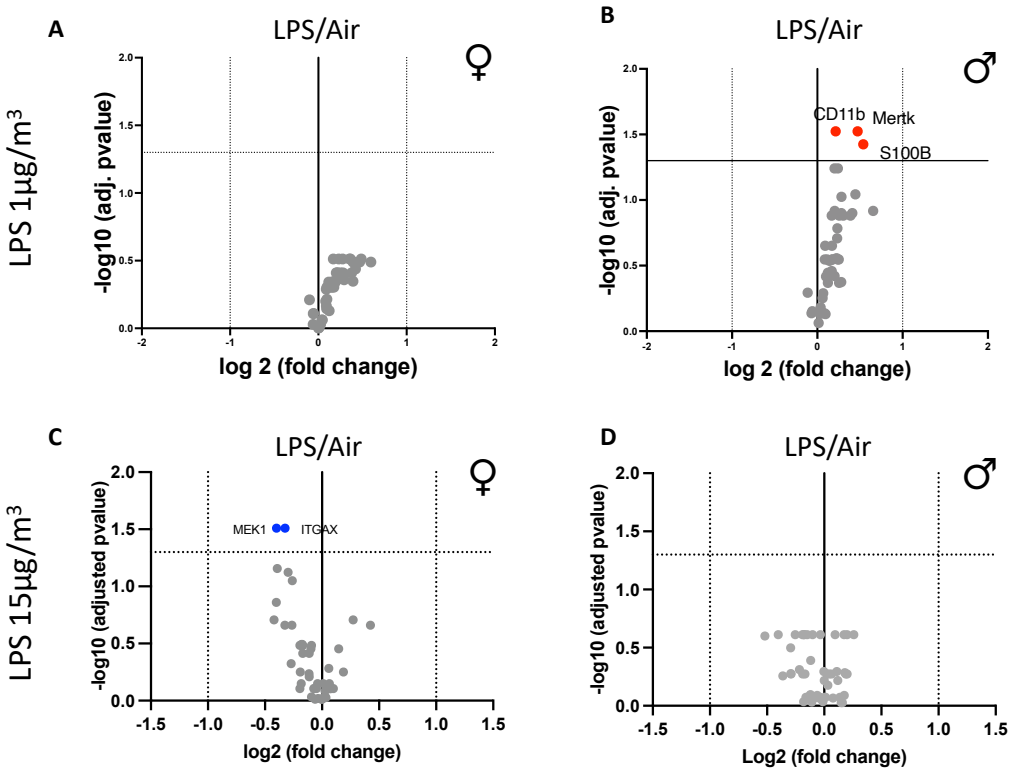
A
LPS/Air
♀
LPS 1µg/m³
-log10 (adj. pvalue)
log 2 (fold change)
B
LPS/Air
♂
CD11b
Mertk
S100B
-log10 (adj. pvalue)
log 2 (fold change)
C
LPS/Air
♀
LPS 15µg/m³
MEK1
ITGAX
-log10 (adjusted pvalue)
log2 (fold change)
D
LPS/Air
♂
-log10 (adjusted pvalue)
Log2 (fold change)

# Chapter 7

## Discussion

The data contained in this dissertation provides 2 distinct mechanisms in which sex affects the response to inflammation. (1) jejunum data shows at the level of the immune response males and females differentially control recruitment of immune cells to tissue, with distinct consequences to tissue function; (2) lung data shows that despite similar responses to immune cell infiltration, males and females differentially control brain sensory information with a distinct consequence to tissue function. During systemic inflammation, circulating inflammatory mediators impact tissue function. The brain is not isolated from the body and is impacted by systemic inflammation. Because the brain provide feedback for these organs, inflammation affects the crosstalk between brain and periphery. Here, we will discuss the two different mechanisms in more detail and infer about their possible function for both brain and tissue, given their close relationship.

From intestine to brain: The intestinal tissue sex specific mechanisms of inflammation

Mucosal tissues are in close proximity with the outside of the body and jejunum is no exception. At the same time the organ has an extensive surface area to facilitate the absorption of nutrients, immune cells are monitoring the tissue to prevent foreign organisms of invading the tissue and both selectivity and defense are tightly controlled. Here, we show that inflammatory responses dysregulate this intricate balance, increasing permeability in female jejunum but not male. We prove that the effect in jejunum

permeability is dependent on TREM2 signaling that recruits CCR2$^{+}$ immune cells to the tissue, augmenting the initial immune response. This effect of TREM2 is also sex-specific, as males use TREM2 signaling to increase glucose transportation without drastically upregulating inflammatory expression, nor changing intestinal permeability (Figure 7.1).

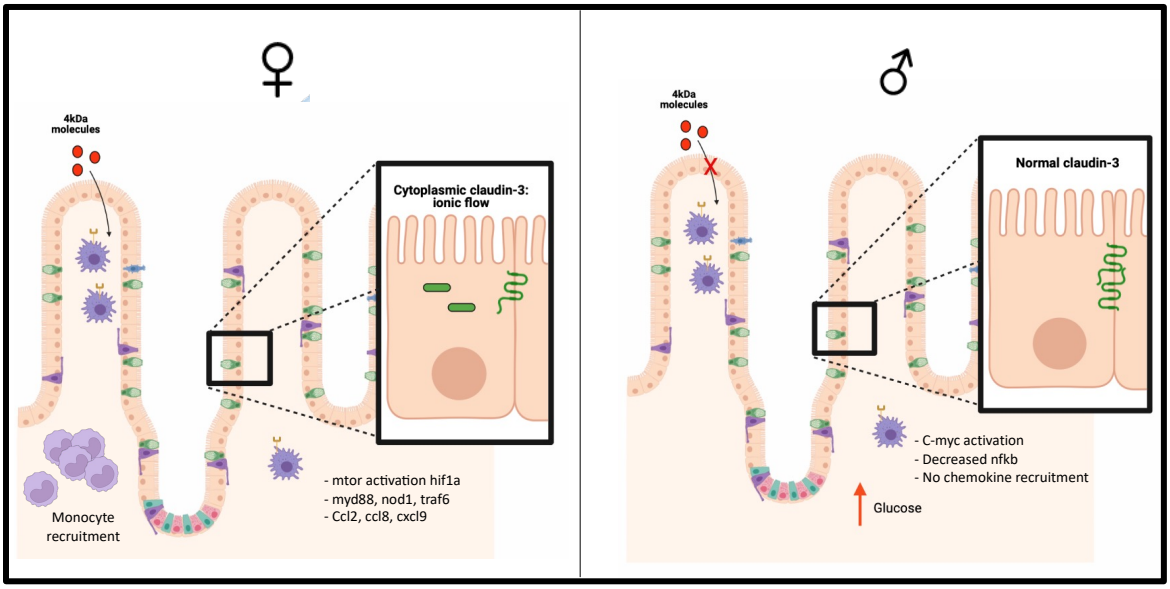


**Figure 7.1 Proposed mechanism of intestinal changes in males and females dependent on TREM2 and CCR2$^{+}$ cells**
Females increase jejunal permeability to ions and 4kDa molecules after IP-LPS, increasing claudin-3 tight-junction internalization. The mechanism is dependent on TREM2 signaling, that increases ccl2, ccl8 and cxcl9 release and culminates with an increase in CCR2$^{+}$ cell recruitment. TREM2 also responds to IP-LPS in a mechanism dependent on mtor activation of hif1a. Males on the other hand do not change intestinal permeability in response to IP-LPS, nor change claudin-3 tight-junction location. Instead there is an increase in glucose transportation to jejunal tissue that is TREM2 dependent. TREM2 elicits c-myc activation, decreases in nfkb and no chemokine recruitment.

Crohn's disease is characterized by immune dysregulations that spans both the innate and adaptive immune system, with T cells and recruited monocytes contributing to pathogenesis. Since the innate immunity drives adaptive, models of Crohn's disease investigation, characterize the response of both, being difficult to separate mechanisms of

disease. One strength of our model is the ability to separate the early innate immune response and understand mechanisms of intestinal pathology with a sex component.

LPS is a well-characterized model of innate inflammatory responses, it drives strong polarization of macrophages in vitro (Orecchioni *et al.*, 2019), and is useful to perturb the system with exacerbated responses. Our model takes advantage of these characteristics of LPS in intestinal response and find a CCL2 dependent mechanism of intestinal permeability present in female but not males. How this drives adaptive immunity differentially between sexes still remains to be solved, but in Crohn's disease the CCL2-CCR2 axis and monocyte migration to tissue are major disease drivers. IL6, TLR and ROS activation further contribute to a positive feedback of monocyte recruitment and differentiation into myeloid populations that drive disease (Bain *et al.*, 2013). Since we show here how CCL2 is driven by innate immunity in females but not males, this could provide a mechanism in which sex contributes to Crohn's disease. In fact, woman are more affected by Chron's Disease than man (Feuerstein and Cheifetz, 2017). Further association between the two must be proven, but the possibility is a very interesting investigative approach to this pathology.

This mechanism of resident versus innate immune cell in sex differences has been demonstrated in other models. High-fat diet induces differences in immune cell recruitment between males and females, with females responding with higher levels of CCR2+ cells (Varghese *et al.*, 2022). Spinal cord injury elicits an acute inflammatory response that results in the recruitment of different types of immune cells, including monocytes and neutrophils. And females recruited more monocytes to the injury site, while males relied

more on resident microglial populations and increased their recruitment (Stewart *et al.*, 2021). Suggesting the sex-specific mechanism of inflammation can be shared among other tissues, with males depending more on resident immune cells, while females rely more on immune cell recruitment during innate immune responses. Interestingly, the paper also compares the immune cell response of recruited versus resident macrophagic populations and shows microglial cells have lower expression of complement proteins C1q and a higher expression of hif1a, suggesting the monocytic population once recruited contribute to complement response with decreased hif1a expression, a profile extremely similar to what was obtained in our model (Chapter 3, 5).

Our data also suggest the relative contribution of the different cell types to sex-differences. Jejunum tissue recruits monocytes in females that are responsible for driving changes in intestinal permeability. While males focus on resident immune cells, that are able to control inflammatory reaction without amplification and recruitment of monocytes. The process is TREM2 dependent, suggesting TREM2 is responsible for this increased recruitment in females but not males and the TREM2 activation is different between sexes.

TREM2 has many different signaling cascades that have been partially uncovered. TREM2 signaling activates phagocytosis, anti-inflammatory response, and metabolic shifts of immune cells (Ulland *et al.*, 2017; Yao *et al.*, 2019). Because females have classically been described to be more phagocytic than males (Scotland *et al.*, 2011), and TLR activates the phagocytic response of myeloid cells (Wu, Chen and Chen, 2009), it is possible that differences between male and female phagocytosis is a direct effect of TREM2 activation in females. Moreover, it is possible the differences observed in this dissertation regarding

function of myeloid cell response and recruitment is because of TREM2 activation toward a phagocytic role in females drives ccl2 recruitment, while TREM2 activation in malers is anti-inflammatory and prevents changes in jejunum permeability. The TREM2 activation toward phagocytosis and metabolic shifts dependent on hif1a uses phosphorylation of SYK protein (Ulland *et al.*, 2017). Future experiments should focus on quantifying pSYk between males and females. This would provide an interesting insight into sex effects in intestinal pathology.

This becomes specially important because TREM2 is involved with Alzheimer's disease and other types of dementia. TREM2 heterozygous loss of function mutations increase by 3-fold the risk of developing Alzheimer's (Guerreiro *et al.*, 2013), while homozygous mutations drive frontotemporal dementia and Nasu-Hakola disease (Paloneva *et al.*, 2002). Alzheimer's is one of the most investigated cognitive diseases in the literature, and the most common type of dementia for individuals older than 75 years old (*What is Alzheimer's Disease?*, 2023). It is non-surprising that many research groups have shown aspects of Alzheimer's disease intertwined with TREM2 function in microglial cells (Jones, 2013; Wang *et al.*, 2022). But TREM2 is expressed throughout the body and can extensively change outcome of inflammatory responses (Chapter 4 of this dissertation). Is it possible that TREM2 contributes to Alzheimer's disease by its effect in periphery inflammation? Which other organ specific effects have a sex effect driven by TREM2, and how much do they contribute to brain disease?

Given the sex-specific effect if the inflammatory response in the periphery, and the connection between gut and brain it is possible this data has implications for sex-specific

brain effects. There are many different routes that the intestinal tissue can use to modulate brain activity. The endotoxin theory of neurodegeneration suggests increases in intestinal permeability drive alterations in the brain by promoting long-term neuroinflammation. This idea is corroborated by several research that investigate the intestine-brain axis (Houser and Tansey, 2017). How much sex affects this regulation remains to be solved.

From lung to brain: Lung tissue and its brain effects

The lung mucosal tissue is also specialized to be in constant contact with the outside world. It requires the exchange of gas through systems, at the same time it needs to prevent foreign organisms and harmful aerosol particles to enter the body. This is a tightly regulated process to avoid hindering gas exchange or facilitating microorganism invasion. But inflammation briefly dysregulates this process, activating immune cell response that can potentially be harmful to tissue. Sex affects the immune response and has influences in lung function, Females have stronger bronchoconstriction than males (Langdeau *et al.*, 2009), and adapt breathing patterns more easily than males to low levels of oxygen (Horiuchi *et al.*, 2019). We hypothesized sex-specific differences would be present during lung inflammation and contribute to dysregulation of lung function.

Here, we show males and females diferentially regulate this response: female NTS is more responsive to changes in lung environment. LPS is capable of driving an increase in the number of excitatory synapses within the NTS, while *Alternaria alternata* drives a decrease in the number of excitatory synapses within the NTS (Figure 7.2).

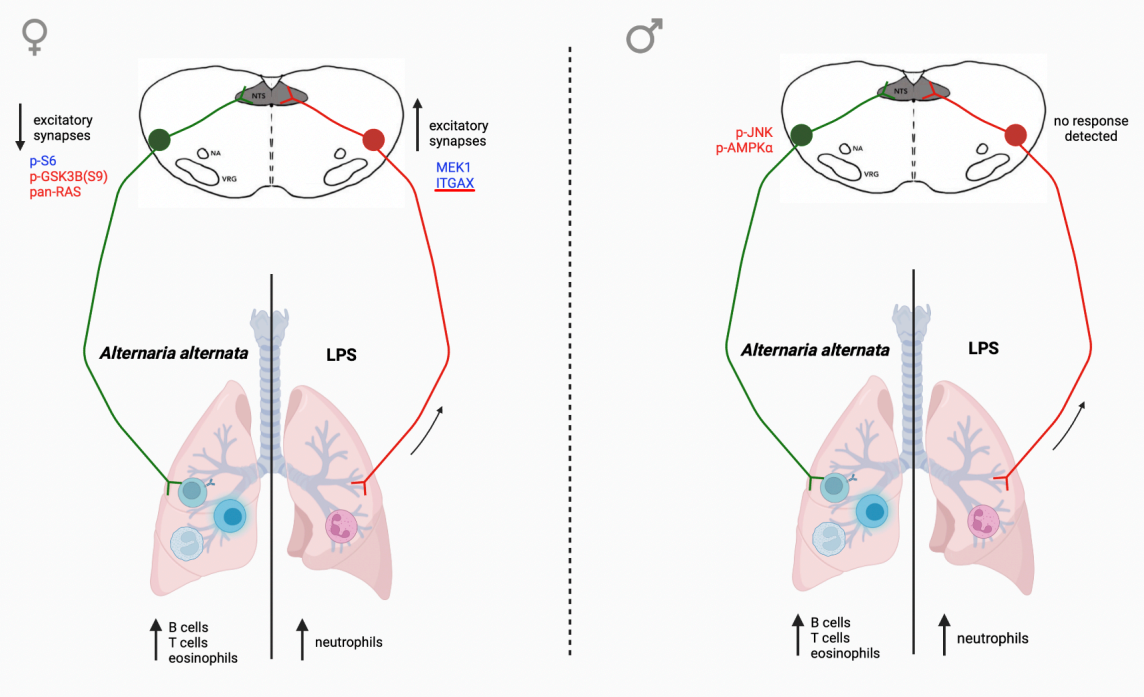


**Figure 7.2 Proposed model in female and male response in the NTS to different types of lung inflammation.**
Females decrease excitatory synapses in number after 7 days of continuous *Alternaria alternata* inhalation, while they increase synaptic number after 7 days of high dose LPS inhalation. We propose the modifications are driven by nociceptor synaptic plasticity independent of neuroinflammation, a mechanism only regulated in females, and which consequence to lung function remains to be investigated.
Males show an altered in signaling cascades within the NTS after Alternaria exposure, while no detected alterations were found in NTS after lung response to LPS.

This response is nociceptor driven and has implication for many different lung functions. The NTS is a region extremely plastic to internal organ alterations. Changes in inflammatory response, particularly allergic are capable of enhancing the nociceptive response within the NTS to an agonist (Spaziano *et al.*, 2015), and in non-human primates direct measurement of neuronal response show an increase after allergic lung inflammation (Chen *et al.*, 2001). This modification has direct consequence in lung function: cough reflexes are initiated by the joint response of nociceptors and mechanoceptors in lung

(Andrani *et al.*, 2019) to expel particles or irritants. Another paper has shown that bronchoconstriction is mediated by NTS activation by nociceptors during allergic responses (Su *et al.*, 2023).

Unfortunately, this dissertation was not able to solve which function this sex-specific NTS response was modulating. This opens up to possibilities (1) either this effect is merely adaptive in female mice driving the same response in male and female lung; (2) this effect mediates breathing rhythmns adaptations to lung differentially between males and females; (3) it drives stronger bronchoconstriction in females. Next experiments are necessary to prove regulation of lung response.

Regardless, the fact that NTS responds in such a sex-specific way has direct implication to lung diseases. During the COVID19 pandemic, many individuals suffered from lung disease and respiratory alterations. Since the control of respiratory reflexes is mediated by the NTS this dissertation provides an insight into mechanistic ways the CNS affects the lung during COVID19 pathology. Is it possible that COVID19 respiratory deficits were caused by mismatched responses between lung environment and NTS driven commands? Moreover, would NTS be responsible for sex differences in lung disease?

Everything, everywhere, all at once

Animal models of disease allows us to separate mechanistically the effects observed. In our IP-LPS model, we were able to separate innate versus adaptive immune response; in the Alternaria model we were able to isolate lung effect and NTS response. This strategy is extremely useful to dissect mechanisms of disease, and in the case of this dissertation, to

show sex specific modulation of response. However, the body experiences things altogether: the intestine is also innervated by nociceptive fibers, IP-LPS also affects the lung, the lung immune cells also secrete inflammatory mediators that could impact intestinal permeability. This section will briefly explore the intertwined connection of the 3 different systems.

Intestinal tissues are innervated by Nav1.8$^{+}$ fibers that respond to inflammation in intestine. These nociceptor fibers have been shown to secrete neuropeptides that protect the intestine from Salmonella infection (Lai *et al.*, 2020). And increases in intestinal permeability are associated with an increase of nociceptive fibers thermal hypersensitivity (Grundy, Erickson and Brierley, 2019), interestingly, this increase correlated with disease severity. These fibers have been shown to induce sex-differences in response dependent of LPS recognition. Mechanical hypersensitivity in sensory fibers is dependent on TLR4 in female sensory fibers, but in males is not (Burton *et al.*, 2019).

Inflammation in mucosal tissue alerts other mucosal tissues. Changes in intestinal immune response would also affect lung-response and vice versa.

IP-LPS model of systemic inflammation affects other organs within the body, including the lung and the brain. IP-LPS has been used to study acute lung injury, and acute respiratory distress syndrome (ARDS). LPS induces increased permeability in lung tissue and affect the expression of a variety of inflammatory markers within the lung (Yue and Guidry, 2019).

In conclusion, sex affects the immune response. We have uncovered two distinct mechanisms that diverge responses in male and female tissues with consequences for brain

health. Moreover, changes in brain function could directly impact peripheral tissues and more research is needed to further understand this crosstalk between brain and periphery.

# References


Abbott, S. (2003) “Molds and other fungi in indoor environments: Summary of biology, known health effects and references.” Available at: https://www.semanticscholar.org/paper/0078232406eed33fa238737f4b7963fd45d92e99 (Accessed: May 22, 2023).

Abrahamsen, B. *et al.* (2008) “The cell and molecular basis of mechanical, cold, and inflammatory pain,” *Science*, 321(5889), pp. 702–705.

Aguzzi, A., Barres, B. A. and Bennett, M. L. (2013) “Microglia: Scapegoat, saboteur, or something else?”

Amorim, M. R. *et al.* (2019) “Neuroinflammation in the NTS is associated with changes in cardiovascular reflexes during systemic inflammation,” *Journal of neuroinflammation*, 16(1), p. 125.

Andrani, F. *et al.* (2019) “Cough, a vital reflex. mechanisms, determinants and measurements,” *Acta bio-medica: Atenei Parmensis*, 89(4), pp. 477–480.

Anhê, F. F. *et al.* (2021) “Metabolic endotoxemia is dictated by the type of lipopolysaccharide,” *bioRxiv*. doi: 10.1101/2021.07.13.452270.

Arnold, A. P. (2020) “Four Core Genotypes and XY* mouse models: Update on impact on SABV research,” *Neuroscience and biobehavioral reviews*. Elsevier BV, 119, pp. 1–8.

Aulock, S. V. *et al.* (2006) “Gender difference in cytokine secretion on immune stimulation with LPS and LTA,” *Journal of interferon & cytokine research: the official journal of the International Society for Interferon and Cytokine Research*, 26(12), pp. 887–892.

Badimon, A. *et al.* (2020) “Negative feedback control of neuronal activity by microglia,” *Nature*, 586(7829), pp. 417–423.

Bain, C. C. *et al.* (2013) “Resident and pro-inflammatory macrophages in the colon represent alternative context-dependent fates of the same Ly6Chi monocyte precursors,” *Mucosal immunology*, 6(3), pp. 498–510.

Bamias, G., Rivera-Nieves, J. and Grisham, M. B. (2018) “Recruitment of Inflammatory and Immune Cells in the Gut,” in *Physiology of the Gastrointestinal Tract*. Elsevier, pp. 1579–1614.

Banks, W. A. *et al.* (2015) “Lipopolysaccharide-induced blood-brain barrier disruption: roles of cyclooxygenase, oxidative stress, neuroinflammation, and elements of the neurovascular unit,” *Journal of neuroinflammation*, 12(1), p. 223.

Barajon, I. *et al.* (2009) “Toll-like receptors 3, 4, and 7 are expressed in the enteric nervous system and dorsal root ganglia,” *The journal of histochemistry and cytochemistry: official journal of the Histochemistry Society*, 57(11), pp. 1013–1023.

Baral, P. *et al.* (2018) “Nociceptor sensory neurons suppress neutrophil and γδ T cell responses in bacterial lung infections and lethal pneumonia,” *Nature medicine*, 24(4), pp. 417–426.

Bartlett, D., Jr and Sant’ambrogio, G. (1976) “Effects of local and systemic hypercapnia on the discharge of stretch receptors in the airways of the dog,” *Respiration physiology*, 26(1), pp. 91–99.

Beurel, E., Grieco, S. F. and Jope, R. S. (2015) “Glycogen synthase kinase-3 (GSK3): regulation, actions, and diseases,” *Pharmacology & therapeutics*, 148, pp. 114–131.

Bianchi, I. *et al.* (2012) “The X chromosome and immune associated genes,” *Journal of autoimmunity*. Elsevier BV, 38(2–3), pp. J187-92.

Biddle, T. A. *et al.* (2023) “Aerosolized aqueous dust extracts collected near a drying lake trigger acute neutrophilic pulmonary inflammation reminiscent of microbial innate immune ligands,” *The Science of the total environment*, 858(Pt 3), p. 159882.

Binnewies, M. *et al.* (2021) “Targeting TREM2 on tumor-associated macrophages enhances immunotherapy,” *Cell reports*, 37(3), p. 109844.

Bohlen, J., Roiuk, M. and Teleman, A. A. (2021) “Phosphorylation of ribosomal protein S6 differentially affects mRNA translation based on ORF length,” *Nucleic acids research*, 49(22), pp. 13062–13074.

Borovikova, L. V. *et al.* (2000) “Vagus nerve stimulation attenuates the systemic inflammatory response to endotoxin,” *Nature*, 405(6785), pp. 458–462.

Bouchon, A., Dietrich, J. and Colonna, M. (2000) “Cutting edge: inflammatory responses can be triggered by TREM-1, a novel receptor expressed on neutrophils and monocytes,” *Journal of immunology* , 164(10), pp. 4991–4995.

Brown, L. S. *et al.* (2019) “Pericytes and Neurovascular Function in the Healthy and Diseased Brain,” *Frontiers in cellular neuroscience*, 13, p. 282.

Burton, M. *et al.* (2019) “Uncovering Cell-Specific Mechanisms in Sex Differences in TLR4-Dependent Pain,” *The journal of pain: official journal of the American Pain Society*. Elsevier, 20(4), p. S1.

Bush, R. K. and Prochnau, J. J. (2004) “Alternaria-induced asthma,” *The Journal of allergy and clinical immunology*, 113(2), pp. 227–234.

Cai, K. C. *et al.* (2016) “Age and sex differences in immune response following LPS treatment in mice,” *Brain, behavior, and immunity*, 58, pp. 327–337.

Card, J. W. *et al.* (2006) “Gender Differences in Murine Airway Responsiveness and Lipopolysaccharide-Induced Inflammation,” *The Journal of Immunology*. doi: 10.4049/jimmunol.177.1.621.

Carrettiero, D. C., Ferrari, M. F. R. and Fior-Chadi, D. R. (2012) “Alpha2-adrenergic receptor distribution and density within the nucleus tractus solitarii of normotensive and hypertensive rats during development,” *Autonomic neuroscience: basic & clinical*, 166(1), pp. 39–46.

Cesaro, A. *et al.* (2009) “Differential expression and regulation of ADAM17 and TIMP3 in acute inflamed intestinal epithelia,” *American journal of physiology. Gastrointestinal and liver physiology*, 296(6), pp. G1332-43.

Chang, R. B. *et al.* (2015) “Vagal Sensory Neuron Subtypes that Differentially Control Breathing,” *Cell*, 161(3), pp. 622–633.

Chen, C. Y. *et al.* (2001) “Extended allergen exposure in asthmatic monkeys induces neuroplasticity in nucleus tractus solitarius,” *The Journal of allergy and clinical immunology*, 108(4), pp. 557–562.

Chen Gang *et al.* (2016) “Comparison of RELMα and RELMβ Single- and Double-Gene-Deficient Mice Reveals that RELMα Expression Dictates Inflammation and Worm Expulsion in Hookworm Infection,” *Infection and immunity*. American Society for Microbiology, 84(4), pp. 1100–1111.

Chen, J. *et al.* (2019) “IL-17 inhibits CXCL9/10-mediated recruitment of CD8+ cytotoxic T cells and regulatory T cells to colorectal tumors,” *Journal for immunotherapy of cancer*. BMJ, 7(1), p. 324.

Chen, Y. *et al.* (2020) “Absorptive transport of amino acids by the rat colon,” *American journal of physiology. Gastrointestinal and liver physiology*, 318(1), pp. G189–G202.

Chen, Z. *et al.* (2018) “Sepsis Upregulates CD14 Expression in a MyD88-Dependent and Trif-Independent Pathway,” *Shock* , 49(1), pp. 82–89.

Cheng, S.-C. *et al.* (2014) “mTOR- and HIF-1α-mediated aerobic glycolysis as metabolic basis for trained immunity,” *Science*, 345(6204), p. 1250684.

Chowdhury, N. U. *et al.* (2021) “Sex and gender in asthma,” *European respiratory review: an official journal of the European Respiratory Society*, 30(162). doi: 10.1183/16000617.0067-2021.

Clarke, L. L. (2009) “A guide to Ussing chamber studies of mouse intestine,” *American journal of physiology. Gastrointestinal and liver physiology*, 296(6), pp. G1151-66.

Corder, K. M. *et al.* (2023) “Behavioral comparison of the C57BL/6 inbred mouse strain and their CB6F1 siblings,” *Behavioural processes*, 207, p. 104836.

Correale, C. *et al.* (2013) “Bacterial sensor triggering receptor expressed on myeloid cells-2 regulates the mucosal inflammatory response,” *Gastroenterology*, 144(2), pp. 346-356.e3.

Crosson, T. *et al.* (2023) “IL-13 promotes sensory-sympathetic neurons crosstalk in asthma,” *bioRxiv*. doi: 10.1101/2023.01.26.525731.

Crowley, M. T. *et al.* (1997) “A Critical Role for Syk in Signal Transduction and Phagocytosis Mediated by Fcγ Receptors on Macrophages,” *The Journal of experimental medicine*. The Rockefeller University Press, 186(7), pp. 1027–1039.

Cruzat, V. *et al.* (2018) “Glutamine: Metabolism and Immune Function, Supplementation and Clinical Translation,” *Nutrients*, 10(11). doi: 10.3390/nu10111564.

Cunningham, M. A. *et al.* (2012) “Estrogen receptor alpha modulates Toll-like receptor signaling in murine lupus,” *Clinical immunology* , 144(1), pp. 1–12.

Cunningham, M. A. *et al.* (2014) “Estrogen Receptor Alpha Binding to ERE is Required for Full Tlr7- and Tlr9-Induced Inflammation,” *SOJ immunology*, 2(1). doi: 10.15226/soji.2014.00107.

Dantzer, R. *et al.* (2008) “From inflammation to sickness and depression: when the immune system subjugates the brain,” *Nature reviews. Neuroscience*, 9(1), pp. 46–56.

Davis, S. F. *et al.* (2004) “Excitatory and inhibitory local circuit input to the rat dorsal motor nucleus of the vagus originating from the nucleus tractus solitarius,” *Brain research*, 1017(1–2), pp. 208–217.

Daws, M. R. *et al.* (2001) “Cloning and characterization of a novel mouse myeloid DAP12-associated receptor family,” *European journal of immunology*, 31(3), pp. 783–791.

Daws, M. R. *et al.* (2003) “Pattern recognition by TREM-2: binding of anionic ligands,” *Journal of immunology* , 171(2), pp. 594–599.

De Schepper, S. *et al.* (2018) “Self-maintaining gut macrophages are essential for intestinal homeostasis,” *Cell*. Elsevier BV, 175(2), pp. 400-415.e13.

Dejanovic, B. *et al.* (2022) “Complement C1q-dependent excitatory and inhibitory synapse elimination by astrocytes and microglia in Alzheimer’s disease mouse models,” *Nature aging*, 2(9), pp. 837–850.

Dempsey, L. A. (2015) “Nociceptors in asthma,” *Nature immunology*. Nature Publishing Group, 16(9), pp. 906–906.

Denning, T. L. *et al.* (2007) “Lamina propria macrophages and dendritic cells differentially induce regulatory and interleukin 17-producing T cell responses,” *Nature immunology*, 8(10), pp. 1086–1094.

Deny, M. *et al.* (2022) “Sex difference in innate inflammatory response and macrophage polarization in Streptococcus agalactiae-induced pneumonia and potential role of microRNA-223-3p,” *Scientific reports*, 12(1), p. 17126.

Deshpande, R. *et al.* (1997) “Estradiol down-regulates LPS-induced cytokine production and NFkB activation in murine macrophages,” *American journal of reproductive immunology* . Wiley, 38(1), pp. 46–54.

Dheer, R. *et al.* (2016) “Intestinal Epithelial Toll-Like Receptor 4 Signaling Affects Epithelial Function and Colonic Microbiota and Promotes a Risk for Transmissible Colitis,” *Infection and immunity*, 84(3), pp. 798–810.

Diogenes, A. *et al.* (2011) “LPS sensitizes TRPV1 via activation of TLR4 in trigeminal sensory neurons,” *Journal of dental research*, 90(6), pp. 759–764.

Doney, E. *et al.* (2023) “Chronic stress exposure alters the gut barrier: sex-specific effects on microbiota and jejunum tight junctions,” *Biological Psychiatry Global Open Science*. doi: 10.1016/j.bpsgos.2023.04.007.

Donohoe, D. R. *et al.* (2011) “The microbiome and butyrate regulate energy metabolism and autophagy in the mammalian colon,” *Cell metabolism*, 13(5), pp. 517–526.

Erickson, M. A. *et al.* (2018) “Genetics and sex influence peripheral and central innate immune responses and bloodbrain barrier integrity,” *PLoS ONE*. doi: 10.1371/journal.pone.0205769.

Erridge, C., Bennett-Guerrero, E. and Poxton, I. R. (2002) “Structure and function of lipopolysaccharides,” *Microbes and infection*. Elsevier BV, 4(8), pp. 837–851.

Evans, A. M. and Hardie, D. G. (2020) “AMPK and the Need to Breathe and Feed: What’s the Matter with Oxygen?,” *International journal of molecular sciences*, 21(10). doi: 10.3390/ijms21103518.

Fanelli, A. *et al.* (1994) “Histamine induced changes in breathing pattern may precede bronchoconstriction in selected patients with bronchial asthma,” *Thorax*, 49(7), pp. 639–643.

Farré, R. *et al.* (2020) “Intestinal Permeability, Inflammation and the Role of Nutrients,” *Nutrients*, 12(4). doi: 10.3390/nu12041185.

Ferreira, S. H. *et al.* (1988) “Interleukin-1 beta as a potent hyperalgesic agent antagonized by a tripeptide analogue,” *Nature*, 334(6184), pp. 698–700.

Feuerstein, J. D. and Cheifetz, A. S. (2017) “Crohn Disease: Epidemiology, Diagnosis, and Management,” *Mayo Clinic proceedings. Mayo Clinic*, 92(7), pp. 1088–1103.

Finnell, J. E., Speirs, I. C. and Tronson, N. C. (2023) “Sex differences in hippocampal cytokine networks after systemic immune challenge,” *bioRxiv*. doi: 10.1101/378257.

Fournier, B. M. and Parkos, C. A. (2012) “The role of neutrophils during intestinal inflammation,” *Mucosal immunology*, 5(4), pp. 354–366.

Freemerman, A. J. *et al.* (2014) “Metabolic reprogramming of macrophages: glucose transporter 1 (GLUT1)-mediated glucose metabolism drives a proinflammatory phenotype,” *The Journal of biological chemistry*, 289(11), pp. 7884–7896.

Frost, P. S. *et al.* (2019) “Neonatal infection leads to increased susceptibility to Aβ oligomer-induced brain inflammation, synapse loss and cognitive impairment in mice,” *Cell death & disease*, 10(4), p. 323.

Fu, C. *et al.* (2019) “Activation of Phox2b-Expressing Neurons in the Nucleus Tractus Solitarii Drives Breathing in Mice,” *The Journal of neuroscience: the official journal of the Society for Neuroscience*, 39(15), pp. 2837–2846.

Galea, I. (2021) “The blood–brain barrier in systemic infection and inflammation,” *Cellular & molecular immunology*. Nature Publishing Group, 18(11), pp. 2489–2501.

Gay, L. *et al.* (2021) “Sexual Dimorphism and Gender in Infectious Diseases,” *Frontiers in immunology*, 12, p. 698121.

Ginhoux, F. *et al.* (2013) “Origin and differentiation of microglia,” *Frontiers in Cellular Neuroscience*, 7. doi: 10.3389/fncel.2013.00045.

Gomez Perdiguero, E., Schulz, C. and Geissmann, F. (2013) “Development and homeostasis of resident myeloid cells: The case of the microglia,” *GLIA*, 61(1), pp. 112–120.

González-Scarano, F. and Baltuch, G. (1999) “Microglia as mediators of inflammatory and degenerative diseases,” *Annual review of neuroscience*, 22, pp. 219–240.

Goodman, W. A., Erkkila, I. P. and Pizarro, T. T. (2020) “Sex matters: impact on pathogenesis, presentation and treatment of inflammatory bowel disease,” *Nature reviews.*

*Gastroenterology & hepatology*. Springer Science and Business Media LLC, 17(12), pp. 740–754.

Griesbeck, M. *et al.* (2015) "Sex Differences in Plasmacytoid Dendritic Cell Levels of IRF5 Drive Higher IFN-α Production in Women," *Journal of immunology* , 195(11), pp. 5327–5336.

Grundy, L., Erickson, A. and Brierley, S. M. (2019) "Visceral Pain," *Annual review of physiology*, 81, pp. 261–284.

Guan, K. *et al.* (2019) "Principles of Allergen Immunotherapy and Its Clinical Application in China: Contrasts and Comparisons with the USA," *Clinical reviews in allergy & immunology*, 57(1), pp. 128–143.

Guerreiro, R. *et al.* (2013) "TREM2 variants in Alzheimer's disease," *The New England journal of medicine*, 368(2), pp. 117–127.

Hall, S. C. and Agrawal, D. K. (2017) "Increased TREM-2 expression on the subsets of CD11c+ cells in the lungs and lymph nodes during allergic airway inflammation," *Scientific reports*, 7(1), p. 11853.

Hamerman, J. A. *et al.* (2006) "Cutting edge: inhibition of TLR and FcR responses in macrophages by triggering receptor expressed on myeloid cells (TREM)-2 and DAP12," *The journal of immunology*. The American Association of Immunologists, 177(4), pp. 2051–2055.

Hausmann, M. *et al.* (2002) "Toll-like receptors 2 and 4 are up-regulated during intestinal inflammation," *Gastroenterology*, 122(7), pp. 1987–2000.

Hayes, T. *et al.* (2018) "Innate Immunity Induced by the Major Allergen Alt a 1 From the Fungus Alternaria Is Dependent Upon Toll-Like Receptors 2/4 in Human Lung Epithelial Cells," *Frontiers in immunology*, 9, p. 1507.

Hernandez-Ramirez, G. *et al.* (2021) "Alternaria as an inducer of allergic sensitization," *Journal of fungi (Basel, Switzerland)*. MDPI AG, 7(10), p. 838.

Herzog, E. *et al.* (2006) "Synaptic and vesicular co-localization of the glutamate transporters VGLUT1 and VGLUT2 in the mouse hippocampus," *Journal of neurochemistry*, 99(3), pp. 1011–1018.

Hiroki, C. H. *et al.* (2021) "Innate Receptors Expression by Lung Nociceptors: Impact on COVID-19 and Aging," *Frontiers in immunology*, 12, p. 785355.

Honda, K. *et al.* (2005) "IRF-7 is the master regulator of type-I interferon-dependent immune responses," *Nature*, 434(7034), pp. 772–777.

Honda, M. *et al.* (2021) "Directly recruited GATA6+ peritoneal cavity macrophages contribute to the repair of intestinal serosal injury," *Nature communications*. Nature Publishing Group UK London, 12(1), p. 7294.

Horiuchi, M. *et al.* (2019) "Sex differences in respiratory and circulatory cost during hypoxic walking: potential impact on oxygen saturation," *Scientific reports*, 9(1), p. 9550.

Houser, M. C. and Tansey, M. G. (2017) "The gut-brain axis: is intestinal inflammation a silent driver of Parkinson's disease pathogenesis?," *NPJ Parkinson's disease*, 3, p. 3.

Huynh, D. *et al.* (2013) "CSF-1 receptor-dependent colon development, homeostasis and inflammatory stress response," *PloS one*, 8(2), p. e56951.

Jacobson, D. L. *et al.* (1997) "Epidemiology and estimated population burden of selected autoimmune diseases in the United States," *Clinical immunology and immunopathology*, 84(3), pp. 223–243.

Jaillon, S., Berthenet, K. and Garlanda, C. (2019) "Sexual Dimorphism in Innate Immunity," *Clinical reviews in allergy & immunology*, 56(3), pp. 308–321.

Jain, A. and Pasare, C. (2017) "Innate Control of Adaptive Immunity: Beyond the Three-Signal Paradigm," *Journal of immunology* , 198(10), pp. 3791–3800.

Jang, M. H. *et al.* (2006) "CCR7 is critically important for migration of dendritic cells in intestinal lamina propria to mesenteric lymph nodes," *Journal of immunology* , 176(2), pp. 803–810.

Jansson-Knodell, C. L. *et al.* (2018) "Not All That Flattens Villi Is Celiac Disease: A Review of Enteropathies," *Mayo Clinic proceedings. Mayo Clinic*, 93(4), pp. 509–517.

Jiang, Z. *et al.* (2005) "CD14 is required for MyD88-independent LPS signaling," *Nature immunology*, 6(6), pp. 565–570.

Jones, B. (2013) "Alzheimer disease: TREM2 linked to late-onset AD," *Nature reviews. Neurology*, p. 5.

Jung, J., Zeng, H. and Horng, T. (2019) "Metabolism as a guiding force for immunity," *Nature cell biology*, 21(1), pp. 85–93.

Kamdar, K. *et al.* (2016) "Genetic and Metabolic Signals during Acute Enteric Bacterial Infection Alter the Microbiota and Drive Progression to Chronic Inflammatory Disease," *Cell host & microbe*, 19(1), pp. 21–31.

Kang, B. *et al.* (2019) "Commensal microbiota drive the functional diversification of colon macrophages," *Mucosal immunology*. Nature Publishing Group, 13(2), pp. 216–229.

Kanter, J. E. *et al.* (2012) "Diabetes promotes an inflammatory macrophage phenotype and atherosclerosis through acyl-CoA synthetase 1," *Proceedings of the National Academy of Sciences of the United States of America*, 109(12), pp. E715-24.

Kelly, B. and O'Neill, L. A. J. (2015) "Metabolic reprogramming in macrophages and dendritic cells in innate immunity," *Cell research*. Springer Science and Business Media LLC, 25(7), pp. 771–784.

Keren-Shaul, H. *et al.* (2017) "A Unique Microglia Type Associated with Restricting Development of Alzheimer's Disease," *Cell*, 169(7), pp. 1276-1290.e17.

Kettenmann, H., Kirchhoff, F. and Verkhratsky, A. (2013) "Perspective Microglia : New Roles for the Synaptic Stripper," *NEURON*. Elsevier, 77(1), pp. 10–18.

Kim, M. *et al.* (2018) "Critical Role for the Microbiota in CX3CR1+ Intestinal Mononuclear Phagocyte Regulation of Intestinal T Cell Responses," *Immunity*, 49(1), pp. 151-163.e5.

Knight, Z. A. *et al.* (2012) "Molecular profiling of activated neurons by phosphorylated ribosome capture," *Cell*, 151(5), pp. 1126–1137.

Ko, R. *et al.* (2015) "Glycogen synthase kinase 3β ubiquitination by TRAF6 regulates TLR3-mediated pro-inflammatory cytokine production," *Nature communications*, 6, p. 6765.

Kollarik, M., Ru, F. and Brozmanova, M. (2010) "Vagal afferent nerves with the properties of nociceptors," *Autonomic neuroscience: basic & clinical*, 153(1–2), pp. 12–20.

Kristiansen, K. A. and Edvinsson, L. (2010) "Neurogenic inflammation: a study of rat trigeminal ganglion," *The journal of headache and pain*, 11(6), pp. 485–495.

Krivan, S. *et al.* (2019) "Increased expression of Toll-like receptors 2, 3, 4 and 7 mRNA in the kidney and intestine of a septic mouse model," *Scientific reports*, 9(1), p. 4010.

Kroemer, G., Mariño, G. and Levine, B. (2010) "Autophagy and the integrated stress response," *Molecular cell*, 40(2), pp. 280–293.

Kubin, L. *et al.* (2006) "Central pathways of pulmonary and lower airway vagal afferents," *Journal of applied physiology*, 101(2), pp. 618–627.

Lai, N. Y. *et al.* (2020) "Gut-Innervating Nociceptor Neurons Regulate Peyer's Patch Microfold Cells and SFB Levels to Mediate Salmonella Host Defense," *Cell*, 180(1), pp. 33-49.e22.

Lampropoulou, V. *et al.* (2016) “Itaconate Links Inhibition of Succinate Dehydrogenase with Macrophage Metabolic Remodeling and Regulation of Inflammation,” *Cell metabolism*, 24(1), pp. 158–166.

Langdeau, J. B. *et al.* (2000) “Airway hyperresponsiveness in elite athletes,” *American journal of respiratory and critical care medicine*. atsjournals.org, 161(5), pp. 1479–1484.

Langdeau, J.-B. *et al.* (2009) “Gender differences in the prevalence of airway hyperresponsiveness and asthma in athletes,” *Respiratory medicine*, 103(3), pp. 401–406.

Lee, S. H. *et al.* (2010) “ERK activation drives intestinal tumorigenesis in Apcmin/+ mice,” *Nature medicine*. Nature Publishing Group, 16(6), pp. 665–670.

Lee, S. H. (2015) “Intestinal permeability regulation by tight junction: implication on inflammatory bowel diseases,” *Intestinal research*, 13(1), pp. 11–18.

van Lengerich, B. *et al.* (2023) “A TREM2-activating antibody with a blood-brain barrier transport vehicle enhances microglial metabolism in Alzheimer’s disease models,” *Nature neuroscience*. Springer Science and Business Media LLC, 26(3), pp. 416–429.

Lerouge, I. and Vanderleyden, J. (2002) “O-antigen structural variation: mechanisms and possible roles in animal/plant–microbe interactions,” *FEMS microbiology reviews*. Oxford Academic, 26(1), pp. 17–47.

Liu, T. *et al.* (2017) “NF-κB signaling in inflammation,” *Signal transduction and targeted therapy*, 2, pp. 17023-.

Louveau, A., Da Mesquita, S. and Kipnis, J. (2016) “Lymphatics in Neurological Disorders: A Neuro-Lympho-Vascular Component of Multiple Sclerosis and Alzheimer’s Disease?,” *Neuron*, 91(5), pp. 957–973.

*LPS from E. coli, Serotype O55:B5 (TLRGRADE®) (Ready-to-Use)* (2022). Available at: https://www.enzolifesciences.com/ALX-581-013/lps-from-e.-coli-serotype-o55-b5-tlrgrade-ready-to-use/ (Accessed: May 21, 2023).

MacMillan, S. and Evans, A. M. (2023) “AMPK facilitates the hypoxic ventilatory response through non-adrenergic mechanisms at the brainstem,” *Pflugers Archiv: European journal of physiology*, 475(1), pp. 89–99.

Martin, J. C. *et al.* (2019) “Single-Cell Analysis of Crohn’s Disease Lesions Identifies a Pathogenic Cellular Module Associated with Resistance to Anti-TNF Therapy,” *Cell*, 178(6), pp. 1493-1508.e20.

Maruyama, K. (2022) “Senso-immunology: crosstalk between nociceptive and immune systems,” *The FEBS journal*, 289(14), pp. 4132–4145.

Mata-Haro, V. *et al.* (2007) "The Vaccine Adjuvant Monophosphoryl Lipid A as a TRIF-Biased Agonist of TLR4," *Science*, 316(5831), pp. 1628–1632.

Mathur, S. *et al.* (2021) "Nociceptor neurons promote IgE class switch in B cells," *JCI insight*, 6(24). doi: 10.1172/jci.insight.148510.

Matott, M. P., Kline, D. D. and Hasser, E. M. (2017) "Glial EAAT2 regulation of extracellular nTS glutamate critically controls neuronal activity and cardiorespiratory reflexes," *The Journal of physiology*, 595(17), pp. 6045–6063.

McCullough, L. D. *et al.* (2016) "Stroke sensitivity in the aged: sex chromosome complement vs. gonadal hormones," *Aging*, 8(7), pp. 1432–1441.

McElrath, C. *et al.* (2021) "Critical role of interferons in gastrointestinal injury repair," *Nature communications*, 12(1), p. 2624.

McKemy, D. D., Neuhausser, W. M. and Julius, D. (2002) "Identification of a cold receptor reveals a general role for TRP channels in thermosensation," *Nature*, 416(6876), pp. 52–58.

Mickle, A. D., Shepherd, A. J. and Mohapatra, D. P. (2016) "Nociceptive TRP Channels: Sensory Detectors and Transducers in Multiple Pain Pathologies," *Pharmaceuticals* , 9(4). doi: 10.3390/ph9040072.

Migale, R. *et al.* (2015) "Specific Lipopolysaccharide Serotypes Induce Differential Maternal and Neonatal Inflammatory Responses in a Murine Model of Preterm Labor," *The American journal of pathology*, 185(9), pp. 2390–2401.

Mills, E. L. *et al.* (2016) "Succinate Dehydrogenase Supports Metabolic Repurposing of Mitochondria to Drive Inflammatory Macrophages," *Cell*, 167(2), pp. 457-470.e13.

Moen, S. H. *et al.* (2019) "Human Toll-like Receptor 8 (TLR8) Is an Important Sensor of Pyogenic Bacteria, and Is Attenuated by Cell Surface TLR Signaling," *Frontiers in immunology*, 10, p. 1209.

Morel, C. *et al.* (2018) "JIP1-Mediated JNK Activation Negatively Regulates Synaptic Plasticity and Spatial Memory," *The Journal of neuroscience: the official journal of the Society for Neuroscience*, 38(15), pp. 3708–3728.

Mostafa, D. H. D. *et al.* (2022) "Characterization of sex-related differences in allergen house dust mite-challenged airway inflammation, in two different strains of mice," *Scientific reports*, 12(1), p. 20837.

Motoyama, E. K. and Finder, J. D. (2011) "Respiratory physiology in infants and children," in *Smith's Anesthesia for Infants and Children*. Elsevier, pp. 22–79.

*Mouse Metabolism Panel Gene List* (2022) *NanoString*. NanoString Technologies, Inc. Available at: https://nanostring.com/resources/mouse-metabolism-panel-gene-list/ (Accessed: May 21, 2023).

Munn, D. H. *et al.* (1999) "Inhibition of T cell proliferation by macrophage tryptophan catabolism," *The Journal of experimental medicine*, 189(9), pp. 1363–1372.

Nakata, K. *et al.* (2006) "Specific messenger RNA expression for signal transduction molecules by lipopolysaccharide in intestinal macrophages," *Clinical and experimental immunology*, 143(3), pp. 484–493.

Nassar, M. A. *et al.* (2004) "Nociceptor-specific gene deletion reveals a major role for Nav1.7 (PN1) in acute and inflammatory pain," *Proceedings of the National Academy of Sciences of the United States of America*. Proceedings of the National Academy of Sciences, 101(34), pp. 12706–12711.

Natale, G. *et al.* (2019) "TREM Receptors Connecting Bowel Inflammation to Neurodegenerative Disorders," *Cells* , 8(10). doi: 10.3390/cells8101124.

*nCounter Mouse Inflammation V2 Panel Gene List* (2021) *NanoString*. NanoString Technologies, Inc. Available at: https://nanostring.com/support-documents/ncounter-mouse-inflammation-v2-panel-gene-list/ (Accessed: May 21, 2023).

Nedrebø, T. and Reed, R. K. (2002) "Different serotypes of endotoxin (lipopolysaccharide) cause different increases in albumin extravasation in rats," *Shock (Augusta, Ga.)*. Ovid Technologies (Wolters Kluwer Health), 18(2), pp. 138–141.

Needleman, P. and Manning, P. T. (1999) "Interactions between the inducible cyclooxygenase (COX-2) and nitric oxide synthase (iNOS) pathways: implications for therapeutic intervention in osteoarthritis," *Osteoarthritis and cartilage / OARS, Osteoarthritis Research Society*, 7(4), pp. 367–370.

Nguyen, A. Q. *et al.* (2020) "Astrocytic Ephrin-B1 Controls Excitatory-Inhibitory Balance in Developing Hippocampus," *The Journal of neuroscience: the official journal of the Society for Neuroscience*, 40(36), pp. 6854–6871.

Nonoguchi, H. A. *et al.* (2022) "Lipopolysaccharide Exposure Differentially Alters Plasma and Brain Inflammatory Markers in Adult Male and Female Rats," *Brain sciences*, 12(8). doi: 10.3390/brainsci12080972.

Nonomura, K. *et al.* (2017) "Piezo2 senses airway stretch and mediates lung inflation-induced apnoea," *Nature*, 541(7636), pp. 176–181.

Norata, G. D. *et al.* (2006) "Dihydrotestosterone Decreases Tumor Necrosis Factor-α and Lipopolysaccharide-Induced Inflammatory Response in Human Endothelial Cells," *The Journal of clinical endocrinology and metabolism*. Oxford Academic, 91(2), pp. 546–554.

Orecchioni, M. *et al.* (2019) "Macrophage Polarization: Different Gene Signatures in M1(LPS+) vs. Classically and M2(LPS-) vs. Alternatively Activated Macrophages," *Frontiers in immunology*, 10, p. 1084.

Ostvik, A. E. *et al.* (2013) "Enhanced expression of CXCL10 in inflammatory bowel disease: potential role of mucosal Toll-like receptor 3 stimulation," *Inflammatory bowel diseases*, 19(2), pp. 265–274.

Overduin, T. S. *et al.* (2023) "Active glucose transport varies by small intestinal region and oestrous cycle stage in mice," *Experimental physiology*. doi: 10.1113/EP091040.

Paloneva, J. *et al.* (2002) "Mutations in two genes encoding different subunits of a receptor signaling complex result in an identical disease phenotype," *American journal of human genetics*, 71(3), pp. 656–662.

Park, B. S. and Lee, J.-O. (2013) "Recognition of lipopolysaccharide pattern by TLR4 complexes," *Experimental & molecular medicine*, 45(12), p. e66.

Pavlov, V. A. *et al.* (2006) "Central muscarinic cholinergic regulation of the systemic inflammatory response during endotoxemia," *Proceedings of the National Academy of Sciences of the United States of America*, 103(13), pp. 5219–5223.

Peng, Q. *et al.* (2010) "TREM2- and DAP12-dependent activation of PI3K requires DAP10 and is inhibited by SHIP1," *Science signaling*, 3(122), p. ra38.

Peng, X. *et al.* (2018) "Continuous Inhalation Exposure to Fungal Allergen Particulates Induces Lung Inflammation While Reducing Innate Immune Molecule Expression in the Brainstem," *ASN neuro*, 10, p. 1759091418782304.

Peterson, D. D. *et al.* (1981) "Effects of aging on ventilatory and occlusion pressure responses to hypoxia and hypercapnia," *The American review of respiratory disease*, 124(4), pp. 387–391.

Peterson, L. W. and Artis, D. (2014) "Intestinal epithelial cells: regulators of barrier function and immune homeostasis," *Nature reviews. Immunology*. Nature Publishing Group, 14(3), pp. 141–153.

Pieterse, E. *et al.* (2016) "Neutrophils Discriminate between Lipopolysaccharides of Different Bacterial Sources and Selectively Release Neutrophil Extracellular Traps," *Frontiers in immunology*, 7, p. 484.

Płóciennikowska, A. *et al.* (2015) “Co-operation of TLR4 and raft proteins in LPS-induced pro-inflammatory signaling,” *Cellular and molecular life sciences: CMLS*, 72(3), pp. 557–581.

Posma, E. *et al.* (2004) “The effect of testosterone on cytokine production in the specific and non-specific immune response,” *American journal of reproductive immunology* . Wiley, 52(4), pp. 237–243.

Prasad, S. *et al.* (2005) “Inflammatory processes have differential effects on claudins 2, 3 and 4 in colonic epithelial cells,” *Laboratory investigation; a journal of technical methods and pathology*, 85(9), pp. 1139–1162.

Pröbstel, A.-K. *et al.* (2020) “Gut microbiota-specific IgA+ B cells traffic to the CNS in active multiple sclerosis,” *Science immunology*, 5(53). doi: 10.1126/sciimmunol.abc7191.

Rath, E. and Haller, D. (2022) “Intestinal epithelial cell metabolism at the interface of microbial dysbiosis and tissue injury,” *Mucosal immunology*, 15(4), pp. 595–604.

Rettew, J. A., Huet, Y. M. and Marriott, I. (2009) “Estrogens augment cell surface TLR4 expression on murine macrophages and regulate sepsis susceptibility in vivo,” *Endocrinology*, 150(8), pp. 3877–3884.

Rettew, J. A., Huet-Hudson, Y. M. and Marriott, I. (2008) “Testosterone reduces macrophage expression in the mouse of toll-like receptor 4, a trigger for inflammation and innate immunity,” *Biology of reproduction*, 78(3), pp. 432–437.

Ribeiro, M. C. *et al.* (2018) “LPS Induces mTORC1 and mTORC2 Activation During Monocyte Adhesion,” *Frontiers in molecular biosciences*, 5, p. 67.

Robinson, D. P. and Klein, S. L. (2012) “Pregnancy and pregnancy-associated hormones alter immune responses and disease pathogenesis,” *Hormones and behavior*, 62(3), pp. 263–271.

Röder, P. V. *et al.* (2014) “The role of SGLT1 and GLUT2 in intestinal glucose transport and sensing,” *PloS one*, 9(2), p. e89977.

Rosenthal, R. *et al.* (2020) “Claudin-15 forms a water channel through the tight junction with distinct function compared to claudin-2,” *Acta physiologica* , 228(1), p. e13334.

Rufo, N. *et al.* (2022) “Stress-induced inflammation evoked by immunogenic cell death is blunted by the IRE1α kinase inhibitor KIRA6 through HSP60 targeting,” *Cell death and differentiation*, 29(1), pp. 230–245.

Sankaran-Walters, S. *et al.* (2013) “Sex differences matter in the gut: effect on mucosal immune activation and inflammation,” *Biology of sex differences*, 4(1), p. 10.

Saruta, M. *et al.* (2009) "High-frequency Haplotypes in the X Chromosome Locus TLR8 Are Associated With Both CD and UC in Females," *Inflammatory bowel diseases*. Oxford Academic, 15(3), pp. 321–327.

Satoh, T. *et al.* (2010) "The Jmjd3-Irf4 axis regulates M2 macrophage polarization and host responses against helminth infection," *Nature immunology*, 11(10), pp. 936–944.

Schafer, D. P. *et al.* (2012) "Microglia sculpt postnatal neural circuits in an activity and complement-dependent manner," *Neuron*, 74(4), pp. 691–705.

Schmid, C. D. *et al.* (2002) "Heterogeneous expression of the triggering receptor expressed on myeloid cells-2 on adult murine microglia," *Journal of neurochemistry*, 83(6), pp. 1309–1320.

Schreiber, J. *et al.* (2006) "Coordinated binding of NF-κB family members in the response of human cells to lipopolysaccharide," *Proceedings of the National Academy of Sciences*, 103(15), pp. 5899–5904.

Schurz, H. *et al.* (2019) "The X chromosome and sex-specific effects in infectious disease susceptibility," *Human genomics*. Springer Science and Business Media LLC, 13(1), p. 2.

*Scn10a Gene Expression Tissue Summary - GXD* (no date). Available at: https://www.informatics.jax.org/tissue/marker/MGI:108029 (Accessed: June 14, 2023).

Scotland, R. S. *et al.* (2011) "Sex differences in resident immune cell phenotype underlie more efficient acute inflammatory responses in female mice," *Blood*, 118(22), pp. 5918–5927.

Seno, H. *et al.* (2009) "Efficient colonic mucosal wound repair requires Trem2 signaling," *Proceedings of the National Academy of Sciences of the United States of America*, 106(1), pp. 256–261.

Shah, S. C. *et al.* (2018) "Sex-Based Differences in Incidence of Inflammatory Bowel Diseases-Pooled Analysis of Population-Based Studies From Western Countries," *Gastroenterology*, 155(4), pp. 1079-1089.e3.

Shuba, Y. M. (2020) "Beyond Neuronal Heat Sensing: Diversity of TRPV1 Heat-Capsaicin Receptor-Channel Functions," *Frontiers in cellular neuroscience*, 14, p. 612480.

Sierra, A. *et al.* (2013) "Janus-faced microglia: Beneficial and detrimental consequences of microglial phagocytosis."

Sina, C., Kemper, C. and Derer, S. (2018) "The intestinal complement system in inflammatory bowel disease: Shaping intestinal barrier function," *Seminars in immunology*, 37, pp. 66–73.

Smith, S. A. *et al.* (2021) “Mitochondrial dysfunction in inflammatory bowel disease alters intestinal epithelial metabolism of hepatic acylcarnitines,” *The Journal of clinical investigation*, 131(1). doi: 10.1172/JCI133371.

Smith-Bouvier, D. L. *et al.* (2008) “A role for sex chromosome complement in the female bias in autoimmune disease,” *The Journal of experimental medicine*, 205(5), pp. 1099–1108.

Smythies, L. E. *et al.* (2005) “Human intestinal macrophages display profound inflammatory anergy despite avid phagocytic and bacteriocidal activity,” *The Journal of clinical investigation*, 115(1), pp. 66–75.

Sonnenberg, G. F. *et al.* (2011) “CD4(+) lymphoid tissue-inducer cells promote innate immunity in the gut,” *Immunity*, 34(1), pp. 122–134.

Spaziano, G. *et al.* (2015) “Exposure to Allergen Causes Changes in NTS Neural Activities after Intratracheal Capsaicin Application, in Endocannabinoid Levels and in the Glia Morphology of NTS,” *BioMed research international*, 2015, p. 980983.

Spitzer, J. A. (1999) “Gender differences in some host defense mechanisms,” *Lupus*, 8(5), pp. 380–383.

Stevens, B. *et al.* (2007) “The Classical Complement Cascade Mediates CNS Synapse Elimination,” *Cell*, 131(6), pp. 1164–1178.

Stewart, A. N. *et al.* (2021) “Acute inflammatory profiles differ with sex and age after spinal cord injury,” *Journal of neuroinflammation*, 18(1), p. 113.

Stroud, D. M. *et al.* (no date) “Contrasting Nav1.8 Activity in Scn10a−/− Ventricular Myocytes and the Intact Heart,” *Journal of the American Heart Association*. American Heart Association, 5(11), p. e002946.

Stunault, M. I. *et al.* (2018) “Metabolism Plays a Key Role during Macrophage Activation,” *Mediators of inflammation*, 2018, p. 2426138.

Su, Y. *et al.* (2023) “Brainstem Dbh + Neurons Control Chronic Allergen-Induced Airway Hyperreactivity,” *bioRxiv : the preprint server for biology*. doi: 10.1101/2023.02.04.527145.

Su, Z.-Z. *et al.* (2003) “Insights into glutamate transport regulation in human astrocytes: cloning of the promoter for excitatory amino acid transporter 2 (EAAT2),” *Proceedings of the National Academy of Sciences of the United States of America*, 100(4), pp. 1955–1960.

Suzuki, M., Hisamatsu, T. and Podolsky, D. K. (2003) “Gamma interferon augments the intracellular pathway for lipopolysaccharide (LPS) recognition in human intestinal

epithelial cells through coordinated up-regulation of LPS uptake and expression of the intracellular Toll-like receptor 4-MD-2 complex," *Infection and immunity*, 71(6), pp. 3503–3511.

Sylvia, K. E. and Demas, G. E. (2018) "Acute intraperitoneal lipopolysaccharide influences the immune system in the absence of gut dysbiosis," *Physiological reports*. doi: 10.14814/phy2.13639.

Takahashi, T. and Iwasaki, A. (2021) "Sex differences in immune responses," *Science (New York, N.Y.)*. American Association for the Advancement of Science (AAAS), 371(6527), pp. 347–348.

Takeda, K. and Akira, S. (2005) "Toll-like receptors in innate immunity," *International immunology*, 17(1), pp. 1–14.

Talavera, K. *et al.* (2020) "Mammalian Transient Receptor Potential TRPA1 Channels: From Structure to Disease," *Physiological reviews*, 100(2), pp. 725–803.

Talbot, S. *et al.* (2015) "Silencing Nociceptor Neurons Reduces Allergic Airway Inflammation," *Neuron*, 87(2), pp. 341–354.

Tavares-Ferreira, D. *et al.* (2022) "Sex differences in nociceptor translatomes contribute to divergent prostaglandin signaling in male and female mice," *Biological psychiatry*. Elsevier BV, 91(1), pp. 129–140.

van Teijlingen Bakker, N. *et al.* (2022) "In macrophages fatty acid oxidation spares glutamate for use in diverse metabolic pathways required for alternative activation," *bioRxiv*. doi: 10.1101/2022.04.13.487890.

Ter Horst, R. *et al.* (2016) "Host and Environmental Factors Influencing Individual Human Cytokine Responses," *Cell*, 167(4), pp. 1111-1124.e13.

Thomma, B. P. H. J. (2003) "Alternaria spp.: from general saprophyte to specific parasite," *Molecular plant pathology*, 4(4), pp. 225–236.

Thorsen, K., Drengstig, T. and Ruoff, P. (2014) "Transepithelial glucose transport and Na+/K+ homeostasis in enterocytes: an integrative model," *American journal of physiology. Cell physiology*, 307(4), pp. C320-37.

Tokuyama, H. *et al.* (2005) "The simultaneous blockade of chemokine receptors CCR2, CCR5 and CXCR3 by a non-peptide chemokine receptor antagonist protects mice from dextran sodium sulfate-mediated colitis," *International immunology*, 17(8), pp. 1023–1034.

Torcia, M. G. *et al.* (2012) “Sex differences in the response to viral infections: TLR8 and TLR9 ligand stimulation induce higher IL10 production in males,” *PloS one*, 7(6), p. e39853.

Turnbull, I. R. *et al.* (2006) “Cutting edge: TREM-2 attenuates macrophage activation,” *The journal of immunology*. The American Association of Immunologists, 177(6), pp. 3520–3524.

Ulland, T. K. *et al.* (2017) “TREM2 Maintains Microglial Metabolic Fitness in Alzheimer’s Disease,” *Cell*, 170(4), pp. 649-663.e13.

Ungaro, R. *et al.* (2017) “Ulcerative colitis,” *The Lancet*, 389(10080), pp. 1756–1770.

Van den Bossche, J. and van der Windt, G. J. W. (2018) “Fatty Acid Oxidation in Macrophages and T Cells: Time for Reassessment?,” *Cell metabolism*, pp. 538–540.

Varghese, M. *et al.* (2022) “Monocyte Trafficking and Polarization Contribute to Sex Differences in Meta-Inflammation,” *Frontiers in endocrinology*, 13, p. 826320.

Vats, D. *et al.* (2006) “Oxidative metabolism and PGC-1beta attenuate macrophage-mediated inflammation,” *Cell metabolism*, 4(1), pp. 13–24.

Viola, M. F. and Boeckxstaens, G. (2021) “Niche-specific functional heterogeneity of intestinal resident macrophages,” *Gut*, 70(7), pp. 1383–1395.

Voehringer, D., Liang, H.-E. and Locksley, R. M. (2008) “Homeostasis and effector function of lymphopenia-induced ‘memory-like’ T cells in constitutively T cell-depleted mice,” *Journal of immunology* , 180(7), pp. 4742–4753.

Wang, S. *et al.* (2022) “TREM2 drives microglia response to amyloid-β via SYK-dependent and -independent pathways,” *Cell*, 185(22), pp. 4153-4169.e19.

Wang, S.-H., Chen, P.-J. and Yeh, S.-H. (2015) “Gender disparity in chronic hepatitis B: Mechanisms of sex hormones,” *Journal of gastroenterology and hepatology*, 30(8), pp. 1237–1245.

Weinstein, Y., Ran, S. and Segal, S. (1984) “Sex-associated differences in the regulation of immune responses controlled by the MHC of the mouse,” *Journal of immunology* , 132(2), pp. 656–661.

*What is Alzheimer’s Disease?* (2023). Available at: https://www.cdc.gov/aging/aginginfo/alzheimers.htm (Accessed: May 23, 2023).

Wilkinson, N. M. *et al.* (2022) “Sex Differences in Immunity,” *Annual review of immunology*, 40, pp. 75–94.

Williams, J. M. *et al.* (2013) "A mouse model of pathological small intestinal epithelial cell apoptosis and shedding induced by systemic administration of lipopolysaccharide," *Disease models & mechanisms*, 6(6), pp. 1388–1399.

Wu, T.-T., Chen, T.-L. and Chen, R.-M. (2009) "Lipopolysaccharide triggers macrophage activation of inflammatory cytokine expression, chemotaxis, phagocytosis, and oxidative ability via a toll-like receptor 4-dependent pathway: validated by RNA interference," *Toxicology letters*, 191(2–3), pp. 195–202.

Xu, W. and Larbi, A. (2018) "Immunity and Inflammation: From Jekyll to Hyde," *Experimental gerontology*, 107, pp. 98–101.

Yackle, K. (2023) "Transformation of Our Understanding of Breathing Control by Molecular Tools," *Annual review of physiology*, 85, pp. 93–113.

Yao, H. *et al.* (2019) "Distinct signaling pathways regulate TREM2 phagocytic and NFκB antagonistic activities," *Frontiers in cellular neuroscience*. Frontiers Media SA, 13, p. 457.

Yip, J. L. K. *et al.* (2021) "The Role of Intestinal Macrophages in Gastrointestinal Homeostasis: Heterogeneity and Implications in Disease," *Cellular and molecular gastroenterology and hepatology*, 12(5), pp. 1701–1718.

Yu, L. C. H., Turner, J. R. and Buret, A. G. (2006) "LPS/CD14 activation triggers SGLT-1-mediated glucose uptake and cell rescue in intestinal epithelial cells via early apoptotic signals upstream of caspase-3," *Experimental cell research*, 312(17), pp. 3276–3286.

Yue, X. and Guidry, J. J. (2019) "Differential Protein Expression Profiles of Bronchoalveolar Lavage Fluid Following Lipopolysaccharide-Induced Direct and Indirect Lung Injury in Mice," *International journal of molecular sciences*, 20(14). doi: 10.3390/ijms20143401.

Yuki, T. and Thurman, R. G. (1980) "Mechanism of the swift increase in alcohol metabolism ('SIAM') in the rat," *Advances in experimental medicine and biology*, 132, pp. 689–695.

Zhang, X. *et al.* (2001) "Estrogen inhibits lipopolysaccharide-induced tumor necrosis factor-alpha release from murine macrophages," *Methods and findings in experimental and clinical pharmacology*, 23(4), pp. 169–173.

Zhao, J. *et al.* (2019) "Neuroinflammation induced by lipopolysaccharide causes cognitive impairment in mice," *Scientific reports*, 9(1), p. 5790.

Zhao, Q. *et al.* (2017) "A novel function of CXCL10 in mediating monocyte production of proinflammatory cytokines," *Journal of leukocyte biology*, 102(5), pp. 1271–1280.

Zhao, Q. *et al.* (2022) “A multidimensional coding architecture of the vagal interoceptive system,” *Nature*, 603(7903), pp. 878–884.

Zhou, J. and Boutros, M. (2020) “JNK-dependent intestinal barrier failure disrupts host-microbe homeostasis during tumorigenesis,” *Proceedings of the National Academy of Sciences of the United States of America*, 117(17), pp. 9401–9412.

Zhou, W. *et al.* (2018) “Glucose stimulates intestinal epithelial crypt proliferation by modulating cellular energy metabolism,” *Journal of cellular physiology*, 233(4), pp. 3465–3475.

Zhu, L.-Q. *et al.* (2010) “GSK-3β Inhibits Presynaptic Vesicle Exocytosis by Phosphorylating P/Q-Type Calcium Channel and Interrupting SNARE Complex Formation,” *The Journal of neuroscience: the official journal of the Society for Neuroscience*. Society for Neuroscience, 30(10), pp. 3624–3633.

Zimmerman, N. P. *et al.* (2008) “Chemokines and chemokine receptors in mucosal homeostasis at the intestinal epithelial barrier in inflammatory bowel disease,” *Inflammatory bowel diseases*, 14(7), pp. 1000–1011.

Zureik, M. *et al.* (2002) “Sensitisation to airborne moulds and severity of asthma: cross sectional study from European Community respiratory health survey,” *BMJ* , 325(7361), pp. 411–414.